

Dissertation

submitted to the
Combined Faculty of Natural Sciences and Mathematics
of the Ruperto Carola University Heidelberg, Germany
for the degree of
Doctor of Natural Sciences

Presented by

Nina Tonn, M.Sc.

born in Darmstadt, Germany

Oral examination: 26.06.2020

SUPPRESSOR OF MAX2 1-LIKE3 (SMXL3), SMXL4 and SMXL5
establish post-embryonic phloem development
in *Arabidopsis thaliana*

Referees:

Prof. Dr. Thomas Greb

Prof. Dr. Rüdiger Hell

Summary

During post-embryonic development, plants rely on the integrity of phloem within their root systems. The phloem is part of the vasculature and transports energy metabolites from leaves into mitotically active regions such as the root apical meristem (RAM). Loss of function of genes regulating phloem development can result in severe changes in root growth and plant body architecture. The redundantly active genes *SUPPRESSOR OF MAX2 1-LIKE3* (*SMXL3*), *SMXL4* and *SMXL5* are central regulators of early phloem formation. However, molecular mechanisms underlying *SMXL3/4/5* gene activities during early phloem development are mostly unknown. The functional relevance of *SMXL3/4/5* protein domains including the EAR motif is also unclear. The aim of my dissertation was to characterise the mode of action of *SMXL3/4/5* during early events of phloem development in detail using *Arabidopsis thaliana* roots as model organ to investigate spatiotemporal tissue formation.

First, I investigated at which developmental steps *SMXL3/4/5* genes are required to promote phloem development in the RAM, how they interact genetically with positive regulators (*OPS*, *BRX*) and how their function is affected by negative regulators (*CLE26*, *CLE45*). I found that *SMXL4/5* function is required to initiate and promote the activities other of of genes regulating phloem development (*OPS*, *BRX*, *BAM3*, *CVP2* and *APL*), and that *SMXL4/5* protein functions are possibly required to attenuate CLE-mediated suppression of phloem differentiation. Furthermore, I examined whether the highly conserved EAR motif of *SMXL5* is functionally relevant to promote early phloem development. Here, I tested whether protein accumulation was altered for EAR motif-mutated *SMXL5* proteins (*SMXL5^{mEAR}*) *in planta*, and if phloem formation could be restored in *smxl4;smxl5* double mutants complemented with *SMXL5^{mEAR}* proteins. My data suggest that *SMXL5* protein function is independent from the EAR motif indicating that *SMXL5* proteins do not act as canonical EAR repressors in the context of phloem development. Last, I aimed at identifying new genes that are functionally related to *SMXL3/4/5* during early phloem development. Therefore, I performed an ethyl

methanesulfonate (EMS)-based mutagenesis of *smxl4;smxl5* double mutants to screen for genetic suppressors that alleviate the phloem defects characteristic for *smxl4;smxl5* mutants. I found that mutagenesis of yet unknown suppressor genes in the *smxl4;smxl5* background could indeed restore phloem development. Further analysis including genome mapping is required to identify candidate genes that result in the suppression of the *smxl4;smxl5* mutant phenotype.

In conclusion, I postulate that *SMXL3*, *SMXL4* and *SMXL5* genes are required to establish the post-embryonic phloem lineage and regulate the phloem-specific developmental program in the RAM. Together, a complex, tightly balanced network of molecular players depending on *SMXL3/4/5* activities ensures the formation of phloem within the root system.

Zusammenfassung

Während ihrer postembryonalen Entwicklung sind Pflanzen auf die Integrität von Phloem in ihren Wurzelsystemen angewiesen. Das Phloem bildet den Teil des Gefäßsystems, der Energiestoffwechselprodukte von Blättern in mitotisch aktive Regionen wie das apikale Wurzelmeristem (RAM) transportiert. Der Funktionsverlust von Genen, die Phloementwicklung regulieren, kann zu schwerwiegenden Veränderungen des Wurzelwachstums und der Architektur des Pflanzenkörpers führen. Die redundant aktiven Gene *SUPPRESSOR OF MAX2 1-LIKE3 (SMXL3)*, *SMXL4* und *SMXL5* sind zentrale Regulatoren der frühen Phloembildung. Die molekularen Mechanismen, die den Genaktivitäten von *SMXL3/4/5* während der frühen Phloementwicklung zugrunde liegen, sind jedoch größtenteils unbekannt. Die funktionale Relevanz von *SMXL3/4/5*-Proteindomänen einschließlich des EAR-Motivs ist ebenfalls unklar. Ziel meiner Dissertation war es, die Wirkungsweise von *SMXL3/4/5* während der frühen Phloementwicklung anhand von *Arabidopsis thaliana*-Wurzeln als Modellorgan für raumzeitliche Gewebebildung detailliert zu charakterisieren.

Zunächst habe ich untersucht, bei welchen Entwicklungsschritten *SMXL3/4/5*-Gene erforderlich sind, um die Phloementwicklung im RAM anzutreiben. Außerdem, wie sie genetisch mit positiven Regulatoren (*OPS*, *BRX*) interagieren und wie ihre Funktion durch negative Regulatoren (*CLE26*, *CLE45*) beeinflusst wird. Ich habe herausgefunden, dass *SMXL4/5*-Gene funktional erforderlich sind, um die Aktivitäten anderer Gene, die Phloementwicklung regulieren (*OPS*, *BRX*, *BAM3*, *CVP2* und *APL*), zu initiieren und zu fördern, und dass *SMXL4/5*-Proteinfunktionen möglicherweise erforderlich sind, um die CLE-vermittelte Inhibierung von Phloemdifferenzierung abzuschwächen. Zusätzlich habe ich untersucht, ob das hochkonservierte EAR-Motiv von *SMXL5*-Proteinen funktional relevant ist, um die frühe Phloementwicklung zu fördern. Hier habe ich getestet, ob die Proteinakkumulation für EAR-Motiv-mutierte *SMXL5*-Proteine (*SMXL5^{mEAR}*) *in planta* verändert wurde und ob Phloembildung in *smx14;smx15*-Doppelmutanten komplementiert mit

SMXL5^{mEAR}-Proteinen wiederhergestellt werden konnte. Meine Daten zeigen auf, dass die SMXL5-Proteinfunktion unabhängig vom EAR-Motiv ist, was darauf hinweist, dass SMXL5-Proteine nicht als kanonische EAR-Repressoren im Kontext von Phloementwicklung agieren. Ein weiteres Ziel dieser Arbeit war, neue Gene zu identifizieren, die während der frühen Phloementwicklung funktional mit *SMXL3/4/5* verbunden sind. Dazu habe ich eine auf Ethylmethansulfonat (EMS) basierende Mutagenese von *smxl4;smxl5*-Doppelmutanten durchgeführt, um nach genetischen Suppressoren zu suchen, welche die für *smxl4;smxl5*-Mutanten charakteristischen Phloemdefekte abschwächen. Ich habe herausgefunden, dass die Mutagenese von noch zu identifizierenden Suppressoren in *smxl4;smxl5*-Doppelmutanten die Phloementwicklung wiederherstellen konnte. Weitere Analysen einschließlich einer Genomkartierung sind erforderlich, um Kandidatengene zu identifizieren, die zur Unterdrückung des *smxl4;smxl5*-Phänotyps führen.

Zusammenfassend postuliere ich, dass die Gene *SMXL3*, *SMXL4* und *SMXL5* erforderlich sind, um die postembryonale Phloemzelllinie zu etablieren und das phloemspezifische Entwicklungsprogramm im RAM zu regulieren. Ein komplexes, fein ausbalanciertes Netzwerk molekularer Akteure stellt abhängig von *SMXL3/4/5*-Aktivitäten die Bildung von Phloem im Wurzelsystems sicher.

Table of Contents

List of Publications	I
List of Abbreviations	II
1. Introduction	1
1.1. The plant vasculature promotes plasticity and growth	1
1.2. From stem cells to sieve elements – phloem development in root tips	3
1.3. Phloem sap transport from source to sink organs	6
1.4. Phloem development and plant growth are interconnected	8
1.4.1. Positive regulators of phloem development	8
1.4.2. Negative regulators of phloem development	11
1.5. SMXL3/4/5 – Initiators of phloem development?	16
1.5.1. SMXL3/4/5 genes are central promoters of phloem development	16
1.5.2. SMXL protein structure is highly conserved	17
1.5.3. Involvement of SMXL3/4/5 proteins in transcriptional regulation	18
1.6. Aim and objectives	20
2. Material and Methods	23
2.1. Model organisms and bacterial strains	23
2.1.1. <i>Arabidopsis thaliana</i>	23
2.1.2. <i>Nicotiana benthamiana</i>	23
2.1.3. <i>Escherichia coli</i>	23
2.1.4. <i>Agrobacterium tumefaciens</i>	25
2.2. Chemicals	25
2.2.1. Antibiotics	25
2.2.2. Dyes	26
2.3. Standard plant work	26
2.3.1. Seed sterilisation and stratification	26
2.3.2. Plant growth and seed collection	26
2.3.3. Genomic DNA isolation	27

TABLE OF CONTENTS

2.3.4.	Genotyping	27
2.3.5.	Agarose gel electrophoresis	28
2.3.6.	Infiltration of <i>Nicotiana benthamiana</i>	28
2.4.	Generation of new transgenic lines	29
2.4.1.	Molecular cloning (GreenGate cloning)	29
2.4.2.	Transformation of <i>E. coli</i>	32
2.4.3.	Transformation of <i>A. tumefaciens</i>	33
2.4.4.	Transformation of <i>A. thaliana</i>	33
2.5.	EMS-based mutagenesis and suppressor screen	34
2.6.	CLE treatments	34
2.7.	Seedling preparation for confocal microscopy	35
2.7.1.	Signal fixation (PFA) and cell wall staining (DirectRed23) of transgenic lines	35
2.7.2.	Cell wall staining (mPS-PI) of mutant lines	36
2.8.	Confocal microscopy	36
2.9.	Root length measurements and Statistics	37
2.10.	Figures and Illustrations	37
3.	Results	39
3.1.	<i>SMXL3/4/5</i> genes activate early phloem regulators	39
3.2.	<i>SMXL5</i> conducts a different role than <i>BRX</i> and <i>OPS</i>	42
3.3.	<i>SMXL4/5</i> act upstream of <i>OPS</i> and <i>BRX</i>	45
3.4.	<i>SMXL5</i> expression in developing SEs restores phloem development	47
3.5.	Enhanced CLE45/BAM3 signalling causes <i>smxl4;smxl5</i> -like protophloem defects	50
3.6.	Enhanced CLE45/BAM3 signalling is still perceived in <i>smxl4;smxl5</i> mutants	54
3.7.	<i>SMXL3/4/5</i> proteins are affected by CLE45/BAM3 signalling	55
3.8.	<i>SMXL3/4/5</i> proteins are affected by BAM3-independent CLE26 signalling	60
	Summary I	61
3.9.	<i>SMXL5</i> protein function in protophloem cells is independent of the EAR motif	63
3.10.	<i>SMXL5</i> proteins potentially interact with TPR2/4 corepressors	66

Summary II	67
3.11. EMS-based mutagenesis of <i>smxl4;smxl5</i> restored protophloem development	68
Summary III	72
4. Discussion	75
4.1. <i>SMXL3/4/5</i> genes promote phloem initiation and SE differentiation in roots	75
4.2. Delayed production of developing SEs <i>smxl4;smxl5</i> double mutants	79
4.3. <i>SMXL3/4/5</i> protein accumulation is affected by CLE signalling	81
4.4. Additional role of <i>SMXL3/4/5</i> proteins in fine-tuning SE differentiation?	82
4.5. The <i>smxl4;smxl5</i> phenotype can be suppressed by second-site mutagenesis	84
4.6. Synchronised development of SEs and CCs via translational control of <i>SMXL5</i> ?	86
4.7. Non-identical roles of <i>SMXL3/4/5</i> in primary and secondary phloem development	88
4.8. Role of <i>SMXL5</i> in non-phloem related cell fate regulation in the SAM?	89
4.9. <i>SMXL5</i> protein function is independent of the EAR motif	92
Conclusion	94
List of Figures	97
List of Tables	99
Bibliography	101
Acknowledgements / Danksagungen	109

List of Publications

Listed here are publications that I wrote or contributed to in the course my dissertation. Of those, some include illustrations or data presented in this dissertation. They are referenced accordingly in the respective figure legends.

First-authorship:

Tonn, N. and Greb, T. (2017) *Radial plant growth*, *Current Biology*. doi: 10.1016/j.cub.2017.03.056.

Co-authorships:

López-Salmerón, V., Cho, H., **Tonn**, N. and Greb, T. (2019) 'The Phloem as a Mediator of Plant Growth Plasticity', *Current Biology*, 29(5). doi: 10.1016/j.cub.2019.01.015.

Wallner, E.-S., **Tonn**, N., Wanke, F., López-Salmerón, V., Gebert, M., Wenzl, C., Lohmann, J. U., Harter, K. and Greb, T. (2019) 'OBERON3 and SUPPRESSOR OF MAX2 1-LIKE proteins form a regulatory module specifying phloem identity', *bioRxiv*. doi: 10.1101/2019.12.21.885863.

Wallner, E. S., **Tonn**, N., Shi, D., Jouannet, V. and Greb, T. (2020) 'SUPPRESSOR OF MAX2 1-LIKE 5 promotes secondary phloem formation during radial stem growth', *Plant Journal*. doi: 10.1111/tpj.14670.

List of Abbreviations

Listed in alphabetical order are abbreviations for genes, organisms, and scientific terms recurring in this dissertation. Gene names are written in capitals and italics.

Agrobacterium	<i>Agrobacterium tumefaciens</i> , <i>A. tumefaciens</i>
<i>APL</i>	<i>ALTERED PHLOEM DEVELOPMENT</i>
Arabidopsis	<i>Arabidopsis thaliana</i> , <i>A. thaliana</i>
<i>BAM3</i>	<i>BARELY ANY MERISTEM3</i>
<i>BRX</i>	<i>BREVIS RADIX</i>
CC	companion cell
<i>CLE</i>	<i>CLAVATA3/EMBRYO SURROUNDING REGION</i>
<i>CLERK</i>	<i>CLE-RESISTANT RECEPTOR KINASE</i>
Clp	caseinolytic protease
<i>CLV</i>	<i>CLAVATA</i>
<i>CRN</i>	<i>CORYNE</i>
<i>CVL1</i>	<i>CVP2-LIKE1</i>
<i>CVP2</i>	<i>COTYLEDON VASCULAR PATTERN2</i>
CZ	central zone
<i>E. coli</i>	<i>Escherichia coli</i>
EAR	ETHYLENE-RESPONSIVE ELEMENT BINDING FACTOR-ASSOCIATED AMPHIPHILIC REPRESSION
gDNA	genomic DNA
HDAC	histone deacetylase
<i>JUL</i>	<i>JULGI</i>
LRR	leucine-rich repeat
<i>MAKR5</i>	<i>MEMBRANE ASSOCIATED KINASE REGULATOR5</i>
MS	Murashige and Skoog (medium)
<i>NAC</i>	<i>NO APICAL MERISTEM</i>
<i>NaKR1</i>	<i>SODIUM POTASSIUM ROOT DEFECTIVE1</i>
<i>NEN</i>	<i>NAC45/86-DEPENDENT EXONUCLEASE-DOMAIN</i>
Nicotiana	<i>Nicotiana benthamiana</i> , <i>N. benthamiana</i>
<i>OBE3</i>	<i>OBBERON3</i>
OC	organising centre
<i>OPL2</i>	<i>OPS-LIKE2</i>
<i>OPS</i>	<i>OCTOPUS</i>
PHD	plant homeodomain
PI4P	phosphatidylinositol-4-phosphate
PI(4,5)P ₂	phosphatidylinositol-4,5-biphosphate
QC	quiescent centre

LIST OF ABBREVIATIONS

RAM	root apical meristem
RM	rib meristem
RBP	RNA binding protein
RLK	receptor-like kinase
<i>RPK2</i>	<i>RECEPTOR PROTEIN LIKE KINASE2</i>
SAM	shoot apical meristem
SC	stem cell
SE	sieve element
<i>SAPL</i>	<i>SISTER OF ALTERED PHLOEM DEVELOPMENT (APL)</i>
<i>SMAX1</i>	<i>SUPPRESSOR OF MAX2 1</i>
<i>SMXL</i>	<i>SUPPRESSOR OF MAX2 1 (SMAX1)-LIKE</i>
<i>SUC2</i>	<i>SUCROSE TRANSPORTER2</i>
<i>WUS</i>	<i>WUSCHEL</i>

Specialis Revelio



1. Introduction

1.1. The plant vasculature promotes plasticity and growth

Plants are sessile, photoautotrophic, multicellular organisms of various forms and sizes that markedly shape our landscape and serve as important renewable energy source. Throughout their development, plants need to be able to perceive temperature, exposure to sunlight, or water availability, communicate exterior changes through the whole plant body and respond via modulation of overall plant growth. Due to limited mobility plants have adapted a variety of structural and molecular tools enabling them to shape and reshape their body forms in response to changing environmental conditions (Tonn and Greb 2017). The plant vasculature plays a crucial role in translating environmental cues into developmental processes to enable plant survival (Cho et al. 2018, Lopez-Salmeron et al. 2019). Therefore, it is important to increase our knowledge on the molecular mechanisms that govern the development of vascular tissues which then promote plasticity and growth.

The plant vasculature spans the whole plant body and mediates continuous supply of water, minerals, energy metabolites and signalling molecules in developing plants (Miyashima et al. 2013, Blob et al. 2018). Morphologically, the vasculature is composed of two main parts, xylem (wood) and phloem (bast), both formed by highly specialised conductive units. In the xylem, tracheary elements transport water and minerals passively from roots to upper plant parts via pressure differences created by water transpiration at the surface of leaves (Miyashima et al. 2013, Blob et al. 2018). In the phloem, sieve elements (SEs) transport the 'phloem sap', carbohydrates and other organic molecules including amino acids, RNAs and signalling molecules, from source to sink organs (Knoblauch et al. 2016). Here, source organs such as leaves are defined by their net production and efflux of sugar molecules, whereas sink organs exhibit a

high demand for energy metabolites and are defined by net influx of sugars. Typical sink organs include meristems, flowers, and storage organs such as fruits (Lalonde et al. 2003). Xylem and phloem tissues are both produced by undifferentiated but elongated (pro)cambial cells, a pool of pluripotent stem cells, subsequently forming interconnected vascular tissues (De Rybel et al. 2016; Ruonala et al. 2017, Miyashima et al. 2013) (**Figure 1**).

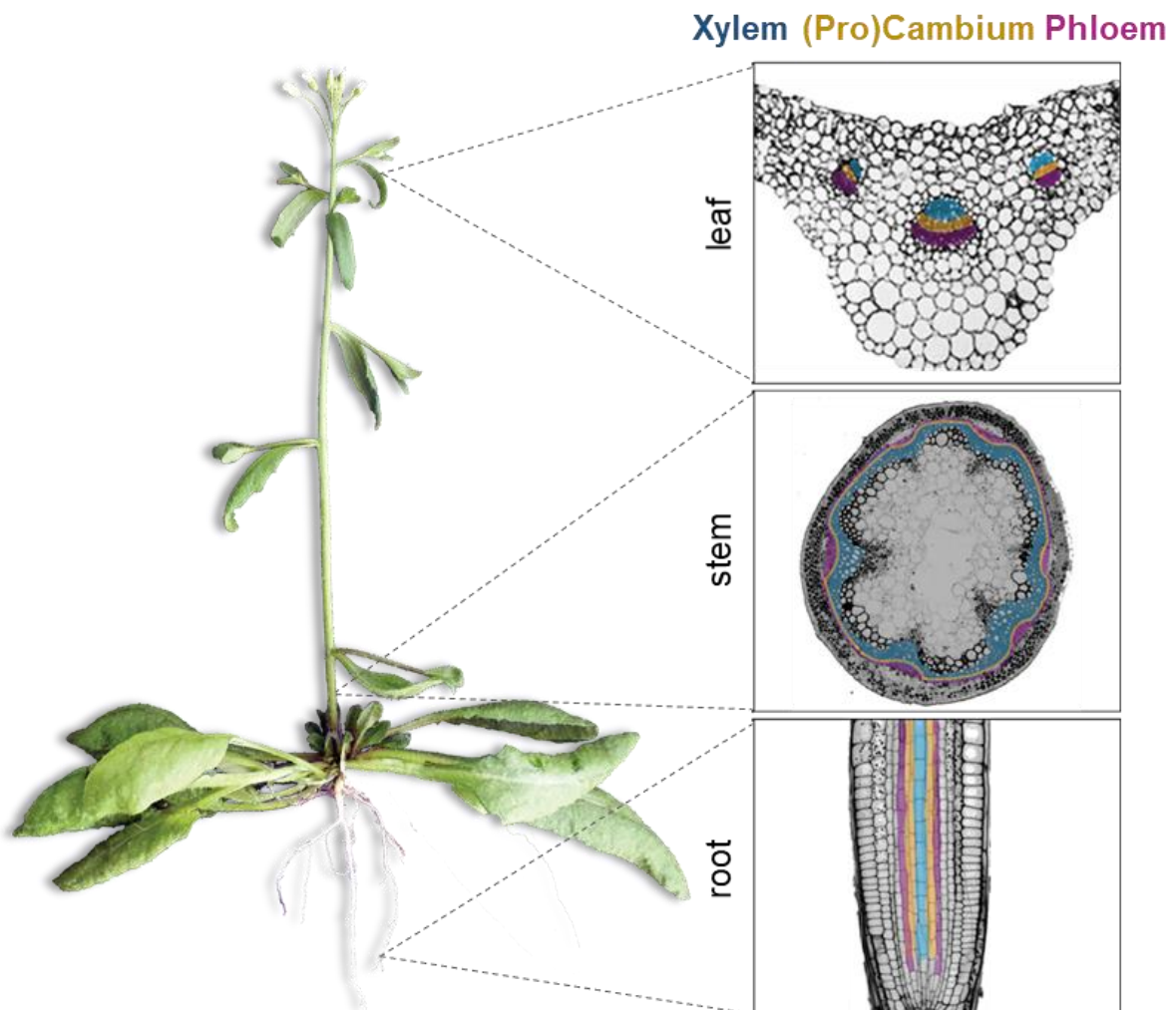


Figure 1: Vascular tissues in Arabidopsis organs. The plant vasculature spans the whole plant body and includes sugar-transporting phloem and water-transporting xylem which are structurally and functionally interconnected. (Pro)cambium cells maintain vascular tissues throughout the plant life cycle. Illustration published in Lopez-Salmeron et al. 2019.

1.2. From stem cells to sieve elements – phloem development in root tips

To enable vascular tissue formation and plant growth in response to environmental cues, continuous formation of new tissues is regulated by meristems, highly organised regions including an organising centre, a pool of self-renewing stem cells and proliferative progenitor cells which eventually differentiate into specialised features like the vasculature (Miyashima et al. 2013). To study the role of meristems for post-embryonic tissue formation we often rely on model plants such as *Arabidopsis thaliana* (Arabidopsis) (Aichinger et al. 2012). Particularly primary roots including root apical meristem (RAM) in the tip serve as an easily accessible model system for spatiotemporal tissue organisation in sink organs (Anne and Hardtke 2018, Blob et al. 2018).

During early post-embryonic development, plants rely specifically on the integrity of phloem within their root systems as it transports energy metabolites into mitotically active regions. Accordingly, defects in early, post-embryonic phloem formation can result in severe changes in root growth and plant body architecture (Wallner et al. 2017, Blob et al. 2018, Cho et al. 2018, John and Nimchuk 2019). A developing root tip can be separated into four developmental zones, the meristematic zone (RAM), transition zone, elongation zone, and differentiation zone (**Figure 2Left**) (Ivanov and Dubrovsky 2013). In the RAM, phloem development starts from phloem stem cells, also called phloem ‘initial cells’, located in the stem cell niche surrounding the organising centre (quiescent centre). Stem cells exiting the quiescent centre give rise to all cell files that form the root (Dolan et al. 1993). In the case of phloem formation, phloem initial cells divide anticlinally and produce SE/procambium precursor cells which subsequently undergo a periclinal cell division to produce two strands of transiently amplifying cells. One strand produces SE precursor cells which eventually differentiate into SEs after a secondary periclinal cell division, the other strand gives rise to procambial cells (Mähönen et al. 2000) (**Figure 2Right**). Phloem strands are built in the process of

differentiation when single SEs become connected via specialised perforated cell walls called sieve plates to form a continuous tube system and enable constant flow of sugar molecules (Dettmer et al. 2014, Knoblauch et al. 2016).

The first phloem strands called protophloem are fully differentiated before the end of the transition zone while other cell types are still elongating (Bonke et al. 2003, Blob et al. 2018). Higher up in roots, in the elongation zone, additional phloem strands called metaphloem functionally replace the protophloem (Ross-Elliott et al. 2017; Lalonde et al. 2003, Mähönen et al. 2014). Developing SEs undergo a series of differentiation steps such as cell wall modification, degradation of cellular organelles including the nucleus, and formation of a fluid cytosol to transport carbohydrates and signalling molecules easily along phloem SEs (**Figure 2ABC**) (Lucas et al. 2013, Furuta et al. 2014, Ross-Elliott et al. 2017). Only mitochondria, an altered version of the smooth ER, and a degenerated cytoplasm remain to account for a basic level of cellular homeostasis (Evert and Eichhorn 2006; Lucas et al. 2013; Anne and Hardtke 2017).

Located adjacent to phloem strands are companion cells (CCs) with enlarged nuclei. Those cells develop in parallel and connect to phloem SEs via cytosolic channels called plasmodesmata, thereby forming a conductive complex and keeping SEs metabolically alive (Mähönen et al. 2000, Oparka and Turgeon 1999; Otero and Helariutta 2017, Evert and Eichhorn 2006). The establishment of SE-CC complexes finalises the formation of the functional transport units of phloem tissues (Otero and Helariutta 2017, Slewinski et al. 2013) visible as two phloem poles in transverse sections of roots (**Figure 2Right**).

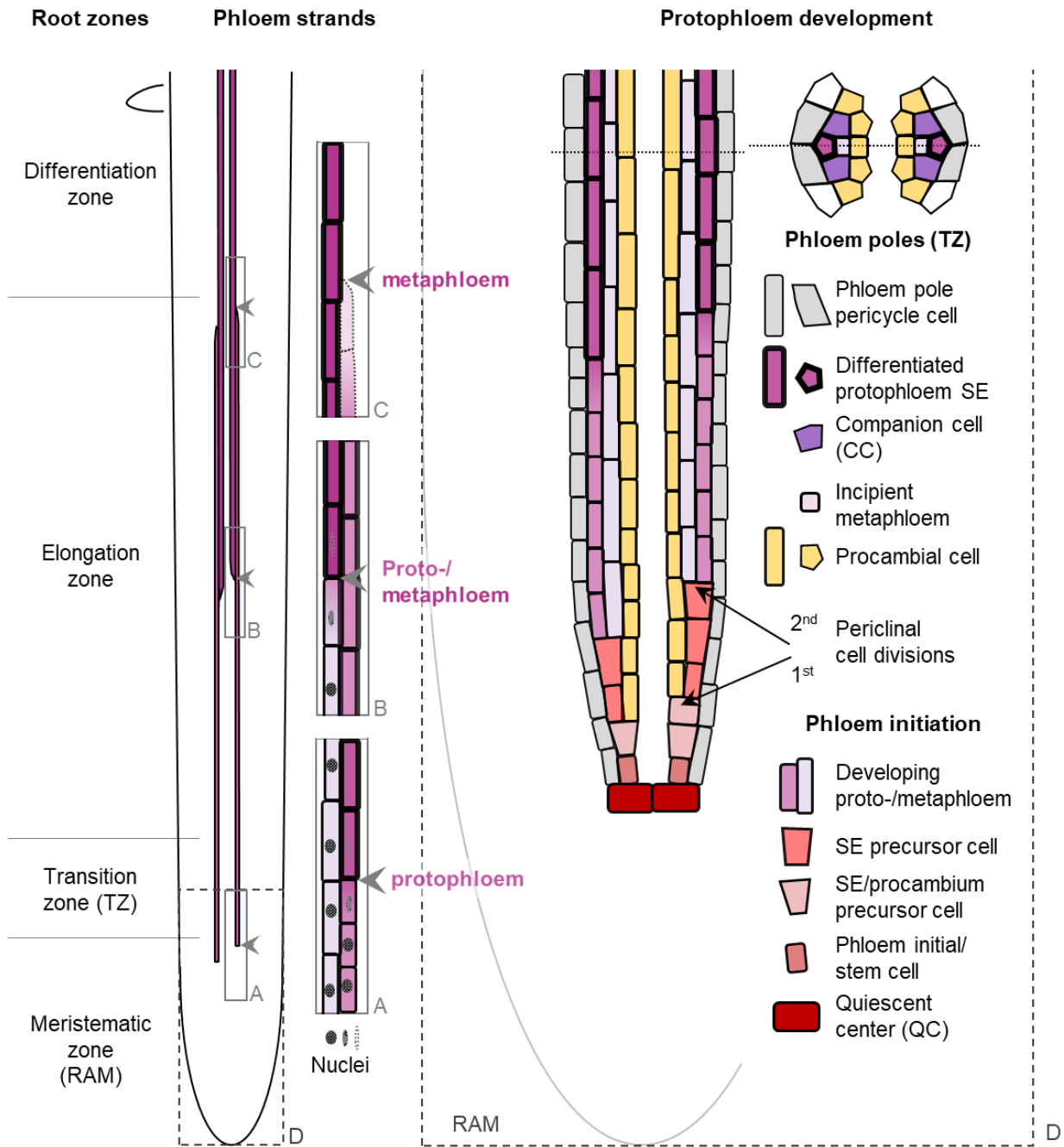


Figure 2: Early phloem development in root tips. (Left) A developing root contains four zones, the meristematic, transition, elongation, and differentiation zone. (A) The first phloem strands called protophloem are fully differentiated before the end of the transition zone. (BC) In the elongation zone, second phloem strands called metaphloem functionally replace the protophloem. (ABC) Developing SEs undergo a series of differentiation steps including cell wall remodelling and enucleation to form functional transport units. **(Right)** (D) In the root apical meristem (RAM), protophloem development is initiated adjacent to the quiescent centre from phloem initial cells producing SE/procambium precursor cells which undergo a periclinal cell division to produce two strands of transiently amplifying cells. One strand produces SE precursor cells which eventually differentiate into protophloem SEs after a secondary periclinal cell division, the other strand gives rise to procambial cells. A cross section depicts both phloem poles in the transition zone (TZ) comprising proto- and metaphloem, companion cells (CC) and phloem pole pericycle (PPP) cells. Illustration based on own data, Bonke et al. 2017, Rodriguez-Villalon 2015 and Ross-Elliott et al. 2017.

1.3. Phloem sap transport from source to sink organs

SE-CC complexes span the whole plant body and thus provide fast and efficient long-distance transport including phloem loading and unloading in source and sink organs, respectively (Otero and Helariutta 2017; Slewinski et al. 2013). The phloem sap comprises carbohydrates and other organic molecules such as amino acids, RNAs and signalling molecules, and moves via osmotically generated pressure differences (Lalonde et al. 2003, Oparka and Turgeon 1999; Blob et al. 2018; Otero and Helariutta 2017). This so-called pressure-flow hypothesis states that in source organ SEs, relatively high concentrations of sucrose, the predominant transport form of sugars, draw water from adjacent xylem elements, thereby increasing the pressure in sieve tubes and consequently moving the phloem sap along the concentration gradient over long distances to sucrose-deprived sink organs. As organic compounds are taken up by sink organs and water diffuses passively out of the phloem, differences in osmotic pressures are maintained, thereby promoting continuous phloem sap transport (Münch 1930, Knoblauch et al. 2016).

Phloem loading and unloading includes symplastic and apoplastic mechanisms. In mesophyll cells of *Arabidopsis* leaves (source organ), sucrose is first released into the apoplast by membrane-bound SWEET transporters (Chen et al. 2012) and subsequently loaded into minor veins by sucrose/proton symporters called SUTs localised at plasma membranes of SE-CC complexes (Durand et al. 2018, Lalonde et al. 2003). Sucrose transporters function as membrane complexes to respond to alterations in the source-sink balance (Lalonde et al. 2003). Although *Arabidopsis* is considered an apoplastic phloem loader (Wippel and Sauer 2012), phloem loading varies depending on plant species, organ and growth state (Lopez-Salmeron et al. 2019). Upon reaching sink organs, phloem unloading happens predominantly symplastically (Lalonde et al. 2003). Phloem sap is first transferred from meta- into protophloem strands in the elongation zone, then translocated by protophloem SEs

until entering still differentiating SEs in the transition zone (Stadler et al. 2005, Ross-Elliott et al. 2017) (**Figure 2B, Figure 3**). Finally, in the meristematic zone, small molecules including sugars and amino acids are exported through plasmodesmata into adjacent tissues at a constant rate, diffusing within the symplast of the root tip. Larger molecules including nucleic acids and proteins are first transported into phloem pole pericycle cells through so-called funnel plasmodesmata and subsequently distributed into adjacent tissues of the root tip (Ross-Elliott et al. 2017) (**Figure 3**). Protophloem unloading supplies mitotically active regions with energy metabolites while metaphloem unloading replenishes energy metabolites of storage tissues in the elongation zone (Ross-Elliott et al. 2017; Lalonde et al. 2003).

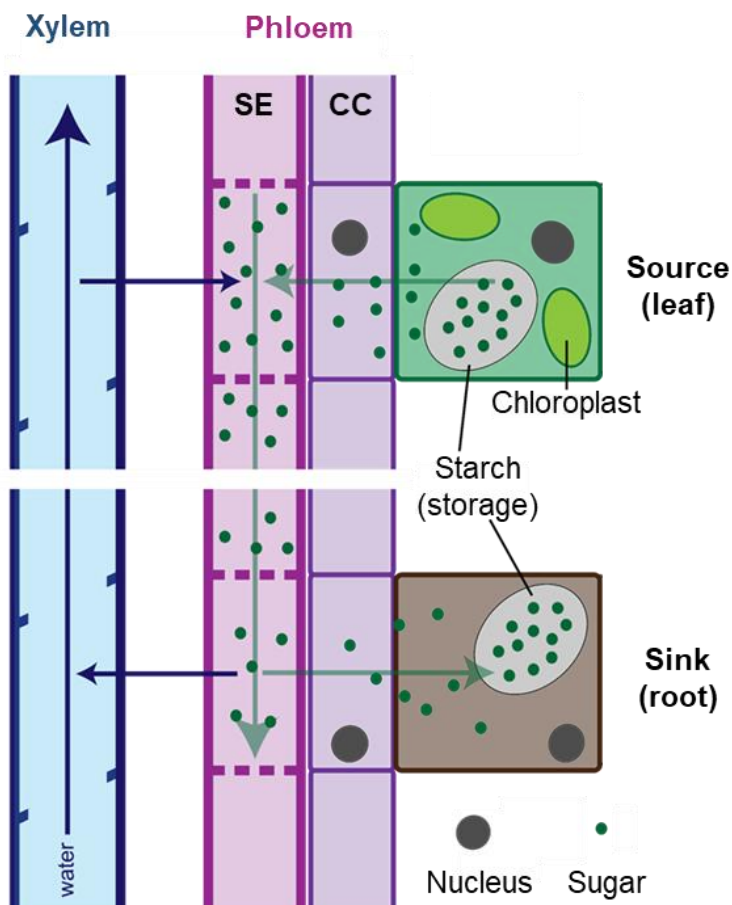


Figure 3: Sugar transport from source to sink organs. Sugar transport is enabled by a functional transport unit comprising sieve elements (SE) and companion cells (CCs). Enucleated SEs are interconnected by sieve plates and are supported by CC by providing regulatory proteins and signalling molecules. CCs promote loading and unloading of sugars in source (leaf) and sink (root) organs, respectively. SE-CC complexes are usually embedded in phloem parenchyma cells and connected via plasmodesmata (not shown). The production of sugar molecules in source organs and their consumption by sink organs creates a pressure gradient which promotes continuous flow of sugars to sink organs. High sugar concentrations in SEs in source organs draw water from the xylem into the phloem. Water uptake into the xylem occurs in

roots from where water flow is driven by transpiration happening at leaf surfaces. Illustration published in Lopez-Salmeron et al. 2019.

1.4. Phloem development and plant growth are interconnected

The phloem is a highly dynamic system that adjusts flow rates and sugar levels in response to sink organ requirements and senses metabolic activity and storage capacity of source organs (Cho et al. 2018). The importance of continuous and plastic formation of SEs becomes most clear in plants with mutations in genes regulating phloem development. For example, *Arabidopsis* mutants with defects in protophloem development over-accumulate sugars in leaves (Wallner et al. 2017, Wu et al. 2017) indicating that the mechanisms regulating early phloem development and sugar distribution are integrated (Cho et al. 2018). In recent years, different early regulators of phloem development were identified (Depuydt et al. 2013; Rodriguez-Villalon et al. 2014; Blob et al. 2018; Rodriguez-Villalon 2016), yet our knowledge of their molecular interactions is still scarce. Overall, regulation of phloem development is highly complex and its impact on overall plant growth in response to environmental changes remains to be investigated more deeply (Lopez-Salmeron et al. 2019).

1.4.1. Positive regulators of phloem development

APL, NACs and NENs promote enucleation of SEs

One of the first described regulators of phloem formation is *ALTERED PHLOEM DEVELOPMENT (APL)*, a gene encoding a MYB coiled-coil-type transcription factor. *APL* is expressed developing SEs and necessary to mediate final steps of SE differentiation in the transition zone of root tips (Bonke et al. 2003) (**Figure 4**). These steps include enucleation and cytoplasmic rearrangement but also transcriptional repression of genes promoting xylem identity in the position of SEs (Bonke et al. 2003, Furuta et al. 2014). In *apl* mutants, cells connected by sieve plates at the position of protophloem strands resemble xylem instead of phloem cells (Truernit et al. 2008). Additionally, seedlings lack periclinal cell divisions that usually precede the formation of protophloem strands (Bonke et al. 2003). Downstream targets of *APL* include the

NO APICAL MERISTEM (*NAC*)-type transcription factors *NAC45* and *NAC86*. Those genes coordinate the expression of *NAC45/86-DEPENDENT EXONUCLEASE-DOMAIN* (*NEN*) proteins *NEN1*, *NEN2* and *NEN4* as well as translocation of *NEN1* and *NEN2* from the cytosol to the nucleus upon enucleation of differentiating SEs (Blob et al. 2018). Furthermore, in both *apl* single and *nac45;nac86* double mutants, nuclei are not fully degraded but the development of sieve plates through modified cell walls still occurs (Bonke et al. 2003; Furuta et al. 2014). Those mutants also grow shorter primary roots than wild type which eventually die, indicating that phloem sap transport into the RAM is significantly impaired (Bonke et al. 2003; Furuta et al. 2014). Taken together, joint activities of *APL*, *NACs* and *NENs* are required for the full degradation of nuclei in differentiating SEs (Bonke et al. 2003, Furuta et al. 2014, Blob et al. 2018).

CVP2, BRX and OPS promote cell wall remodelling of SEs

Another set of genes involved in (proto)phloem differentiation are *COTYLEDON VASCULAR PATTERN2* (*CVP2*) and its redundantly acting partner *CVP2-LIKE1* (*CVL1*). *CVP2* and *CVL1* encode phosphoinositide-5-phosphatases balancing phosphatidylinositol-4,5-bisphosphate ($PI(4,5)P_2$) levels during SE differentiation (Rodriguez-Villalon et al. 2015). *CVP2* was first described as important factor to regulate the establishment and organisation of interconnected, specialised vascular cells into discrete vascular bundles in cotyledons, mature leaves and inflorescence stems (Carland et al. 1999). *CVP2* is first expressed in developing SEs in the meristematic zone earlier than *APL* (Rodriguez-Villalon et al. 2014) (**Figure 4**). *cvp2;cvl1* double mutants display short roots with discontinuous protophloem strands where SEs with thickened cell walls are intermitted by cells without perforated sieve plates called 'gap cells' (Rodriguez-Villalon et al. 2015). These findings suggested an essential role of *CVP2*-regulated $PI(4,5)P_2$ levels in cell wall thickening and timing of (proto)phloem differentiation. Conversely, gap cells are not observed in *apl* single mutants in which the formation of modified cell walls and perforated sieve plates is

unaffected (Bonke et al. 2003, Rodriguez-Villalon et al. 2015). Together, these observations indicate that *APL* and *CVP2/CVL1* genes regulate different steps of SE differentiation.

As for *apl* mutants, primary roots of *cvp2;cvl1* double mutants are reduced in length, again demonstrating that regulation of phloem differentiation and root growth are tightly interconnected (Rodriguez-Villalon 2016). Short primary roots were discovered as prominent macroscopic defects also in *BRX*-deficient plants. *BRX* (*BREVIS RADIX*) was first identified as a regulator of cell proliferation and elongation in the growth zone of the root tip mediating abscisic acid (ABA) signalling (Mouchel et al. 2004, Rodrigues et al. 2009). *BRX* encodes a polarly localised, membrane associated protein regulating auxin efflux in developing protophloem strands and subjected to endocytic recycling and degradation upon auxin treatment (Scacchi et al. 2009, Marhava et al. 2018). *BRX* is expressed earlier than *CVP2*, in SE precursor cells, and accumulates on the rootward plasma membrane (Scacchi et al. 2009; Scacchi et al. 2010) (**Figure 4**). Recently, it was shown that *BRX* acts together with the AGC kinase PROTEIN KINASE ASSOCIATED WITH *BRX* (*PAX*) to modulate auxin gradients and thus the timing of SE differentiation (Marhava et al. 2018). *brx* single mutants are short-rooted and display developing protophloem strands where SEs are irregularly intermitted by gap cells similar to *cvp2;cvl1* double mutants. Gap cells in *brx* mutants exhibit decreased auxin responsiveness (Breda et al. 2017, Kang and Hardtke 2016, Gujas et al. 2012, Rodriguez-Villalon et al. 2014) possibly resulting in altered auxin levels in the whole RAM (Mähönen et al. 2014, Sabatini et al. 1999).

Like *BRX*, another gene being expressed early during phloem development is *OCTOPUS* (*OPS*). The gene encodes a polarly localised, membrane associated protein on the shootward plasma membrane of the developing phloem lineage, firstly expressed in SE/procambium precursor cells (Truernit et al. 2012, Rodriguez-Villalon et al. 2014) (**Figure 4**). Similar to *cvp2;cvl1* and *brx* mutants, primary roots of *OPS*-deficient plants produce protophloem strands intermitted by gap cells indicating that

OPS, too, is involved in timing of SE differentiation. In all three cases (*cvp2;cvl1*, *brx*, *ops*), gap cells neither degrade their nuclei nor form connective sieve plates, consequently causing decreased transport of phloem sap to the RAM (Truernit et al. 2012, Breda et al. 2017). Another member of the *OPS*-like protein family, *OPS-LIKE2* (*OPL2*), acts redundantly with *OPS* during phloem differentiation though it is more broadly expressed in the root tip. In *ops;opl2* double mutants, root length is further reduced than in *ops*, and gap cells appear in protophloem as well as metaphloem files (Aguila Ruiz Sola et al. 2017). It was shown that increased *OPS* activity can rescue the gap cell phenotype in *brx* and *cvp2;cvl1* mutants in a quantitative way (Breda et al. 2017, Rodriguez-Villalon et al. 2014, Rodriguez-Villalon et al. 2015). Furthermore, gap cell phenotypes of *ops* and *brx* mutants are additive in *brx;ops* double mutants indicating that both genes fulfil parallel functions in the context of protophloem development (Breda et al. 2017; Kang and Hardtke 2016; Scacchi et al. 2009). Together, these observations suggest tightly balanced, dose-dependent interaction of positive regulators of SE differentiation.

1.4.2. Negative regulators of phloem development

CLE45/BAM3 act antagonistically to BRX and OPS

Together with timely expression of positive regulators, cell-to-cell communication via signalling molecules balances timing of cell divisions and differentiation during phloem development (Fukuda and Hardtke 2019, John and Nimchuk 2019). For example, CLAVATA3/EMBRYO SURROUNDING REGION45 (CLE45) peptides signalling was shown to suppress SE differentiation by counteracting *BRX* and *OPS* activities (Depuydt et al. 2013, Rodriguez-Villalon 2016). CLE45 belongs to a group of 32 partially redundant, endogenous signalling molecules giving rise to 27 distinct bioactive CLE peptides, 14 of which were identified as being specifically 'root-active' in *Arabidopsis* (Cock et al. 2001, Hazak et al. 2017). It was shown that exogenous

application of CLE45 or transgenically enhanced CLE45 dosage prevent SEs from differentiating, and that overexpression of a modified, less active version of the CLE45 peptide mirrors the *brx* and *ops* gap cell phenotype (Breda et al. 2019, Kang and Hardtke 2016). CLE45 is expressed and probably secreted in developing protophloem strands where it is recognised by the membrane associated receptor protein BARELY ANY MERISTEM3 (BAM3) (Depuydt et al. 2013, Hazak et al. 2017, Breda et al. 2019). BAM3 is a leucine-rich repeat (LRR) receptor-like kinase (RLK) first expressed in SE/procambium precursor cells (Hazak et al. 2017) (**Figure 4**).

brx and *ops* single mutant gap cell phenotypes can be rescued by a second-site mutation of *BAM3* rendering BRX and OPS as antagonists of CLE45/BAM3-mediated inhibition of phloem differentiation (Depuydt et al. 2013, Rodriguez-Villalon et al. 2014, Breda et al. 2017; Kang and Hardtke 2016). BRX influences *BAM3* transcription whereas OPS proteins interfere physically with CLE45 signaling components including the BAM3 protein (Breda et al. 2019). OPS has therefore been proposed as key antagonist and ‘cellular insulator’ of CLE45/BAM3 signalling (Breda et al. 2017; Kang and Hardtke 2016, Breda et al. 2019). *BAM3* expression is increased in *brx* and *brx;ops* mutants which supports previous reports that the effects of *BRX* and *OPS* loss of function are additive (Rodriguez-Villalon et al. 2014, Breda et al. 2017, Breda et al. 2019).

CLE45 signalling is enhanced by MAKR5 and CRN|CLV2

Recently, it was shown that CLE45/BAM3 signalling is enhanced by distinct membrane associated proteins including MEMBRANE ASSOCIATED KINASE REGULATOR5 (MAKR5), CORYNE (CRN) and CLAVATA2 (CLV2) (Depuydt et al. 2013; Hazak et al. 2017; Kang and Hardtke 2016; Rodriguez-Villalon et al. 2014, Breda et al. 2019). MAKR5 proteins are expressed in developing protophloem SEs and adjacent cells and is recruited to the plasma membrane in response to CLE45 treatment. MAKR5 accumulation is abolished in *bam3* mutants rendering it as amplifier of CLE45 signalling

downstream of BAM3 (Kang and Hardtke 2016, Hazak et al. 2017). Second-site mutations in the *MAKR5* gene can partially rescue the *brx* gap cell phenotype and *makr5* single mutants are partially resistant to CLE45 treatments (Kang and Hardtke 2016).

In the context of CLE45 signalling, protein-protein interaction was detected between BAM3 and CRN (Kang and Hardtke 2016, Hazak et al. 2017). CRN is a pseudokinase forming a heterodimer with the receptor kinase CLAVATA2 (CLV2) which stabilises BAM3 association at the membrane. Both CRN and CLV2 are expressed in most tissues in the root tip but accumulate in the vascular cylinder, and second-site mutations in *CRN* or *CLV2* substantially rescue the *brx* phenotype (Somssich et al. 2016, Hazak et al. 2017). BAM3 accumulation but not *BAM3* gene expression is significantly reduced in *crn* mutants, indicating that CRN|CLV2 heterodimers are required for full perception of CLE45 signalling. Yet, while *bam3* mutants are entirely insensitive to CLE45 treatment, *crn* and *cvp2* show only partial resistance to CLE45 (Depuydt et al. 2013; Hazak et al. 2017; Rodriguez-Villalon et al. 2014, Breda et al. 2019).

CLE26 signalling is perceived by CRN|CLV2

CLE26 is another root-active peptide involved in the suppression of phloem differentiation expressed towards the end of SE differentiation (**Figure 4**). Unlike for CLE45, the receptor recognising the CLE26 peptide is still unknown. It was shown, though, that CLE26 signalling requires CRN|CLV2 for its full perception (Hazak et al. 2017; Rodriguez-Villalon et al. 2015). In fact, it was proposed that not only CLE45 and CLE26, but perception of all root-active CLE peptides requires the CRN|CLV2 heterodimer suggesting that suppression of protophloem differentiation is a shared response of all root-active CLE peptides (Hazak et al. 2017). As OPS physically interacts with BAM3 and thus interferes with CRN|CLV2 signalling components, OPS probably also modulates signaling strength of other CLE pathways, thus extending its

role as a key antagonist and cellular insulator of CLE-mediated repression of phloem differentiation (Breda et al. 2019). Taken together, a complex molecular framework balances the timing of SE differentiation in the developing phloem strands (Rodriguez-Villalon et al. 2014, Breda et al. 2019) (**Figure 4**).

CLE25 signalling represses phloem initiation

So far, I discussed CLE peptides primarily as antagonists of SE differentiation toward the end of the meristematic zone (Hazak et al. 2017, Breda et al. 2019). However, molecular mechanisms underlying the establishment of phloem development, phloem initiation, are still largely unknown (Ren et al. 2019). Recent data suggest that the root-active CLE25 peptide is primarily involved in counteracting the initiation of phloem development in the meristematic zone (Ren et al. 2019). CLE25 is first expressed in SE/procambium stem cells (**Figure 4**) during post-embryonic root development in the RAM and is recognised by a heterodimeric receptor complex of CLE-RESISTANT RECEPTOR KINASE (CLERK) and CLV2 (CLERK|CLV2). CLERK is first expressed in SE/procambium precursor cells (**Figure 4**) and was previously reported to be a crucial component for the perception of root-active CLE peptides independent of CRN|CLV2. *clerk* mutants show an earlier appearance of developing of SEs compared to wild type (Anne et al. 2018). Conversely, transgenic plants expressing a dominant negative version of CLE25 (recognised by CLERK|CLV2) develop short roots with delayed occurrence of SEs. This delay is due to compromised periclinal divisions of SE precursor cells and discontinuous SE differentiation (Ren et al. 2019). Notably, a similar mutant phenotype led to the discovery of SUPPRESSOR OF MAX2 1 (SMAX1)-LIKE proteins SMXL3, SMXL4 and SMXL5 as central regulators and potential initiators of post-embryonic phloem formation (**Figure 4**) (Wallner et al. 2017).

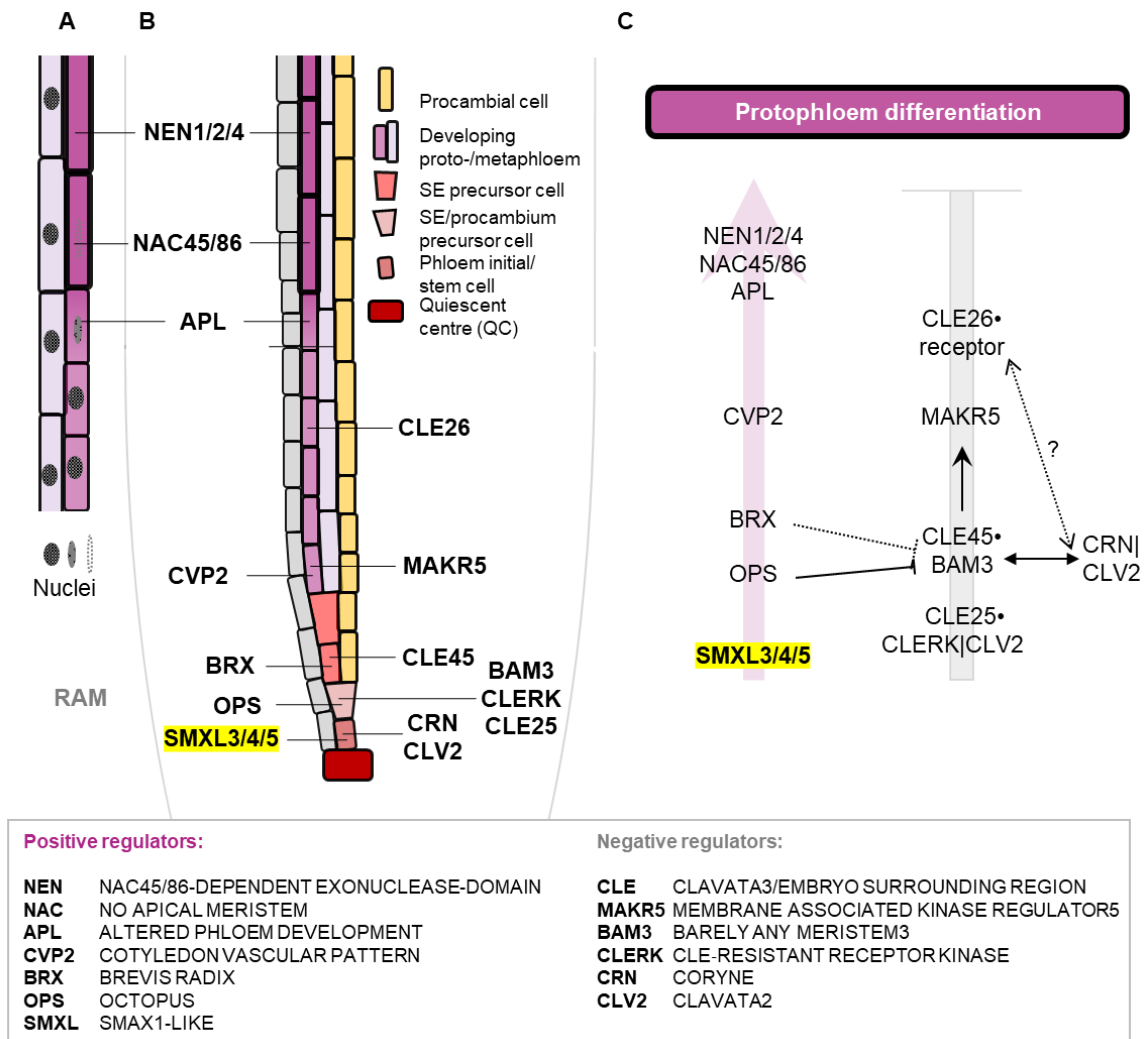


Figure 4: Early regulators of phloem development. Early phloem development is governed by sequential expression and antagonistic activities of positive and negative phloem regulators. (A) Sieve element (SE) differentiation includes cell wall remodelling (thickening) and enucleation. (B) Sequential expressions of phloem regulators correspond to different steps of protophloem strand formation in the RAM. (C) An interactive molecular network balances the timing of protophloem initiation and differentiation. OPS, BRX and CVP2 promote cell wall remodelling of developing SEs. APL, NACs and NENs promote successive enucleation of differentiating SEs. CLE peptide binding to receptor kinases and subsequent downstream signalling counteract protophloem differentiation in developing SEs. CLE45/BAM3 signalling recruits MAKR5 in developing SEs and is further enhanced by physical interaction of BAM3 with the CRN|CLV2 heterodimer. CLE26 (receptor so far unknown) signalling is also perceived by CRN|CLV2. OPS and BRX counteract CLE45/BAM3 signalling in developing SEs by physical interaction of OPS with BAM3 and transcriptional regulation of *BAM3* through *BRX*. Earlier steps of protophloem development (phloem initiation) correlate with the expression of *SMXL3/4/5*, though it is yet unknown how *SMXL3/4/5* interact with other phloem regulators. Phloem initiation is counteracted by CLE25 peptide binding to the CLERK|CLV2 heterodimer. For details, please see text. Solid lines direct interaction, dotted lines indicate indirect interaction via (unknown) downstream signalling. Single dot after CLE peptide indicates binding to receptor. (AB) Illustrations based on own data, (BC) regulators and scheme based on data published in Rodriguez-Villalon et al. 2014, Rodriguez-Villalon et al. 2015, Hazak et al. 2017, Depuydt et al. 2013, Bonke et al. 2003, Wallner et al. 2017, Anne et al. 2018, Somssich et al. 2016, Gujas et al. 2020, Kang and Hardtke 2016, Blob et al. 2018, Furuta et al. 2014).

1.5. SMXL3/4/5 – Initiators of phloem development?

1.5.1. SMXL3/4/5 genes are central promoters of phloem development

Of all known promoters of phloem development in Arabidopsis, *SUPPRESSOR OF MAX2 1 (SMAX1)-LIKE3 (SMXL3)*, *SMXL4* and *SMXL5* were discovered most recently as functionally redundant, cell-autonomous key regulators of phloem formation (Wallner et al. 2017, Wu et al. 2017, Cho et al. 2018, Wallner et al. 2020). *SMXL3/4/5* genes encode nuclear localised proteins of largely unknown function. In the RAM, *SMXL3/4/5* genes are first expressed in phloem initial cells (**Figure 4**) and subsequently in developing proto- and metaphloem strands. Unlike *SMXL4*, *SMXL3* and *SMXL5* are also expressed in procambial cells, and *SMXL3* expression extends further to phloem pole pericycle cells (Wallner et al. 2017). All combinations of double mutants of *SMXL3/4/5* genes fail to produce continuous protophloem strands of differentiated SEs concomitant with delayed or missing second periclinal cell divisions of SE precursor cells (Wallner et al. 2017). Additionally, *smxl4;smxl5* (and other combinations of) double mutants over-accumulate anthocyanins and carbohydrates in leaves and suffer from defective phloem transport from source to sink organs (Wu et al. 2017).

The same phenotype has also been discovered in mutants where *SMXL4* and *SMXL5* expression is silenced, further supporting the importance of *SMXL4* and *SMXL5* for phloem formation and function (Wu et al. 2017). In line with deficient supply of energy metabolites into sink organs, RAM size is gradually decreased in *smxl4;smxl5* double mutants as seedlings grow, resulting in short and eventually dying primary roots and the production of numerous adventitious roots of varying length. Loss of function of all three genes is lethal and plants die in the seedling state (Wallner et al. 2017). In aerial parts of Arabidopsis plants, *SMXL3/4/5* are active in the cambium and cambium-derived phloem tissues in the stem base, highlighting their importance of those genes

not only during primary, but also during secondary growth (Cho et al. 2018, Wallner et al. 2020). Still, little is known about how *SMXL3/4/5* interact with other regulators of phloem development (**Figure 4**).

1.5.2. SMXL protein structure is highly conserved

In total, Arabidopsis plants produce eight SMXL protein family members (*SMAX1*, *SMXL2/3/4/5/6/7/8*) involved in different aspects of plant physiology and development while sharing a conserved protein architecture (Stanga et al. 2013, Moturu et al. 2018, Machin et al. 2019, Soundappan et al. 2015) (**Figure 5A**). Although they were described as non-DNA binding factors with overlapping roles as transcriptional regulators during different developmental processes (Machin et al. 2019, Villaecija-Aguilar et al. 2019, Moturu et al. 2018, Walker et al. 2019), little is known about how SMXL proteins act. Structurally, SMXLs are large proteins with up to nine highly conserved domains, though only four domains have been characterised so far (Machin et al. 2019). These domains include a double caseinolytic protease ('double Clp') domain with nuclear localisation signal (Stanga et al. 2013, Liang et al. 2016), two p-loop NTPases and a short ETHYLENE-RESPONSIVE ELEMENT BINDING FACTOR (ERF)-ASSOCIATED AMPHIPHILIC REPRESSION (EAR) motif (Jiang et al. 2013, Zhou et al. 2013, Moturu et al. 2018, Walker et al. 2019). *SMAX1*, *SMXL2* and *SMXL6/7/8* proteins contain the FRGKT degron motif required for phytohormone-induced proteasomal degradation (Jiang et al. 2013, Zhou et al. 2013, Soundappan et al. 2015). Interestingly, this degron is missing in *SMXL3/4/5* proteins (**Figure 5B**) (Wallner et al. 2017, Bythell-Douglas et al. 2017, Moturu et al. 2018, Walker et al. 2019). Consequently, *SMXL3/4/5* are not subjected to proteasomal degradation upon perception of phytohormones such as exogenous karrikins (→ *SMAX1*, *SMXL2*) or endogenous strigolactones (→ *SMXL6-8*) (Wallner et al. 2017, Jiang et al. 2013, Zhou et al. 2013, Wang et al. 2015, Conn et al. 2015, Stanga et al. 2016, Liang et al. 2016, Li et al. 2016). SMXL proteins structurally resemble chaperon-like proteins most closely

related to HEAT SHOCK PROTEIN 101 (HSP101) (Soundappan et al. 2015; Stanga et al. 2013)

1.5.3. Involvement of SMXL3/4/5 proteins in transcriptional regulation

Very recently, it was revealed that the SMXL5 protein physically interacts with OBERON3 (OBE3) (Wallner 2018), a plant homeodomain (PHD)-finger protein potentially reading and binding to specifically modified histone tails which are indicative for actively transcribed or silent chromatin regions (Sanchez and Zhou 2011). Genetic interactions between *SMXL5* and *OBE3* further support an OBE3-dependent regulatory role of SMXL5 during phloem development and suggest that SMXL3/4/5 proteins act in chromatin remodelling complexes to modify gene transcription when recruited by OBE3 (Wallner et al. 2019). Other studies showed that SMXL proteins interact with the TOPLESS(TPL)-RELATED protein TPR2 in Arabidopsis (Wang et al. 2015). TPL and TPR proteins act as corepressors incapable of DNA binding that link transcriptional regulators such as histone deacetylases (HDACs) to chromatin remodelling complexes. Thereby, TPL/TPRs play a key role in hormone signalling and development (Long et al. 2006, Krogan and Long 2009, Causier et al. 2012, Martin-Arevalillo et al. 2017).

TPL/TPR corepressors were shown to interact with transcription regulators via the EAR motif conserved in these proteins (Kieffer et al. 2006, Szemenyei et al 2008, Pauwels et al 2010, Zhu et al. 2010). The EAR motif is defined by six consecutive amino acids forming the consensus sequences Leu-x-Leu-x-Leu (LxLxL), the most predominant transcriptional repression motif identified in plants so far (Ohta et al. 2001). Proteins possessing an EAR motif ('EAR repressors') coordinate responses to environmental and developmental stimuli via recruitment of corepressors involved in chromatin remodelling (Kagale and Rozwadowski 2011). As introduced before, Arabidopsis SMXL proteins all share one conserved EAR motif and therefore qualify as EAR

repressors. EAR motifs of SMXL3/4/5/6/7/8 (LxLxL/I) are most similar to the consensus sequence (LxLxL) compared to EAR motifs of SMAX1 and SMXL2 (FxLxQ/E). All are closely related to the EAR-2 motif found in the SMXL rice ortholog D53 (FxLxL) (Soundappan et al. 2015, Ma et al. 2017, Wallner et al. 2017) (**Figure 5C**). It was shown that tetramerisation of the rice TPR2 protein was mediated by the EAR-2 motif LxLxL of the SMXL rice orthologue D53 suggesting that SMXL proteins could be involved in stabilisation of TPL/TPR-nucleosome complexes and thus formation of repressive chromatin structures (Ma et al. 2017, Martin-Arevalillo et al. 2017). Therefore, a potential function of SMXL proteins in transcriptional regulating via EAR motif-mediated interaction with TPL/TPR corepressors was proposed (Smith and Li 2014, Soundappan et al. 2015, Wang et al. 2015, Liu et al. 2017, Ma et al. 2017).

Figure 5 (next page): Developmental involvement and functional domains of SMXL proteins. (A) Arabidopsis possesses eight SUPPRESSOR OF MAX2 1 (SMAX1)-LIKE (SMXL) proteins (SMAX1, SMXL2/3/4/5/6/7/8) resembling the *Arabidopsis thaliana* HEAT SHOCK PROTEIN101 (AtHSP101) and involved in different aspects of plant physiology and development. (B) SMXL protein domains are highly conserved and include a double caseinolytic protease ('double Clp') domain with nuclear localisation signal, two p-loop NTPases and a short ETHYLENE-RESPONSIVE ELEMENT BINDING FACTOR-ASSOCIATED AMPHIPHILIC REPRESSION (EAR) motif. All proteins except SMXL3/4/5 contain a FRGKT degron motif required for phytohormone-induced proteasomal degradation. (C) The EAR motif represents a predominant transcriptional repression motif in plants and is defined by six consecutive amino acids, Leu-x-Leu-x-Leu (LxLxL). EAR motifs of SMXL3/4/5/6/7/8 (LxLxL/I) are most similar to the consensus sequence (LxLxL) compared to EAR motifs of SMAX1 and SMXL2 (FxLxQ/E). All are closely related to the EAR-2 motif of the SMXL rice ortholog D53 (FxLxL). Illustration based on (A) Stanga et al. 2013, Machin et al. 2012, (B) Moturu et al. 2018, (C) Soundappan et al. 2015.

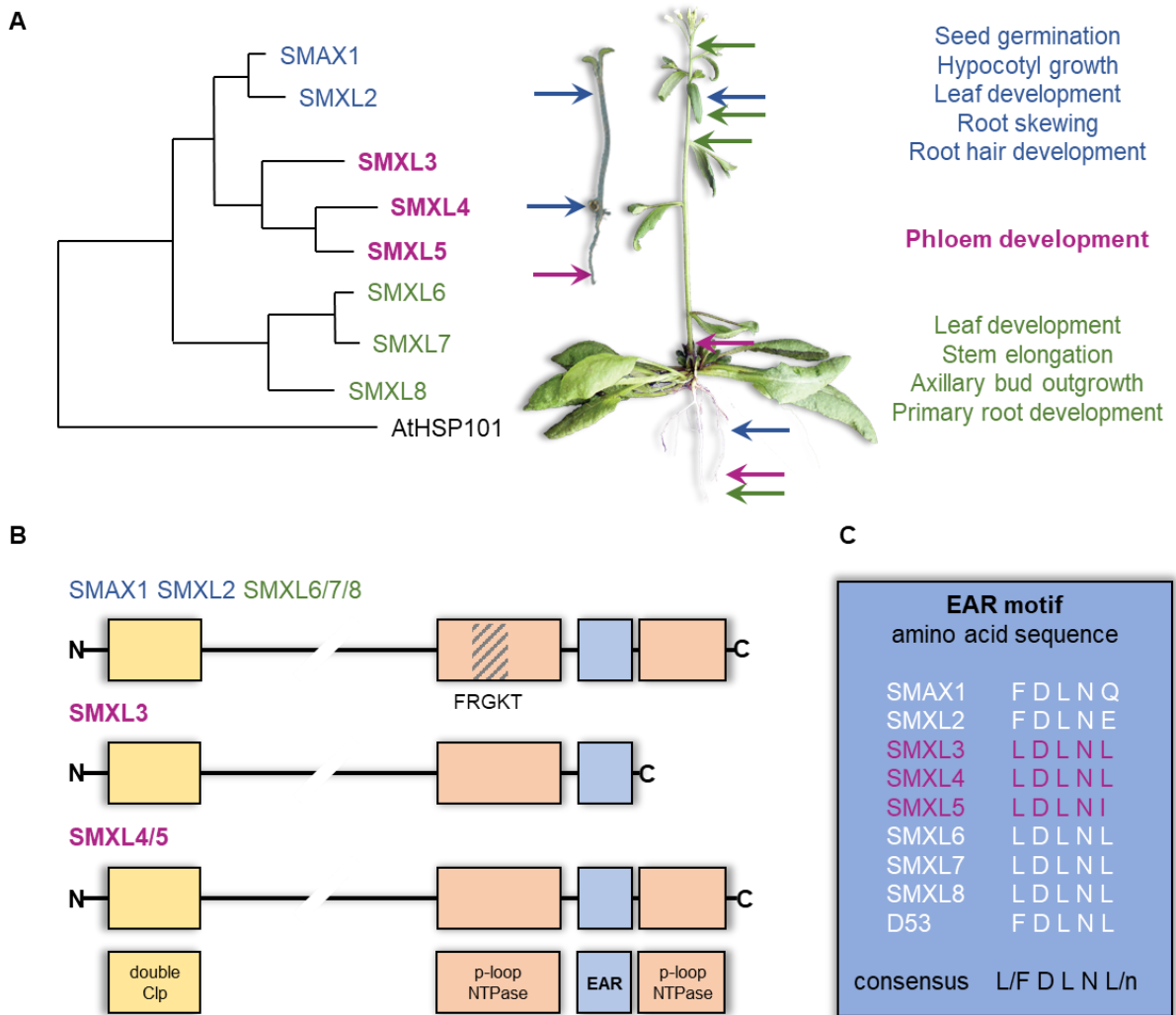


Figure 5: Developmental involvement and functional domains of SMXL proteins.

1.6. Aim and objectives

SMXL3/4/5 proteins are central regulators of phloem formation (Wallner et al. 2017, Wallner et al. 2019, Wallner et al. 2020, Cho et al. 2018). However, our knowledge on molecular mechanisms underlying *SMXL3/4/5* gene activities is still fragmentary. Moreover, the functional relevance of SMXL3/4/5 protein domains including the EAR motif is yet unclear. My aim was to characterise the mode of action of *SMXL3/4/5* during early events of phloem development in detail using *Arabidopsis* roots as a model organ for the spatiotemporal regulation of tissue formation. Working under the hypothesis that *SMXL3/4/5* are essential to initiate phloem development in the RAM, I developed three objectives:

- (1) How do *SMXL3/4/5* genes interact with other phloem regulators to promote early, post-embryonic phloem development?** To narrow down at which steps *SMXL3/4/5* genes are primarily required during phloem development, I compared gene expression patterns of known early phloem regulators (*OPS*, *BRX*, *BAM3*, *CVP2*, *APL*) in wild type and *smxl4;smxl5* double mutants and analysed the restoration of phloem development by heterologous expression of *SMXL5*. Furthermore, I investigated how *SMXL5* interacts genetically with positive regulators of phloem development (*OPS*, *BRX*) and tested the effect of CLE signalling (*CLE26*, *CLE45*) on *SMXL3/4/5*.
- (2) Is the EAR motif relevant for *SMXL5* protein function during phloem development?** To investigate whether the highly conserved EAR motif of *SMXL5* is functionally relevant to promote phloem development, I tested whether protein accumulation was altered for EAR motif-mutated *SMXL5* proteins (*SMXL5^{mEAR}*) *in planta*, and if phloem formation could be restored in *smxl4;smxl5* double mutants complemented with *SMXL5^{mEAR}* proteins. I also performed co-expression assays between *SMXL5* as a putative EAR repressor and the TPL-RELATED corepressors *TPR2* and *TPR4*.
- (3) Which other genes are functionally related to *SMXL3/4/5* in early phloem development?** Last, I aimed at identifying new genes that are functionally related to *SMXL3/4/5* during early phloem development. Therefore, I performed an ethyl methanesulfonate (EMS)-based mutagenesis of *smxl4;smxl5* double mutants to screen for genetic suppressors alleviating the phloem defects characteristic for *smxl4;smxl5* mutants.

2. Material and Methods

If not noted otherwise, methods and details concerning media, buffers and solutions used can be found in *Arabidopsis: A Laboratory manual* by Glazebrook and Weigel (2002).

2.1. Model organisms and bacterial strains

2.1.1. *Arabidopsis thaliana*

Arabidopsis thaliana (L.) Heynh. of the ecotype Columbia (Col-0) (*Arabidopsis*) was used as model plant to generate loss of function mutants and transgenic lines for subsequent analyses. Double loss of function mutants were generated by crossing. Transgenic lines were generated by molecular cloning ('GreenGate', Lampropoulos et al. 2013), plasmid amplification via *E. coli* and subsequent transformation using *Agrobacteria*, and/or by crossing of stable transgenic lines with non-transgenic plants of various genetic backgrounds. All lines described in this dissertation, their origin and reference of publication are listed in **Table 1**.

2.1.2. *Nicotiana benthamiana*

Nicotiana benthamiana (*N. benthamiana*, *Nicotiana*) plants were provided by the group of Prof. Dr. Karin Schumacher, grown in the greenhouse at the Centre for Organismal Studies (COS, Heidelberg, Germany) at approximately 25 °C, watered daily and used for transient protein expression.

2.1.3. *Escherichia coli*

Escherichia coli (*E. coli*) genotype DH5 α : F⁻, end A1, hsdR17 (rk⁻, mk⁺), gyrA96, relA1, supE44, L⁻, recA1, 80dlacZM15, Δ (lacZYA-argF)U196 (Hanahan, 1983) strains was used for molecular cloning and plasmid amplification/isolation. *E. coli* were grown at 37 °C overnight in liquid LB medium on a shaker (180 rpm to an OD600 > 1) (Innova® 44, New Brunswick Scientific Co., USA.) or plated on LB plates in an

incubator (UN110, Memmert, Büchenbach, Germany). Depending on the transformed plasmid, antibiotics (see 2.2.1) were added to the medium to select transformed (positive) colonies.

Table 1: Arabidopsis lines used in this dissertation. All plant lines are described in the plants database of the Greb lab (COS, Heidelberg, Germany).

Line	Origin	Reference
<i>APL:ER-VENUS/smxl4;smxl5</i>	This dissertation	Wallner et al. 2019
<i>APL:SMXL5-VENUS/smxl4;smxl5</i>	This dissertation	Wallner et al. 2019
<i>bam3 (bam3-2)</i>	Hardtke lab	DeYoung et al. 2005
<i>BAM3:BAM3-CITRINE/smxl4;smxl5</i>	This dissertation	Wallner et al. 2019
<i>BAM3:BAM3-CITRINE/wild type</i>	Hardtke lab	Rodriguez-Villalon et al. 2014
<i>BAM3:ER-VENUS/smxl4;smxl5</i>	This dissertation	Wallner et al. 2019
<i>BAM3:SMXL5-VENUS/smxl4;smxl5</i>	This dissertation	Wallner et al. 2019
<i>brx (brx-2)</i>	Hardtke lab	Rodrigues et al. 2009
<i>BRX:BRX-CITRINE/smxl4;smxl5</i>	This dissertation	Wallner et al. 2019
<i>BRX:BRX-CITRINE/wild type</i>	Hardtke lab	Rodriguez-Villalon et al. 2014
<i>brx;smxl5</i>	This dissertation	
<i>CVP2:ER-VENUS/smxl4;smxl5</i>	This dissertation	Wallner et al. 2019
<i>CVP2:NLS-VENUS/smxl4;smxl5</i>	This dissertation	Wallner et al. 2019
<i>CVP2:NLS-VENUS/wild type</i>	Hardtke lab	Rodriguez-Villalon et al. 2014
<i>CVP2:SMXL5-VENUS/smxl4;smxl5</i>	This dissertation	Wallner et al. 2019
<i>ops (ops-2)</i>	Hardtke lab	Truernit et al. 2012
<i>OPS:ER-VENUS/smxl4;smxl5</i>	This dissertation	Wallner et al. 2019
<i>OPS:OPS-mGFP/smxl4;smxl5</i>	This dissertation	Wallner et al. 2019
<i>OPS:OPS-mGFP/wild type</i>	Hardtke lab	Rodriguez-Villalon et al. 2014
<i>OPS:SMXL5-VENUS/smxl4;smxl5</i>	This dissertation	Wallner et al. 2019
<i>ops;smxl5</i>	This dissertation	
<i>smxl3 (smxl3-1)</i>	Greb lab	Wallner et al. 2017
<i>SMXL3:ER-YFP/wild type</i>	Greb lab	Wallner et al. 2017
<i>SMXL3:SMXL3-YFP/smxl3;smxl5</i>	Greb lab	Wallner et al. 2017
<i>smxl4 (smxl4-1)</i>	Greb lab	Wallner et al. 2017
<i>SMXL4:BRX-VENUS/smxl4;smxl5</i>	This dissertation	Wallner et al. 2019
<i>SMXL4:ER-YFP/wild type</i>	Greb lab	Wallner et al. 2017
<i>SMXL4:SMXL4-YFP/bam3</i>	This dissertation	Wallner et al. 2019
<i>SMXL4:SMXL4-YFP/ops;smxl4</i>	This dissertation	Wallner et al. 2019
<i>SMXL4:SMXL4-YFP/smxl4;smxl5</i>	Greb lab	Wallner et al. 2017
<i>SMXL4:SMXL5-VENUS/smxl4;smxl5</i>	This dissertation	Wallner et al. 2019
<i>smxl4;smxl5</i>	Greb lab	Wallner et al. 2017
<i>smxl5 (smxl5-1)</i>	Greb lab	Wallner et al. 2017
<i>SMXL5:ER-YFP/wild type</i>	Greb lab	Wallner et al. 2017
<i>SMXL5:SMXL5mEAR-VENUS/smxl4;smxl5</i>	This dissertation	
<i>SMXL5:SMXL5-YFP/ops;smxl5</i>	This dissertation	Wallner et al. 2019
<i>SMXL5:SMXL5-YFP/smxl4;smxl5</i>	Greb lab	Wallner et al. 2017
wild type	Greb lab	

2.1.4. *Agrobacterium tumefaciens*

Agrobacterium tumefaciens (*A. tumefaciens*, Agrobacteria) genotypes C58C1: Rif^R with pSoup plasmid (Tet^R) or ASE: Kan^R, Cam^R with pSoup+ plasmid (Tet^R) (Ashby 1988, Fraley 1985, Hellens 2000) were used for transformation of *Arabidopsis thaliana* or infiltration of *N. benthamiana* leaves. Agrobacteria strains were grown at 28 °C overnight in liquid YEB medium on a shaker (180 rpm to an OD₆₀₀ > 1) (Innova® 44, New Brunswick Scientific, USA) or plated on YEB plates in an incubator (UN110, Memmert, Büchenbach, Germany). Depending on the transformed plasmid and the used strain, antibiotics (see 2.2.1) were added to the medium to select transformed colonies.

2.2. Chemicals

Standard chemicals were shared between the research groups of Prof. Dr. Jan Lohmann and Prof. Dr. Thomas Greb and are listed in our common and officially accessible Dangerous Materials Registry Information System (DaMaRIS) that is provided by the University of Heidelberg, Germany.

2.2.1. Antibiotics

Antibiotics were aliquoted in microcentrifuge tubes and stored at -20 °C (except for hygromycin, stored at +4°C). Dilutions (1:1000, 1:2000) as indicated for the selection of bacteria and transformed plants are in reference to aliquoted stocks.

Antibiotics stocks:

100 mg/mL ampicillin (Sigma-Aldrich; St. Louis, USA)

25 mg/mL chloramphenicol in ethanol (Roth; Karlsruhe, Germany)

50 mg/mL kanamycin (Roth; Karlsruhe, Germany)

100 mg/mL Spectinomycin (Sigma-Aldrich; St. Louis, USA)

100 mg/mL Sulfadiazine (Sigma-Aldrich; St. Louis, USA)

10 mg/mL tetracycline in ethanol (Sigma-Aldrich; St. Louis, USA)

100 mg/mL rifampicin (Sigma-Aldrich; St. Louis, USA)

Hygromycin B (50 mg/mL, Roche; Basel, Switzerland)

2.2.2. Dyes

Ethidium bromide solution (0.025 %) was stored at room temperature in dropper bottle (Roth; Karlsruhe, Germany) and added to liquid agarose gels before performing gel electrophoresis. DirectRed23 dye (Sigma-Aldrich; St. Louis, USA) was stored at room temperature and freshly added to ClearSee solution (Kurihara et al. 2015) before performing confocal microscopy. Propidium iodide dye (Sigma-Aldrich; St. Louis, USA) was stored at 4 °C and freshly added to Schiff reagent (Truernit et al. 2008).

2.3. Standard plant work

2.3.1. Seed sterilisation and stratification

Seeds were liquid-sterilised using 70 % ethanol supplemented with 0.2 % Tween-20 (Roth; Karlsruhe, Germany) for a minimum of 15 min, washed twice with 100 % ethanol and air dried under sterile conditions. Sterile seeds were stratified in microcentrifuge tubes containing dH₂O, or on 0.5 Murashige and Skoog (MS) medium plates containing 1 % sucrose at 4 °C in the dark for a minimum of 48 hrs.

2.3.2. Plant growth and seed collection

To collect next generation seeds, seeds stratified in tubes were distributed to soil and grown on standard soil (Patzer, Sinntal-Altengronau, Germany) in growth chambers under long day (LD) conditions (16 h light, 8 h dark) at 21 °C for four to six weeks, then transferred to a drying chamber (constant light) for two weeks before collection.

Plates containing stratified seeds were transferred to growth chambers with LD conditions and grown vertically for up to 5 days, depending on the experiment.

2.3.3. Genomic DNA isolation

For gDNA isolation, rosette leaves were collected in 2 mL microcentrifuge tubes containing glass beads and placed in liquid nitrogen immediately. Next, leave tissue was disrupted by placing the tubes in frozen racks and grinding the material for 30-45 sec using the TissueLyser II (Qiagen, Venlo, Netherlands). 300 μ L extraction buffer was added to the grinded material, tubes were inverted several times and centrifuged for three min at room temperature at maximal speed. The supernatant was transferred into a new microcentrifuge tube containing 300 μ L isopropanol, inverted several times and centrifuged at maximal speed at room temperature for five min. The supernatant was discarded, and the pellet washed with 500 μ L 70 % ethanol for 10-15 min. The pellet was dried for at least one hour at room temperature and dissolved in 150 μ L 1x TE buffer by incubation at 65 °C for 10 min while shaking. Samples were stored at 4 °C if genotyping was performed within 24 hrs, otherwise at -20 °C.

2.3.4. Genotyping

Genotyping was performed with 5 μ L of gDNA dissolved in 1x TE buffer using the Taq DNA Polymerase (recombinant) kit (Thermo-Scientific; Waltham, USA), or the JumpStart REDTaq ReadyMix kit (Sigma-Aldrich, St. Louis, USA). PCRs and thermocycler settings were set up as recommended by the manufacturer. Genotyping primers were designed using CLC Main Workbench 7 (CLC Bio Qiagen, Aarhus, Denmark). For Open Reading Frame (ORF) amplification from cDNA, "ACTA" sequences were added to the 5' prime end to allow restriction of PCR products by DNA restriction enzymes at added recognition sites. Primers used for mutant genotyping are listed in **Table 2**.

Table 2: Primers used for mutant genotyping in this dissertation. All primers are described in the primers database of the Greb lab (COS, Heidelberg, Germany).

Used for	Primer names	Primer sequence (5' → 3')
<i>bam3</i>	bam3-LP	CTGCAACTTCTTCTCCGTTTG
	bam3-RP	GATTCCTTCGAAACTCGGATC
<i>brx</i>	brx-RP	GTCAGTGTTTGCTTCCTCTCTATG
	brx-LP	TATTCCTTGTCTAGGTAAGAATCC
	brx insert	TGATCCATGTAGATTTCCCGGACATGAA
<i>ops</i>	ops-RP	TCTTCCTCTAAAAAGCCTCCG
	ops-LP	CACACCGTTGGTTTGGTTAAC
<i>SALK insert</i>	SALK-LBa1	TGGTTCACGTAGTGGGCCATCG
<i>smx14</i>	smx14-LP	TTGAAGCCATGGAAGAATCTG
	smx14-RP	ACAAAGAACAATGCGGTCAAG
<i>smx15</i>	smx15-LP	TGTCTCATTGAAGCCAAAACC
	smx15-RP	AATGGTGCAAGAATTCTGACG

2.3.5. Agarose gel electrophoresis

Agarose was melted in 1x TAE using a conventional microwave. To visualize DNA bands, one drop ethidium bromide solution 0.025 % in dropper bottle per 25 mL agarose solution was added and the gel was solidified in a gel tray with an appropriate comb. The percentage of agarose ranged between 0.5 and 2 % depending on the experiment and expected DNA fragment size. The electrophoresis was run in 1x TAE at 110 V for 25 min and DNA bands were visualized using a UV Transilluminator (VWR International, Darmstadt, Germany).

2.3.6. Infiltration of *Nicotiana benthamiana*

In preparation for infiltrating *Nicotiana* leaves, single *Agrobacterium* (C58C1) colonies were picked from YEB plates and incubated in 3 μ L of liquid YEB containing rifampicin (1:2000), tetracycline (1:2000) and spectinomycin (1:2000) antibiotics at 28 °C for up to 24 hrs until the mixture was no longer transparent. Alternatively, *Agrobacterium* frozen in glycerol were added to the medium and incubated in the same way. Next, each preculture was added to 10 mL YEB containing the same antibiotics and incubated overnight at 28 C while shaking. Cultures with OD₆₀₀ of 1-1.5 were centrifuged at 4000 rpm for five min at room temperature and the pellet was resuspended in 5 mL induction

buffer (Stock: 10 mM MES pH 5.5, 10 mM MgSO₄, 150 µM acetosyringone). After mixing Agrobacteria carrying the construct of interest with Agrobacteria expressing *35S:P19* in a 1:2 ratio, cultures were incubated at room temperature in the dark for 2-3 hrs (Voinnet et al. 2003; Scholthof 2006). Four week-old *Nicotiana* leaves were infiltrated with Agrobacteria cultures of desired combinations using a 1 ml syringe (Becton Dickinson S.A., Madrid, Spain) and infiltrated leaves were harvested and imaged (Nikon A1, Nikon Instruments, Tokyo, Japan) for transient gene expression three days after infiltration.

2.4. Generation of new transgenic lines

2.4.1. Molecular cloning (GreenGate cloning)

All constructs generated in this dissertation were cloned using the GreenGate (GG) system (Lampropoulos et al. 2013) with corresponding, empty entry vectors (*pGGA000-pGGF000*) and the destination vector *pGGZ003* using the restriction enzyme FastDigest (FD) Eco31I (Thermo-Scientific, Waltham, USA).

Primer design and gene cloning: In preparation for entry module creation, genes of interest were amplified and 5'-flanked with Eco31I enzyme recognition sites and GG module (*pGGA-pGGF*) specific, four-base sequences in a PCR reaction using correspondingly designed primers (**Table 3**) and the Phusion High-Fidelity DNA Polymerase (Thermo-Scientific; Waltham, USA). Entry module-specific primers were designed using CLC Main Workbench 7 (CLC Bio Qiagen, Aarhus, Denmark). PCR products were separated by agarose gel electrophoresis, exercised based on the expected band length using a UV Transilluminator (VWR International, Darmstadt, Germany) and purified using the Wizard® SV Gel and PCR Clean-Up System (Promega, Madison, USA) for gel purification.

Table 3: Primers used for gene cloning in this dissertation. All primers are described in the primers database of the Greb lab (COS, Heidelberg, Germany).

Used for	Primer name	Primer sequence (5' → 3')
<i>pNT9</i>	pCVP2-for	AACAGGTCTCAACCTCACAACTACCTAACTGATG
	pCVP2-rev	AACAGGTCTCATGTTTGTGCTTCTTCTCTGCAAG
<i>pNT18</i>	TPR4-CDS-for	AACAGGTCTCAGGCTCAATGTCGTCACTCAGCAGAG
	TPR4-CDS-ref	AACAGGTCTCACTGATCCCCTCGGTTGTTGATCTGAC
<i>pNT19</i>	TPR2-CDS-for	AACAGGTCTCAGGCTCAATGTCGTCTTTG
	TPR2-CDS-rev	AACAGGTCTCACTGATCCCCTTTGAATCTG
<i>pNT42</i>	pSMXL4-for	AACAGGTCTCAACCTACCATGTCGAACCCTCCAATTG
	pSMXL4-rev	AACAGGTCTCATGTTTCAAAAACCCACCTTAAATC
<i>pNT48</i>	pBAM3-for	AACAGGTCTCAACCTGGTGGTTGGAGATG
	pBAM3-rev	AACAGGTCTCATGTTTGTAAACATCAGAAAAATAAAAAAC
<i>pNT51</i>	pOPS-for	AACAGGTCTCAACCTCAATGATGAATTATACTTACGTGGG
	pOPS-rev	AACAGGTCTCATGTTGACGGGAAATGGTGGTTAATC
<i>pNT71</i>	BRX-CDS-for	AACAGGTCTCAGGCTCAATGTTTTCTTGCATAGCTTG
	BRX-CDS-rev	AACAGGTCTCACTGAGAGGTAAGTGTGTTTGTATTCTC

Entry vector creation: Purified gene fragments and empty entry vectors were digested separately using the FD Eco31I enzyme, then purified using the QIAquick PCR Purification Kit (Qiagen, Venlo, Netherlands). Ligation was performed with a ratio of 5:1 (insert:vector) as calculated by the NEBioCalculator (<https://nebiocalculator.neb.com/#!/ligation>) using the T4 DNA Ligase (Thermo-Scientific; Waltham, USA). After heat inactivation for 20 min at 65 °C, plasmids were amplified using chemically competent *E. coli* (DH5 α) growing on ampicillin (1:2000) containing LB plates, isolated using the QIAprep Spin Miniprep Kit (Qiagen, Venlo, Netherlands), test-digested using individual combinations two or more FD enzymes, and send for Sanger sequencing (Eurofins, Ebersberg, Germany). Entry modules are listed in **Table 4**.

Destination vector creation: To generate the final vector construct, entry modules and the empty destination vector were added to the same reaction mix including ATP, T4 DNA ligase and the FD Eco31I enzyme, and combined to one destination module via the GreenGate reaction (Lampropoulos et al. 2013). Another ligation and heat inactivation step followed the reaction to increase the efficiency. Plasmids were amplified using competent *E. coli* (DH5 α) growing on spectinomycin (1:1000) containing LB plates, then re-plated on either spectinomycin or ampicillin containing LB

plates to test for false-positive colonies. Transformed (positive) colonies were isolated using the QIAprep Spin Miniprep Kit (Qiagen, Venlo, Netherlands). Destination modules were test digested using individual combinations two or more FD enzymes and send for Sanger sequencing (Eurofins , Ebersberg, Germany). Destination vectors are listed in **Table 5**.

Table 4: Entry vectors cloned and used in this dissertation. *pNT* entry vectors were created in this dissertation. Entry vectors created by others and used for destination vector creation are also listed including their origin and reference of publication. All plasmids are described in the plasmid database of the Greb lab (COS, Heidelberg, Germany).

Entry vector	Construct	Origin	Reference
<i>pD00587</i>	mVENUS	Schumacher lab	
<i>pDS34</i>	pGGA004	Jan Lohmann lab	Lampropoulos et al. 2013
<i>pGGA006</i>	pUBC10	Jan Lohmann lab	Lampropoulos et al. 2013
<i>pGGC015</i>	mCherry	Jan Lohmann lab	Lampropoulos et al. 2013
<i>pGGD007</i>	linker-NLS	Jan Lohmann lab	Lampropoulos et al. 2013
<i>pGGE009</i>	UBC10 terminator	Jan Lohmann lab	Lampropoulos et al. 2013
<i>pGGF007</i>	KanR	Jan Lohmann lab	Lampropoulos et al. 2013
<i>pNT9</i>	pCVP2	This dissertation	Wallner et al. 2019
<i>pNT18</i>	TPR4	This dissertation	
<i>pNT19</i>	TPR2	This dissertation	
<i>pNT42</i>	pSMXL4	This dissertation	Wallner et al. 2019
<i>pNT48</i>	pBAM3	This dissertation	Wallner et al. 2019
<i>pNT51</i>	pOPS	This dissertation	Wallner et al. 2019
<i>pNT71</i>	BRX	This dissertation	Wallner et al. 2019
<i>pVL101</i>	pSW394	Wolf lab	
<i>pVL11</i>	pGGZ003	Jan Lohmann lab	Lampropoulos et al. 2013
<i>pVL119</i>	mCherry (pGGD003)	Jan Lohmann lab	Lampropoulos et al. 2013
<i>pVL20</i>	SMXL5 terminator	Greb lab	Schuerholz, Lopez-Salmeron et al. 2018
<i>pVL25</i>	APL terminator	Greb lab	Schuerholz, Lopez-Salmeron et al. 2018
<i>pVL28</i>	pSMXL5	Greb lab	Schuerholz, Lopez-Salmeron et al. 2018
<i>pVL35</i>	APL	Greb lab	Schuerholz, Lopez-Salmeron et al. 2018
<i>pVL50</i>	B-Dummy (pGGB003)	Jan Lohmann lab	Lampropoulos et al. 2013
<i>pVL51</i>	D-Dummy (pGGD002)	Jan Lohmann lab	Lampropoulos et al. 2013
<i>pVL53</i>	SulfR (pGGF012)	Jan Lohmann lab	Lampropoulos et al. 2013
<i>pVL63</i>	Signal Peptide (ER)	Jan Lohmann lab	Lampropoulos et al. 2013
<i>pVL66</i>	Rbcs term (pGGE001)	Jan Lohmann lab	Lampropoulos et al. 2013
<i>pVL69</i>	mGFP (pGGD001)	Jan Lohmann lab	Lampropoulos et al. 2013
<i>pVL70</i>	YFP/VENUS (pGGC023)	Greb lab	Schuerholz, Lopez-Salmeron et al. 2018
<i>pVL71</i>	HDEL	Jan Lohmann lab	Lampropoulos et al. 2013

Table 5: Destination vectors cloned in this dissertation. Respective entry vectors are listed in **Table 4**. All plasmids are described in the plasmids database of the Greb lab (COS, Heidelberg, Germany).

Destination vector	Entry vectors (modules)						
	A	B	C	D	E	F	Z
<i>APL:ER-VENUS</i> (pNT68)	pVL35	pVL63	pVL70	pVL71	pVL66	pVL53	pVL11
<i>APL:SMXL5-VENUS</i> (pNT10)	pVL35	pVL50	pVL84	pD00587	pVL25	pVL53	pVL11
<i>BAM3:ER-VENUS</i> (pNT50)	pNT48	pVL63	pVL70	pVL71	pVL66	pVL53	pVL11
<i>BAM3:SMXL5-VENUS</i> (pNT49)	pNT48	pVL50	pVL84	pD00587	pVL66	pVL53	pVL11
<i>CVP2:ER-VENUS</i> (pNT69)	pNT9	pVL63	pVL70	pVL71	pVL66	pVL53	pVL11
<i>CVP2:SMXL5-VENUS</i> (pNT16)	pNT9	pVL50	pVL84	pD00587	pVL66	pVL53	pVL11
<i>OPS:ER-VENUS</i> (pNT53)	pNT51	pVL63	pVL70	pVL71	pVL66	pVL53	pVL11
<i>OPS:SMXL5-VENUS</i> (pNT52)	pNT51	pVL50	pVL84	pD00587	pVL66	pVL53	pVL11
<i>SMXL4:BRX-VENUS</i> (pNT72)	pNT42	pVL50	pNT71	pD00587	pVL66	pVL53	pVL11
<i>SMXL5:SMXL5^{mEAR}-VENUS</i> (pNT3)	pVL28	pVL50	pVL96	pD00587	pVL20	pVL53	pVL11
<i>35S:SMXL5^{mEAR}-VENUS</i> (pNT55)	pDS34	pVL50	pVL96	pD00587	pVL66	pVL53	pVL11
<i>35S:TPR2-mGFP</i> (pNT32)	pDS34	pVL50	pNT19	pVL69	pVL66	pVL53	pVL11
<i>35S:TPR4-mGFP</i> (pNT33)	pDS34	pVL50	pNT18	pVL69	pVL66	pVL53	pVL11

2.4.2. Transformation of *E. coli*

Chemically competent *E. coli* (DH5 α) were thawed on ice before adding ligation mixes containing entry or destination vectors and incubation on ice for 15-20 min. For re-transformation, 1 μ L of previously purified plasmids was added to the bacteria. Bacteria were heat shocked in a water bath at 42 °C for 45 sec, placed on ice for two min, then 800 μ L of liquid SOC medium was added. After incubation for 1 hour at 37 °C while shaking, bacteria were distributed on ampicillin (entry vectors) or spectinomycin (destination vectors) containing LB plates using glass beads and incubated overnight (for 8-10 hrs) at 37 °C in the dark. Single colonies were picked and incubated overnight in 3 μ L liquid LB containing antibiotics at 37 °C, shaking, before continuing with plasmid

isolation, test digestion and Sanger sequencing. In the case of destination modules, colonies picked from spectinomycin plates were re-streaked on either spectinomycin or ampicillin plates first to detect false positive colonies before continuing with overnight incubation.

2.4.3. Transformation of *A. tumefaciens*

Agrobacteria (C58C1) were thawed on ice before mixing with 500 L of purified plasmids, incubated on ice for five min, frozen in liquid nitrogen for five min, and heat shocked for five min at 37 °C while shaking. 800 µL of liquid YEB medium was added and the agrobacteria were incubated for 2-4 hrs at 28 °C while shaking. 200 µL of the bacterial solution were spread on YEB plates containing rifampicin (1:2000), tetracycline (1:2000) and spectinomycin (1:2000) and grown at 28 °C in the dark for three days until colonies appeared.

To generate glycerol stocks, individual colonies were picked and grown in 10 µL liquid YEB containing the same antibiotics for up to 24 hrs until the medium was no longer transparent. 250 µL of agrobacteria were mixed with 750 µL sterile glycerol (80-100 %), immediately frozen in liquid nitrogen and stored at -80 °C.

2.4.4. Transformation of *A. thaliana*

Transgenic Arabidopsis lines were generated using the floral dip method (Clough and Bent 1998). In preparation for stable transformation of *A. thaliana*, single Agrobacteria (C58C1) colonies were picked from YEB plates and incubated in 3 µL of liquid YEB containing rifampicin (1:2000), tetracycline (1:2000) and spectinomycin (1:2000) antibiotics at 28 °C for up to 24 hrs until the mixture was no longer transparent. Alternatively, Agrobacteria frozen in glycerol were added to the medium and incubated in the same way. Next, each preculture was added to 200 mL YEB containing the same antibiotics and incubated overnight at 28 °C while shaking. Densely grown cultures were centrifuged at 4000 rpm for 1 five min and the pellet was resuspended in 200 mL

5 % sucrose solution. Just before floral dipping, Silwet (Spiess-Urania Chemicals, Hamburg, Germany) was added to a final concentration of 0.02 % and flowering Arabidopsis plants were dipped into the bacterial solution for five min, then covered by plastic bags and incubated overnight in the dark before resumed growth of the transformed plants under LD conditions. Repeated transformation of the same plant after one week was performed to enhance the efficiency. After collecting seeds, T1 transformants were selected on 0.5 MS plates containing sulfadiazine (1:2000) and chloramphenicol (1:2000) and transferred to soil after 2 weeks.

2.5. EMS-based mutagenesis and suppressor screen

Ethyl methanesulfonate (EMS)-based mutagenesis was performed based on Page and Grossniklaus 2002. Approximately 8000 seeds of *smx14;smx15* double mutants (M0 generation) were exposed to a calculated sub-saturation level of EMS (Sigma-Aldrich, St. Louis, USA) (0.3 %) for 12 hrs. Immediately after, M1 seeds were transferred to soil and grown in the greenhouse at the Centre for Organismal Studies (COS, Heidelberg, Germany) at approximately 25 °C. Seeds of twelve M1 parental plants were pooled and collected as one family in the M2 generation resulting in 338 families for further analysis. Per analysed family, approximately 2500 seedlings were sequentially screened for seedlings with suppressed *smx14;smx15* phenotype, i.e. wild type-like primary roots indicative of restored protophloem development. Suppressors of the *smx14;smx15* phenotype were transferred to soil to analyse the M3 generation and generate backcrosses with *smx14;smx15* mutants.

2.6. CLE treatments

CLE peptides (unmodified) were obtained by custom synthesis at a 50-60 mg scale with > 85 % purity (Genscript, USA). Dried peptides were dissolved in dH₂O and aliquoted in microcentrifuge tubes to prepare 1 mM stock solutions. Aliquoted stock

solutions were stored at -20 °C. For treatments, CLE peptides were diluted in autoclaved 0.5 MS medium to a final concentration of 50 nM.

Seeds of transgenic lines were sterilised, then stratified for a minimum of 48 hrs in the dark on 0.5 MS plates containing 1 % sucrose. To induce germination and growth, plates were placed vertically in LD growth chambers for three days before transferring individual seedlings to another set of 0.5 MS plates containing 1 % sucrose (MOCK) and 50 nM of synthetic CLE45 or CLE26 peptides (CLE treatment). After 24 hrs, seedlings were fixed and cleared in preparation for confocal microscopy (see below).

Seeds of mutant lines were sterilised, then stratified for a minimum of 48 hrs in the dark on 0.5 MS plates containing 1 % sucrose (MOCK) and 50 nM of synthetic CLE45 peptides (CLE treatment). To induce germination and growth, plates were placed vertically in LD growth chambers for two or five days, depending on the following analysis, and prepared for confocal microscopy or scanned for root length measurements, respectively.

2.7. Seedling preparation for confocal microscopy

2.7.1. Signal fixation (PFA) and cell wall staining (DirectRed23) of transgenic lines

To preserve fluorescent signals, seedlings of transgenic lines were fixed in 4 % (w/v) PFA dissolved in PBS solution for one hour on ice under vacuum, then washed twice with 1x PBS solution, and cleared in ClearSee solution (Kurihara et al. 2015) for a minimum of two days at room temperature and protected from light on a slowly rocking plate.

Cleared seedlings were stained with 0.01 % (w/v) DirectRed23 dye (Sigma-Aldrich; St. Louis, USA) diluted in ClearSee solution for 30 min, then washed with ClearSee solution for a min of 30 min before continuing with confocal microscopy.

2.7.2. Cell wall staining (mPS-PI) of mutant lines

Fixation and cell wall staining via mPS-PI was performed based on Truernit et al. 2008. 2 days after germination, seedlings grown on vertical plates were fixed in a fixative of 50 % methanol and 10 % acetic acid on ice and kept at 4 °C in the dark for a minimum of 24 hrs. Seedlings were rinsed with dH₂O and incubated in 1 % periodic acid for 40 min at room temperature before being rinsed again with dH₂O and incubated in Schiff reagent (100 mM sodium metabisulfite, 0.15 N HCl) with propidium iodide (PI) at a final concentration of 100µg/mL for two hrs until plants were visibly stained. Seedlings were then transferred to microscope slides, covered with chloral hydrate solution (Stock: 4 g chloral hydrate, 1 mL glycerol, 2 mL dH₂O) and kept at room temperature over night in a closed environment. Next day, excel chloral hydrate was replaced by several drops of Hoyer's solution (Stock: 30 g gum Arabic, 200 g chloral hydrate, 20 g glycerol, 50 mL dH₂O), seedlings were covered by cover slips and left for the mounting solution to set for seven or more days before continuing with confocal microscopy.

2.8. Confocal microscopy

For confocal microscopy, the Leica TCS SP8 microscope (Leica Microsystems; Mannheim, Germany) including a 20x multi immersion objective (used for fluorescence microscopy) and 63x glycerol immersion objective (used for microscopy of mPS-PI stained mutants) was used. To visualize fluorescent proteins, the argon laser combined with HyD detectors was used while cell wall staining (DirectRed23 and mPS-PI) was visualised by the DPSS laser. YFP (yellow fluorescent protein) was excited at 514 nm and emission detected in a range of 520-540 nm, and GFP (green fluorescent protein) was excited at 488 nm and emission detected in a range of 500-575 nm. Cell walls stained with DirectRed23 and mPS-PI were excited at 561 nm (DPSS laser) and emission was detected at 590-690 nm. Images were saved and reviewed using the Leica Application Suite X (LAS X) software.

2.9. Root length measurements and Statistics

Seedlings grown on vertical plates were scanned five or seven days after germination using a commercial scanner (Epson America, Long Beach, USA). Root lengths were measured using the Simple Neurite Tracker Plugin in ImageJ 1.49d (Schindelin et al. 2012).

Statistics were performed using GraphPad Prism version 6.01 (GraphPad Software, La Jolla, USA). Means were calculated from measurements with sample sizes as indicated in the respective figure legends. Error bars represent \pm standard deviation. All analyzed datasets were prior tested for homogeneity of variances by the Levene statistic. One-way ANOVA was performed using a confidence interval (CI) of 95 % and a post-hoc Tukey test for comparisons of five or more data sets of homogenous variances. Graphs were generated in GraphPad Prism version 6.01 (GraphPad Software, La Jolla, USA).

2.10. Figures and Illustrations

Data presented in this dissertation was assembled into figures using Adobe Photoshop CS6 and Adobe Illustrator CS6 (Adobe, San Jose, USA). Illustrations and schemes were created using Adobe Photoshop CS6, Adobe Illustrator CS6 (Adobe, San Jose, USA) and Microsoft PowerPoint (Microsoft, Washington, U.S.).

3. Results

SMXL3, SMXL4 and SMXL5 proteins are central regulators of phloem development (Wallner et al. 2017, Wallner et al. 2019, Wallner et al. 2020, Cho et al. 2018), yet how *SMXL3/4/5* genes promote sieve element (SE) formation in interaction with other phloem regulators has not been studied in detail. Here, I show that *SMXL3/4/5* genes are essential to activate downstream (proto)phloem regulators in the RAM, supporting the hypothesis that *SMXL3/4/5* play a key role in promoting the initiation of protophloem development. Furthermore, my data suggest that SMXL5 protein function is independent from the ETHYLENE-RESPONSIVE ELEMENT BINDING FACTOR-ASSOCIATED AMPHIPHILIC REPRESSION (EAR) motif LxLxL, indicating that individual SMXL3/4/5 proteins do not act as canonical EAR repressors in the context of phloem development. Finally, I show that mutagenesis of yet unknown suppressor genes in *smxl4;smxl5* double mutants can restore phloem development.

3.1. *SMXL3/4/5* genes activate early phloem regulators

Previous data show that the impairment of phloem development is most pronounced in mutants without two functional *SMXL4/5* genes compared to other phloem regulators (Wallner et al. 2017). Thus, I hypothesised that *SMXL3/4/5* genes act in the initiation of protophloem development and subsequently regulate the expression of downstream genes promoting SE differentiation. To test this hypothesis, I generated transgenic lines to study gene expression of early phloem regulators in the RAM of *smxl4;smxl5* double mutants and compared them to the expression in respective wild type backgrounds using confocal microscopy. To cover the first cells that establish the phloem lineage, I used previously published transcriptional and translational reporters for SE/procambium precursor cells (*OPS:OPS-mGFP*, *BAM3:BAM3-CITRINE*), SE precursor cells (*BRX:BRX-CITRINE*) and developing protophloem cells (*CVP2:NLS-VENUS*) (Rodriguez-Villalon et al. 2014, Hazak et al. 2017). Regarding the time point, I looked at reporter activity and protophloem development in the RAM two days after

germination when root development of *smxl4;smxl5* mutants still resembles the wild type (Wallner et al. 2017). Compared to the wild type situation, reporter activity is reduced in *smxl4;smxl5* in all four cases concomitant with loss of developing protophloem SEs (**Figure 6**). More precisely, in *smxl4;smxl5* double mutants, OPS-mGFP fusion protein levels are barely detectable along the entire developing protophloem strand whereas the levels of BRX-CITRINE and BAM3-CITRINE fusion proteins are decreased but otherwise unchanged with regard to the position where they firstly appeared (**Figure 6A-C'**). *CVP2* reporter activity (nuclear VENUS protein) is decreased and appears in the RAM later in *smxl4;smxl5* than in wild type, indicating that the development of protophloem cells is delayed (**Figure 6DD'**). Notably, in wild type, I detected activities of *OPS* and *BRX* reporters already adjacent to the quiescent centre (QC) in phloem initial cells (**Figure 6E-H'**) which is earlier in development than previously reported (Rodriguez-Villalon et al. 2014). Taken together, my findings on phloem reporter gene activity in *smxl4;smxl5* double mutants support the hypothesis that early *SMXL4/5* gene activity in phloem initial cells is required for the gene activities of other phloem regulators which thereafter act downstream to regulate phloem formation. As *OPS* and *BRX* are positive regulators of phloem development and expressed as early as *SMXL3/4/5*, this observation underlined the question of how *SMXL4/5* interact genetically with either of both genes.

Figure 6 (next page): Activities of early phloem genes are reduced in *smxl4;smxl5* double mutants. (A-D') Comparison of (AA') *OPS:OPS-mGFP*, (BB') *BRX:BRX-CITRINE*, (CC') *BAM3:BAM3-CITRINE* and (DD') *CVP2:NLS-VENUS* reporter activities in (ABCD) wild type and (A'B'C'D') *smxl4;smxl5* double mutants two days after germination. Asterisks depict protophloem strands. Arrows indicate earliest detectable reporter activities in *smxl4;smxl5* double mutants. (E-H') (E-F') *OPS:OPS-mGFP* and (G-H') *BRX:BRX-CITRINE* close to the quiescent centre in (EE'GG') wild type and (FF'HH') *smxl4;smxl5*. (A-H) Arrows indicate earliest detectable activities. Cell walls are stained with DirectRed23. E'F'G'H' are without cell wall staining. n = 10. Scale bars represent 50 μ m. Data published in Wallner et al. 2019.

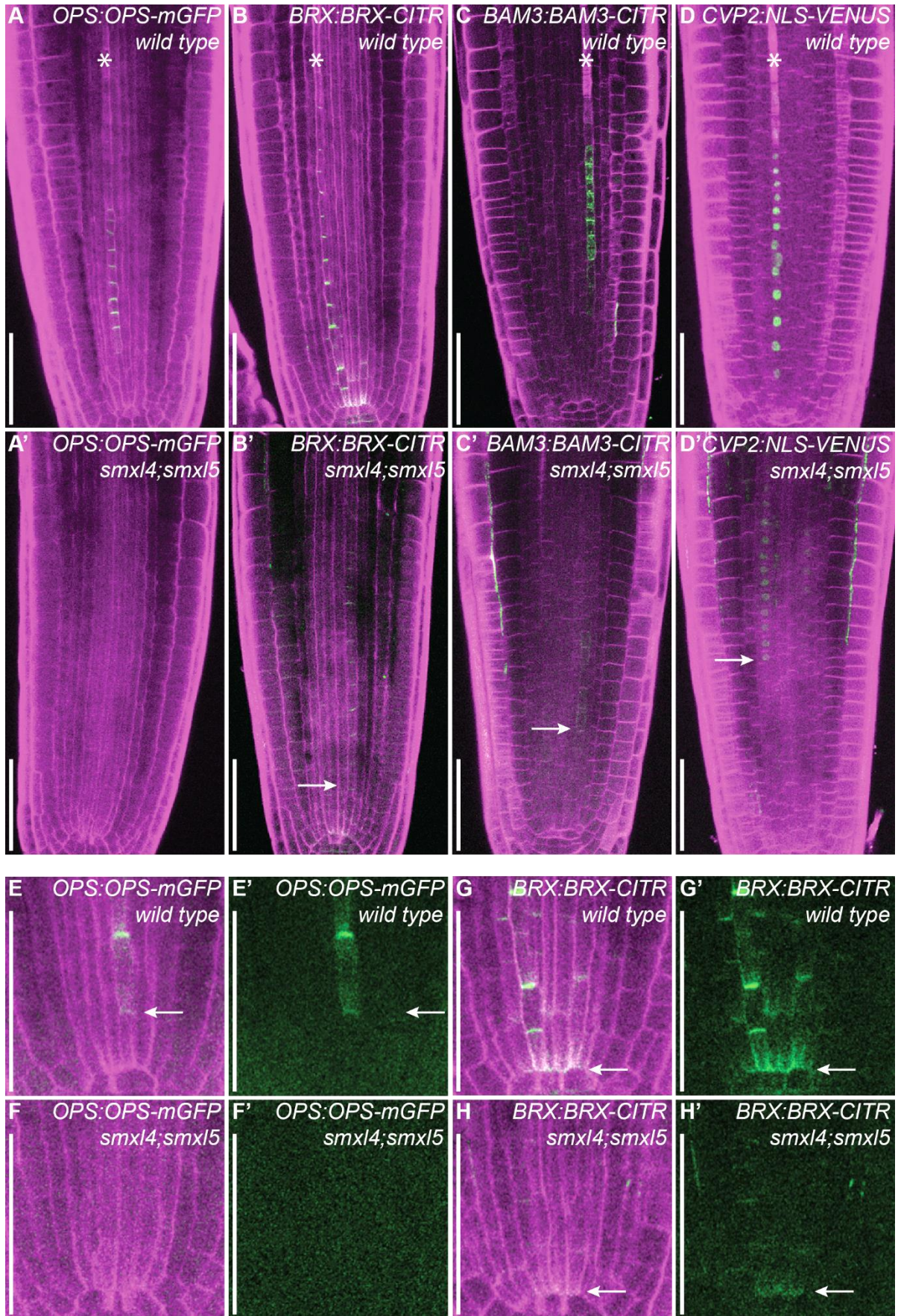


Figure 6: Activities of early phloem genes are reduced in *smx14;smx15* double mutants.

3.2. *SMXL5* conducts a different role than *BRX* and *OPS*

While performing phloem reporter analyses, I discovered that expression of *BRX* and *OPS* genes already occurred in phloem initial cells where *SMXL3/4/5* genes are also active (Wallner et al. 2017). *BRX* and *OPS* encode membrane associated proteins located polarly in rootward and shootward membranes of developing phloem cells, respectively (Scacchi et al. 2009, Truernit et al. 2012). It was shown that the combinational loss of *BRX* and *OPS* gene functions results in an increased number of gap cells compared to *brx* and *ops* single mutants and occasional loss of one protophloem strand (Breda et al. 2017). Still, phloem development in *brx;ops* double mutants is not as strongly affected as in *smxl4;smxl5* double mutants where both protophloem strands are missing (Wallner et al. 2017). To investigate how *SMXL5* interacts genetically with *BRX* and *OPS*, I generated double mutants combining *SMXL5* loss of function with loss of function in either *BRX* or *OPS*. To analyse the phenotypes of *brx;smxl5* and *ops;smxl5* double mutants, I measured primary root length five days after germination and imaged protophloem development in the RAM two days after germination using wild type, *smxl4;smxl5* and respective single mutants as references (*smxl5*, *brx*, *ops*) (Wallner et al. 2017, Breda et al. 2017, Rodriguez-Villalon et al. 2014). As shown in **Figure 7A-C**, wild type and *smxl5* single mutants are long-rooted and form two protophloem strands whereas primary roots of *smxl4;smxl5* double mutants are short and do not develop differentiated SEs. Primary roots of *brx* and *ops* single mutants are shorter than wild type roots but not as short as *smxl4;smxl5* roots and form protophloem strands with varying degrees of intermitting gap cells (**Figure 7B**). Primary roots of *brx;smxl5* and *ops;smxl5* double mutants are as reduced in length as roots of *smxl4;smxl5*. However, protophloem development in *brx;smxl5* and *ops;smxl5* double mutants differs substantially from that of *smxl4;smxl5*. In both double mutants, the impairment of SE differentiation ranges from gap cells intermitting one protophloem strand up to the loss of differentiated SEs altogether (**Figure 7BC**). For example, *brx;smxl5* phenotypes included primary roots with one or both protophloem strands

intermitted by gap cells (50 %), roots with only one continuous protophloem strand (21 %), roots with only one strand intermitted by gap cells (13 %), and roots forming no protophloem strands altogether (24 %). In *ops;smx15* double mutants, the phenotypic penetrance is even higher based on the finding that no roots develop two complete protophloem strands but only one continuous strand (26 %) or only one strand intermitted by gap cells (5 %). Most roots are lacking both protophloem strands altogether (64 %) (**Figure 7BC**). Considering that protophloem development in *smx15* single mutants appears wild type-like, my findings indicated independent effects of *SMXL5* and *BRX/OPS* genes in early protophloem development. Furthermore, protophloem development in *ops;smx15* double mutants is more severely impaired than in *brx;smx15* double mutants. As protophloem development in *ops* single mutants is also more deficient than in *brx* single mutants (**Figure 7BC**), this suggests that *OPS* gene function is more important than *BRX* to promote SE differentiation. Combined with previous findings that *OPS* gene expression is most reduced in *smx14;smx15* double mutants compared to *BRX* (**Figure 6**), this could also indicate that *OPS* activity depends more strongly on *SMXL5* (and *SMXL4*) than *BRX*.

Taken together, my analyses show that loss of *SMXL5* function in *brx* and *ops* mutant backgrounds results in a combination of an increased number of gap cells and loss of protophloem strands indicating that *SMXL5*, *BRX* and *OPS* genes conduct different roles in promoting SE differentiation. Furthermore, considering decreased *BRX* and *OPS* gene expression in *smx14;smx15* double mutants, my findings suggest that as *SMXL4/5* genes act upstream of *BRX* and *OPS* during phloem development.

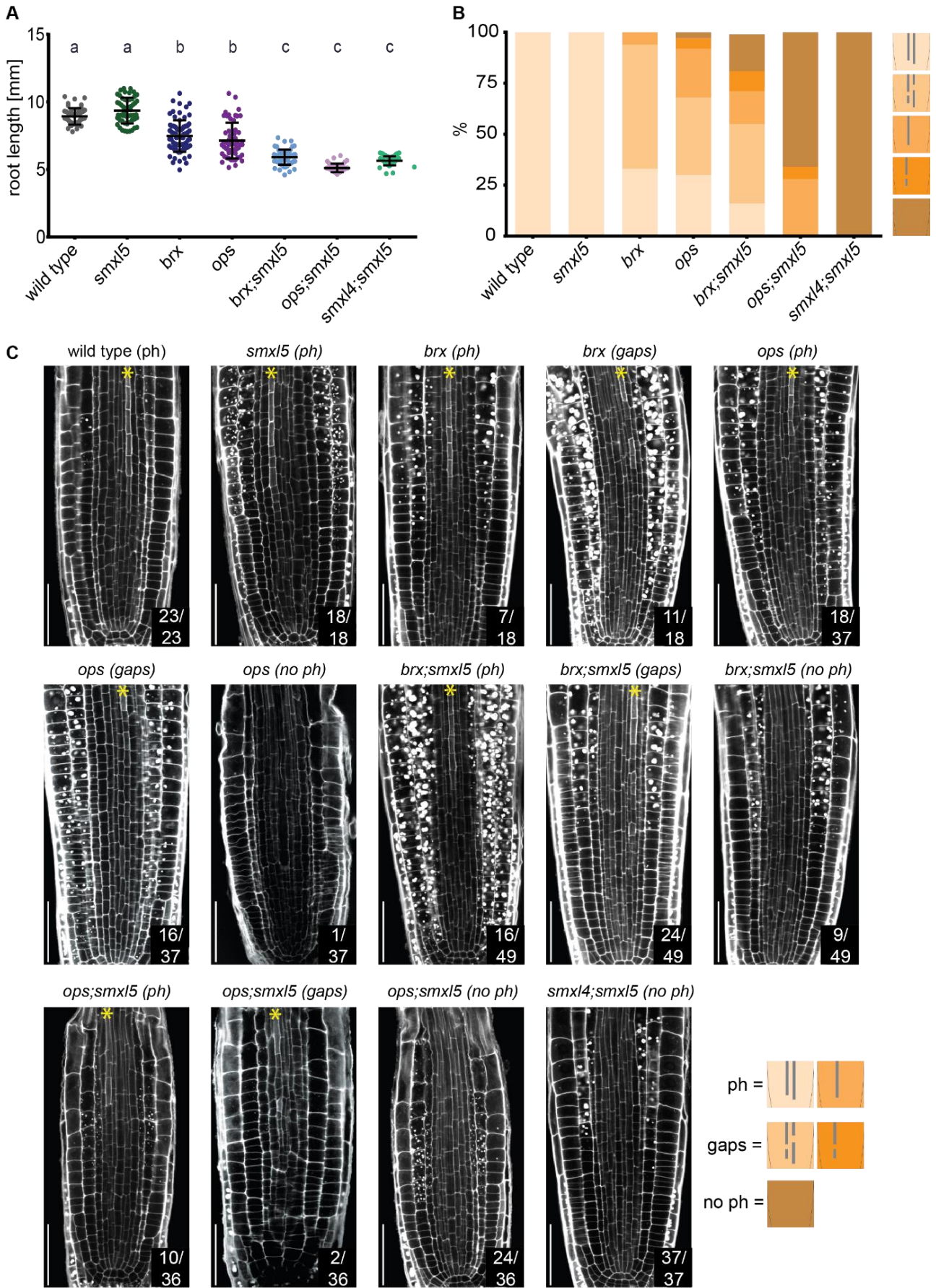


Figure 7: Genetic interaction of *SMXL5* with *BRX* and *OPS*. (See legend next page.)

Figure 7: Genetic interaction of *SMXL5* with *BRX* and *OPS*. Primary root length is decreased and protophloem defects are increased in *brx;smxl5* and *ops;smxl5* mutants compared to *brx* and *ops* single mutants. **(A)** Root length measurements five days after germination in wild type, *smxl5*, *brx*, *ops*, *brx;smxl5*, *ops;smxl5* and *smxl4;smxl5* mutants. $n = 38-76$. Statistical groups (a, b, c) determined by one-way ANOVA and post-hoc Tukey's test (95 % CI). Shown is one representative experiment of three repetitions. **(B)** Phenotypic characterisation of protophloem development two days after germination in wild type, *smxl5*, *brx*, *ops*, *brx;smxl5*, *ops;smxl5* and *smxl4;smxl5* mutants. **(C)** Protophloem development two days after germination wild type, *smxl5*, *brx*, *ops*, *brx;smxl5*, *ops;smxl5* and *smxl4;smxl5* mutants. Cell walls are stained by mPS-PI. Scale bars represent 50 μm . ph – protophloem strand(s), gaps – gap cells in protophloem strand(s). (BC) $n = 18-49$. Data published in Wallner et al. 2019.

3.3. *SMXL4/5* act upstream of *OPS* and *BRX*

So far, I showed that short primary roots and impaired protophloem development in *smxl4;smxl5* double mutants are concomitant with reduced gene expression of early phloem regulators including *OPS* (**Figure 6**). Conversely, to test whether *OPS* loss of function affected *SMXL4* and *SMXL5* activities, I compared *SMXL4/5* protein accumulation in *ops* single mutant roots with wild type-like roots of *smxl4* and *smxl5* single mutants. I used previously published *SMXL* protein marker lines (*SMXL4:SMXL4-YFP/smxl4;smxl5*, *SMXL5:SMXL5-YFP/smxl4;smxl5*, Wallner et al. 2017) as controls and cross them with *ops* mutants to generate transgenic lines expressing *SMXL4-YFP* and *SMXL5-YFP* fusion proteins in *smxl4;ops* and *smxl5;ops* backgrounds, respectively. Again, I imaged fusion protein accumulation and protophloem development in the RAM two days after germination. *SMXL4-YFP* and *SMXL5-YFP* fusion protein accumulation, subcellular localisation, and the site of the first expression in the phloem cell lineage are not altered in *ops;smxl4* and *ops;smxl5* backgrounds, respectively, compared to *smxl4;smxl5* mutants (**Figure 8**). Consequently, as the loss of *OPS* function does not affect *SMXL4/5* activity but combinational loss of *SMXL4* and *SMXL5* functions strongly reduced *OPS* activity (**Figure 6**), I conclude that *SMXL4/5* genes act upstream of *OPS* during phloem development.

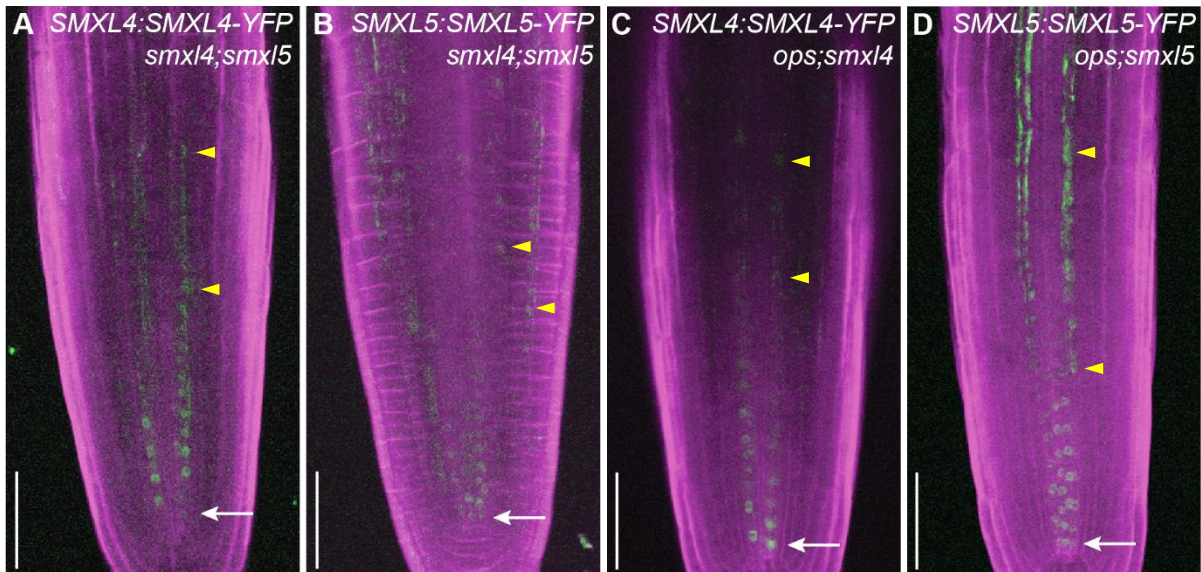


Figure 8: OPS is not required to stimulate SMXL4 and SMXL5 gene activities during early steps of protophloem development. (AB) SMXL4:SMXL4-YFP and SMXL5:SMXL5-YFP reporter activities in *smxl4;smxl5* mutants. (CD) SMXL4:SMXL4-YFP and SMXL5:SMXL5-YFP reporter activities in (C) *ops;smxl4* and (D) *ops;smxl5* mutants, respectively. (A-D) White arrows indicate reporter activities closest to the quiescent centre. Yellow arrowheads point at background signal. Cell walls are stained with DirectRed23. $n = 10$. Scale bars represent 50 μm . Data published in Wallner et al. 2019.

As for OPS, BRX expression is also reduced in *smxl4;smxl5* double mutants (Figure 6). To test whether reduction in BRX gene expression is also causative for impaired phloem development of *smxl4;smxl5* mutants, I expressed BRX (fused to VENUS) as one of the early promoters of phloem development under the SMXL4 promoter in the *smxl4;smxl5* double mutant background. Unlike SMXL3 and SMXL5 which are also expressed in phloem-associated tissues, SMXL4 promoter activity is most restricted to protophloem (and metaphloem) strands (Wallner et al. 2017). I found that the BRX-VENUS fusion protein expressed under the SMXL4 promoter restores root length and SE differentiation in *smxl4;smxl5* as well as the control (SMXL4:SMXL4-YFP/*smxl4;smxl5*, Wallner et al. 2017) (Figure 9ABG). These findings support the hypothesis that reduced BRX activity is one cause for impaired protophloem development in *smxl4;smxl5* double mutants, and that BRX acts downstream of SMXL4/5.

In short, my findings indicate that *SMXL5*, *BRX* and *OPS* regulate different steps of protoxylem development with *SMXL4/5* genes acting upstream of both *OPS* and *BRX*. On the other hand, *OPS* gene activity does not affect *SMXL4/5* activity during initial steps of xylem development.

3.4. *SMXL5* expression in developing SEs restores xylem development

As shown in **Figure 6**, *SMXL4/5* gene activities in xylem initial cells are required for gene expression of subsequent xylem regulators such as *OPS* and *BRX* (xylem initial cells), *BAM3* (SE/procambium precursor cells) and *CVP2* (developing SEs). Being expressed latest in this sequence of developmental steps, *CVP2* encodes a phosphoinositide-5-phosphatase that promotes cell wall remodelling by regulating the timing of SE differentiation (Rodriguez-Villalon et al. 2015). Although *smxl4;smxl5* double mutants develop *CVP2* expressing cells (**Figure 6**), differentiation into SEs with thickened cell walls is missing in those mutants. These findings suggest that both xylem initiation and timing of SE differentiation depend on *SMXL4/5* gene activity.

To investigate at which developmental step *SMXL5* activity is required to rescue SE differentiation, I generated transgenic lines expressing the *SMXL5*-VENUS fusion protein in the *smxl4;smxl5* background under the control of promoters of different xylem regulators. These promoters included *pSMXL4* and *pOPS* (xylem initial cells), *pBAM3* (SE/procambium precursor cells), *pCVP2* (early developing SEs) and *pAPL* (late developing SEs), thereby covering all sequential steps of early xylem development. Additionally, I generated promoter reporter lines expressing VENUS localised to the endoplasmic reticulum (ER) under the control of the same aforementioned promoters in the *smxl4;smxl5* background. I found that under the control of *pSMXL4*, *pOPS*, *pBAM3*, and *pCVP2*, expression of *SMXL5*-VENUS is sufficient to restore root length and SE differentiation in *smxl4;smxl5* (**Figure 9A-E**). This is in line with the observation that reporter signals (VENUS) of the same promoters

are detectable in *smxl4;smxl5* double mutants (**Figure 9H-J**). On the contrary, SMXL5-VENUS expressed under the control of the *APL* promoter does not result in root length restoration in *smxl4;smxl5*, nor is *APL* promoter activity detectable two days after germination (**Figure 9FK**). To ensure that the *APL* promoter was at all functional, I compared its activity in wild type as well as in *smxl4;smxl5*. In wild type, I detected VENUS signal (**Figure 10**) confirming that the *APL* promoter is functional along the protophloem strand and further suggesting that SE differentiation is arrested in *smxl4;smxl5* double mutants before *APL* expression is upregulated.

Taken together, I show that the expression of *SMXL5* not only in phloem initial and SE precursor cells, but also in early developing SEs is effective to trigger SE differentiation, resulting in restored phloem development and root growth.

Figure 9 (next page): *SMXL5* expression restores protophloem development under the control of heterologous promoters. (A) Root length measurements five days after germination. *SMXL5* expression under the control of *SMXL4*, *OPS*, *BAM3* and *CVP2* promoters restores root length to wild type root length. *BRX* expression under the control of *SMXL4* promoter restores root length to wild type root length. Statistical groups determined by one-way ANOVA and post-hoc Tukey's test (95 % CI). n = 37 – 75. (B-F) Expression of SMXL5-VENUS fusion proteins under the control of different heterologous promoters. *SMXL5* expression under the control of *SMXL4*, *OPS*, *BAM3* and *CVP2* promoters restores protophloem development. (G) Expression of the BRX-VENUS fusion protein expressed under the control of the *SMXL4* promoter restores protophloem development. (H-J) *OPS:ER-VENUS*, *BAM3:ER-VENUS* and *CVP2:ER-VENUS* reporters are active in *smxl4;smxl5* mutants. (K) *APL:ER-VENUS* reporter is not active in *smxl4;smxl5* mutants. (B-K) Cell walls are stained with DirectRed23. n = 10. Scale bars represent 50 μ m. Data published in Wallner et al. 2019.

RESULTS

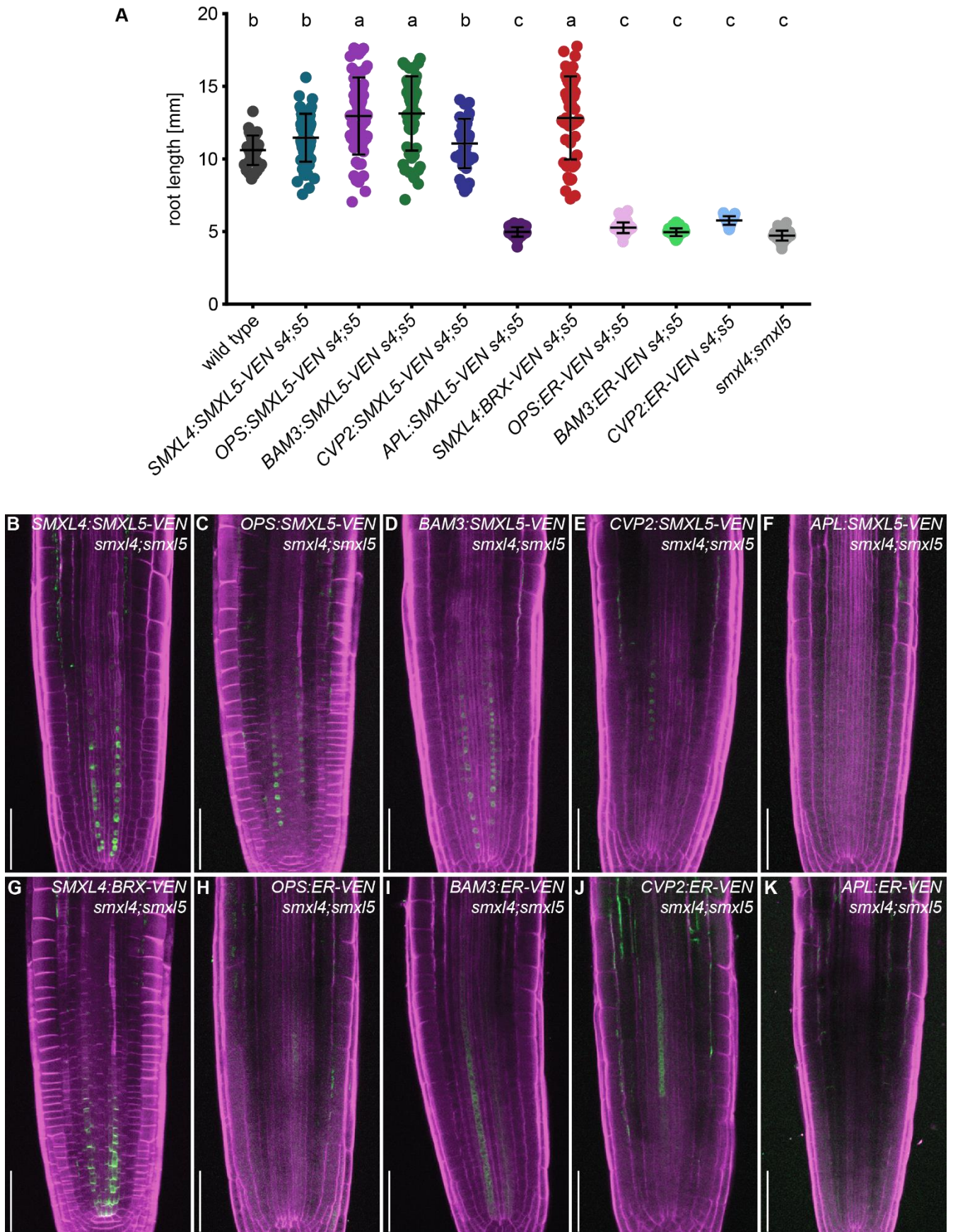


Figure 9: *SMXL5* expression restores protophloem development under the control of heterologous promoters.

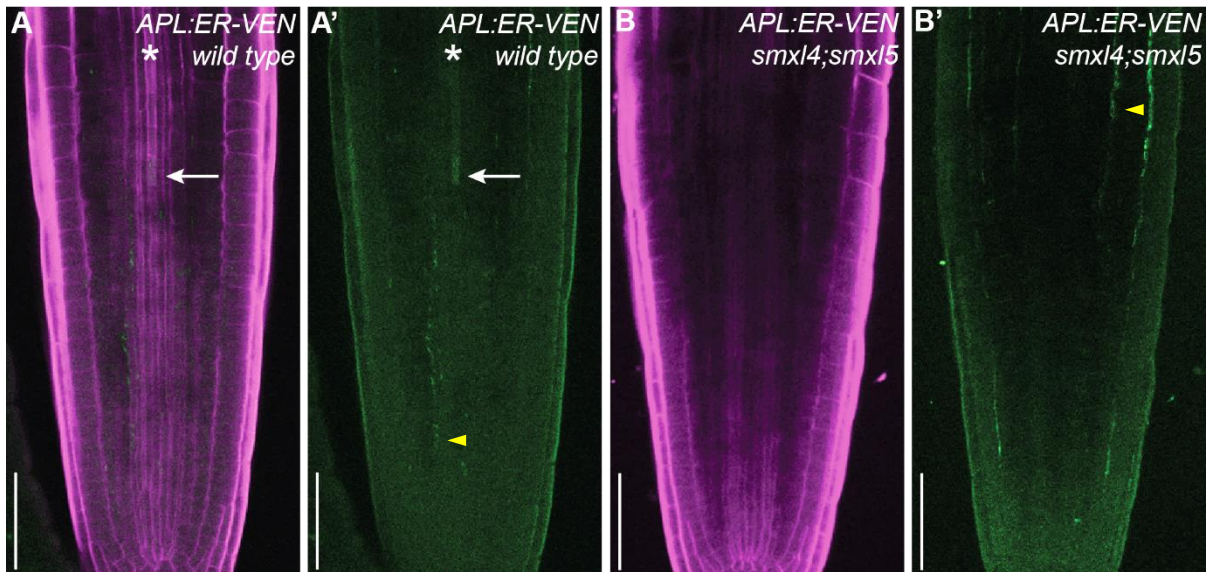


Figure 10: *APL* is not active in *smx14;smx15* double mutants. Comparison of *APL:ER-VENUS* reporter activities in (**AA'**) wild type and (**BB'**) *smx14;smx15* double mutants two days after germination. (**AB**) Asterisks depict protophloem strands. White arrows indicate earliest detectable reporter activities. Yellow arrowheads point at background signal. Cell walls are stained with DirectRed23. $n = 10$. Scale bars represent 50 μm . Data published in Wallner et al. 2019.

3.5. Enhanced CLE45/BAM3 signalling causes *smx14;smx15*-like protophloem defects

Above, I showed that the short root phenotype serves as an indication for the degree of phloem defects in mutant backgrounds such as enhanced numbers of gap cells and loss of protophloem strands (**Figure 7**). The appearance of gap cells interrupting the development of continuous protophloem strands was previously linked to increased activities of regulators suppressing protophloem development in these cells including the membrane-associated receptor-like kinase BAM3 (Depuydt et al. 2013, Rodriguez-Villalon et al. 2014, Breda et al. 2017; Kang and Hardtke 2016). BAM3 is expressed in protophloem strands and inhibits SE differentiation upon binding the root-active peptide hormone CLE45, subsequently causing reduction in root length (Depuydt et al. 2013, Rodriguez-Villalon 2015). As phloem formation is most affected in *smx14;smx15* compared to *brx*, *ops*, *brx;smx15* and *ops;smx15* mutants, I hypothesised that CLE45/BAM3 activity is strongly enhanced in developing SEs of *smx14;smx15* double

mutants, consequently causing impaired phloem formation and a dramatic reduction in root length.

To investigate whether root growth of already short *smx14;smx15* seedlings is additionally impaired by the inhibitory effect of CLE45/BAM3 signalling, I subjected *smx14;smx15* mutants to a CLE45 treatment. I placed seeds directly on medium containing the CLE45 peptide and measured root length five days after germination including wild type, *smx13*, *smx14*, *smx15*, and *bam3* mutants to the treatment. *bam3* single mutants served as controls as they are insensitive and develop long roots regardless of CLE45 (Depuydt et al. 2013). When grown on CLE45-containing medium, wild type and *smx1* single mutants are significantly shorter compared to MOCK conditions (only medium) whereas *bam3* remains long-rooted under both conditions (**Figure 11A**). Notably, primary roots of all CLE45-sensitive plants (wild type, *smx13/4/5* single mutants) are reduced to the exact same length as *smx14;smx15* double mutants under either MOCK or CLE45 conditions (**Figure 11A**). This suggested that endogenous CLE45 signalling is enhanced in *smx14;smx15* mutants compared to wild type and *smx1* single mutants.

Having done primary root length analysis as first indication of impaired phloem development, I additionally analysed SE differentiation upon CLE45 treatment in the RAM two days after germination using cell wall staining and confocal microscopy. At this earlier timepoint, the treatment did not yet alter the overall RAM architecture of wild type or mutant plants (**Figure 11B-F'**). However, upon CLE45 treatment, wild type and *smx1* single mutants did not develop differentiated SEs based on cell wall staining and thus resembled the impaired phloem development in the RAM of *smx14;smx15* double mutants (**Figure 11B'-F'**). In the case of *smx14;smx15*, no differences were observed upon CLE45 treatment compared to MOCK conditions (**Figure 11FF'**).

Together, these observations demonstrate that enhanced CLE45/BAM3 signalling causes *smxl4;smxl5*-like protophloem defects already in young seedlings (two days after germination) when overall RAM architecture and root length show no apparent effects. Furthermore, my findings show that enhanced CLE45 signalling has no further effect on *smxl4;smxl5* double mutants at the level of root architecture even after five days of treatment.

Figure 11 (next page): CLE45-treated plants resemble *smxl4;smxl5* double mutants. (A) Root length measurements five days after germination in wild type, *bam3*, *smxl3*, *smxl4*, *smxl5*, and *smxl4;smxl5* mutants. Plants were grown on 0.5 MS medium without (MOCK) or with 50 nM CLE45. *bam3* mutants are insensitive to CLE45 and were used as control. Under CLE45 conditions, wild type and *smxl* single mutant roots are as short as *smxl4;smxl5* double mutant roots. *smxl4;smxl5* root length is unaffected under CLE45 conditions. Statistical groups (a, b, c) determined by one-way ANOVA and post-hoc Tukey's test (95 % CI). n = 28-47. Shown is one representative experiment of three repetitions. **(B-F')** Protophloem development in root tips two days after germination in wild type, *smxl3*, *smxl4*, *smxl5*, and *smxl4;smxl5* mutants. Plants were grown on 0.5 MS medium without (MOCK) or with 50 nM CLE45. n = 15. (B-E) Under MOCK conditions, wild type and *smxl* single mutants developed protophloem strands (indicated by asterisks). (B'-E') Under CLE45 conditions, protophloem development is impaired in wild type and *smxl* single mutants. (F-F') *smxl4;smxl5* phloem development is impaired both under MOCK and CLE45 conditions, but the overall RAM architecture is not affected under CLE45 conditions. Scale bars represent 50 μ m.

RESULTS

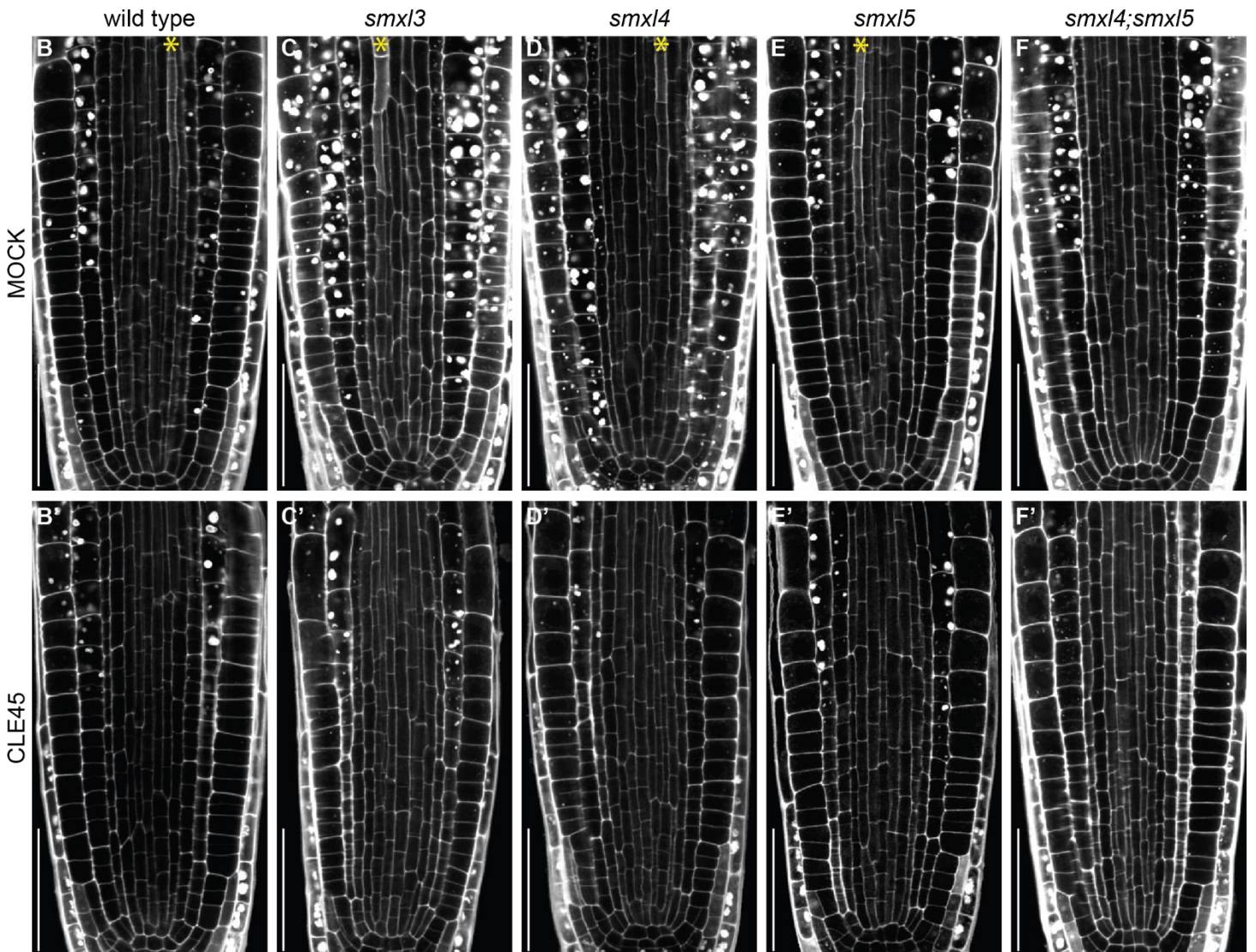
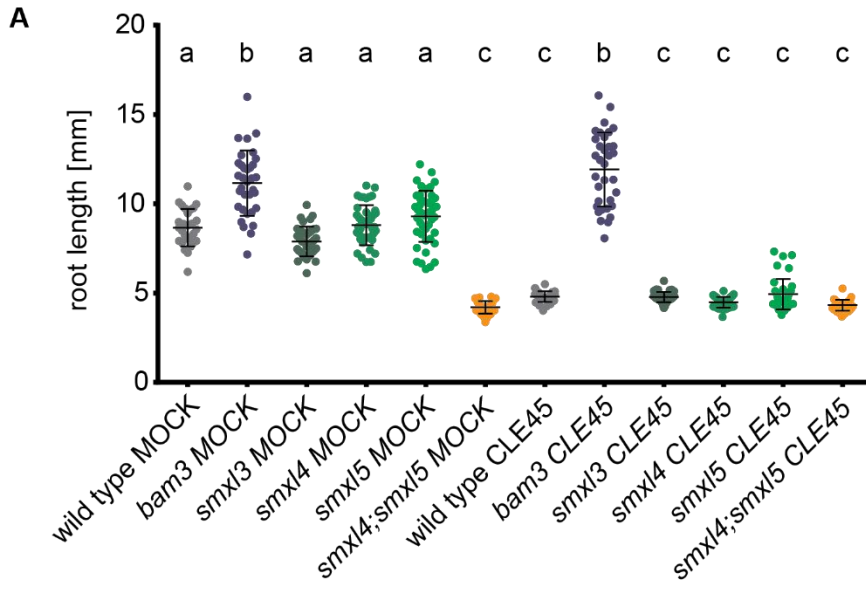


Figure 11: CLE45-treated plants resemble *smx14;smx15* double mutants.

3.6. Enhanced CLE45/BAM3 signalling is still perceived in *smx14;smx15* mutants

smx14;smx15 double mutants exhibit residual activity phloem regulators including *BRX*, *BAM3* and *CVP2* (**Figure 6**) indicating that protophloem developmental program is not entirely abolished in double mutants. However, CLE45 treatment did not result in further impairment of root growth in *smx14;smx15* (**Figure 11**). Together, these observations suggested that in the double mutant, CLE45/BAM3-mediated suppression of protophloem development outbalances those pathways that promote SE differentiation. To test the effect of exogenous CLE45 application at the cellular level, I used promoter reporter lines expressing the *CVP2:NLS-VENUS* transgene in wild type and *smx14;smx15* backgrounds to visualise developing SEs. The nuclear localised, fluorescent VENUS protein expressed under the control of *pCVP2* has repeatedly been used as reporter to monitor changes in *CVP2* promoter activity upon CLE treatments (Rodriguez-Villalon et al. 2014, Hazak et al. 2017, Anne et al. 2018). Three days after germination, I transferred wild type and *smx14;smx15* seedlings expressing the *CVP2:NLS-VENUS* transgene to either MOCK (only medium) or CLE45-containing medium and compared VENUS protein signal after 24 hrs. Under MOCK conditions, *CVP2* promoter activity was comparably low in the *smx14;smx15* background as opposed to wild type which was in line with my previous observations (**Figure 6**). After 24-hour CLE45 treatment, *CVP2* promoter activity was delayed and reduced in wild type, and reduced in *smx14;smx15* double mutants compared to respective MOCK conditions (**Figure 12**). Together with **Figure 9**, these findings show that enhanced CLE45/BAM3 signalling is still perceived in *smx14;smx15* double mutants but has no downstream effect on root length.

Figure 12 (next page): *smx14;smx15* double mutants perceive enhanced CLE45/BAM3 signalling. Comparison of *CVP2:NLS-VENUS* reporter activity expressed in developing SEs in wild type and *smx14;smx15* double mutants. Three-day old seedlings were transferred to 0.5 MS medium without (MOCK) or with 50 nM CLE45. Reporter activity (nuclear VENUS protein) was analysed after 24 hrs. (**A-B'**) Under MOCK conditions, *CVP2* activity is comparably low in *smx14;smx15* mutants compared to wild type. (**C-D'**) Under CLE45 conditions, *CVP2* activity is delayed and reduced in wild type, but also reduced in *smx14;smx15* double mutants compared to MOCK. (ABCD) Cell walls are stained with DirectRed23. n = 10. Scale bars represent 50 μ m.

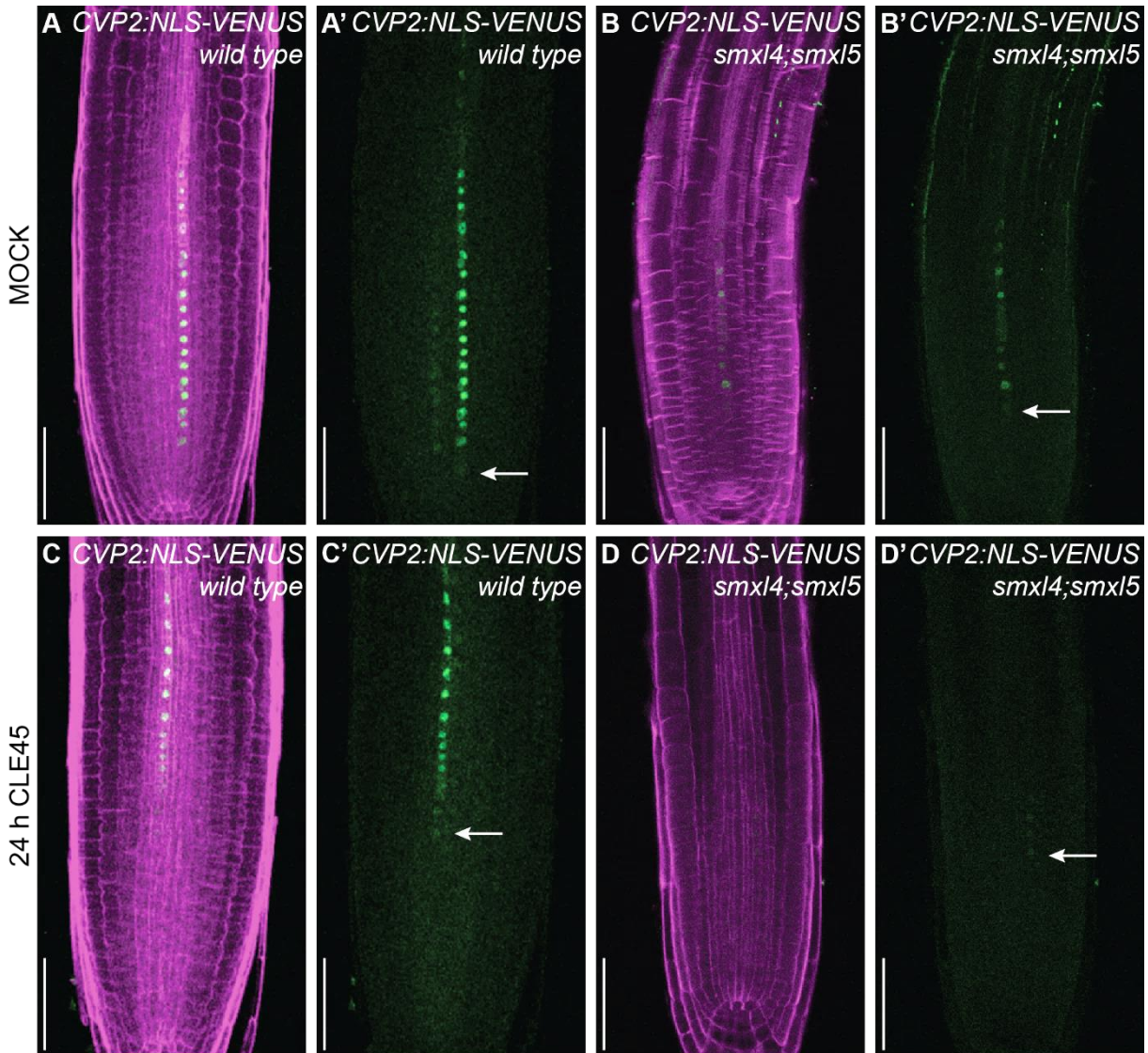


Figure 12: *smxl4;smxl5* double mutants perceive enhanced CLE45/BAM3 signalling.

3.7. SMXL3/4/5 proteins are affected by CLE45/BAM3 signalling

SE differentiation is gradually regulated by a complex molecular framework including additive and dose-dependent effects of promoters and inhibitors of protophloem development (Rodriguez-Villalon et al. 2014, Breda et al. 2019, Marhava et al. 2019). To test whether CLE45/BAM3-dependent inhibition of protophloem development had an effect on *SMXL3/4/5* promoter activity, I treated previously published *SMXL3/4/5* promoter reporter lines (*SMXL3/4/5:ER-YFP*, Wallner et al. 2017) with CLE45 three days after germination using the *CVP2* promoter reporter line as treatment control. After 24-hour CLE45 treatment, seedlings were fixed and imaged to monitor changes

in *SMXL3/4/5* promoter activity based on the ER-localised, fluorescent YFP protein. As a result, YFP signal was detectable in all three reporter lines under MOCK conditions and did not reveal apparent differences in strength or distribution upon CLE45 treatment (**Figure 13B-D'**). In contrast, VENUS protein signal driven by the *CVP2* promoter was reduced in strength and delayed along the protophloem strand upon CLE45 treatment (**Figure 13AA'**) confirming that the treatment had worked. Based on fluorescent reporter proteins, these results suggest that *SMXL3/4/5* promoter activities are not affected by CLE45/BAM3 signalling, indicating that *SMXL3/4/5* act upstream of CLE45/BAM3.

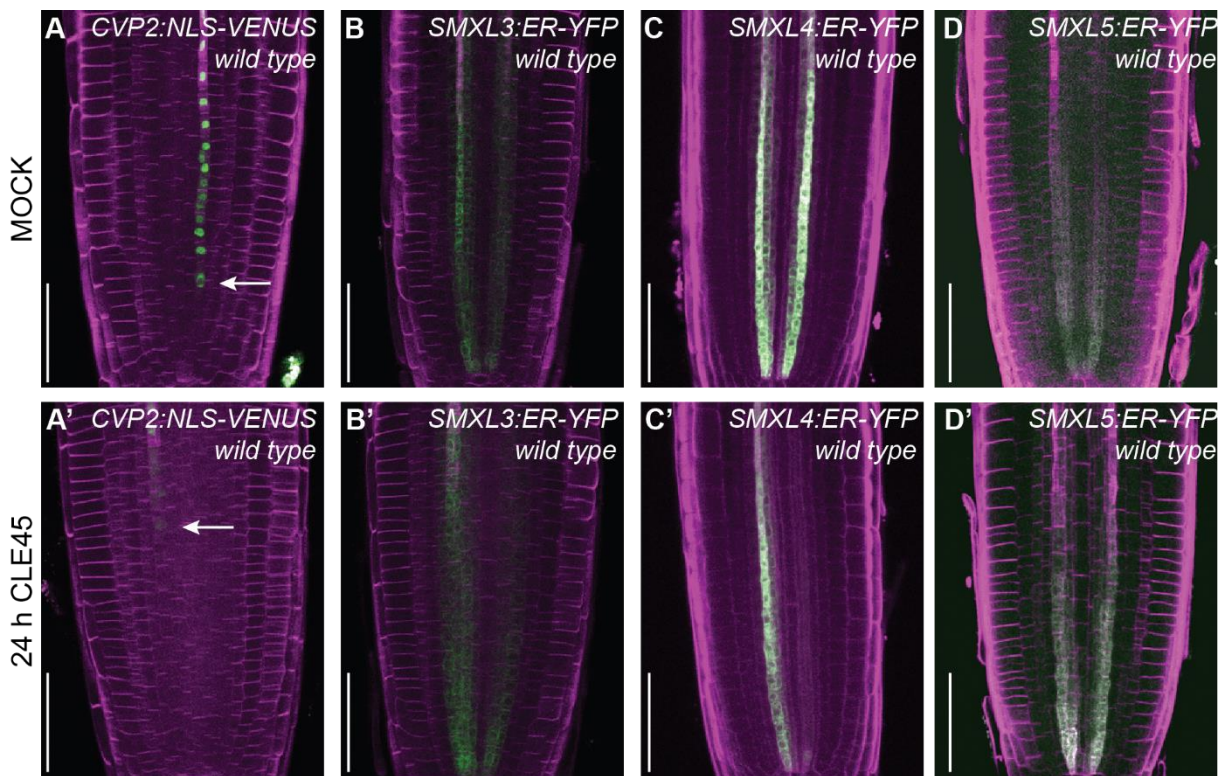


Figure 13: *SMXL3/4/5* promoter activities are not affected by CLE45/BAM3 signalling. Comparison of *SMXL3/4/5:ER-YFP* reporter activities under MOCK and CLE45 conditions. *CVP2:NLS-VENUS* reporter activity was used as treatment control. Two-day old seedlings were transferred to 0.5 MS medium without (MOCK) or with 50 nM CLE45. Reporter activities were analysed after 24 hrs. Shown is one representative experiment of three repetitions. $n = 10$. (**AA'**) *CVP2* activity is delayed and reduced upon CLE45 treatment. (**B-D'**) *SMXL* reporter activities display no apparent differences under MOCK and CLE45 conditions. (A-D') Cell walls are stained with DirectRed23.

Having discovered that CLE45/BAM3 signalling does not affect *SMXL3/4/5* promoter activities, next I tested whether *SMXL3/4/5* protein accumulation was influenced by CLE45/BAM3 signalling. Therefore, I performed a similar experiments using previously published *SMXL3/4/5* translational fusion lines (*SMXL3/4/5:SMXL3/4/5-YFP*, Wallner et al. 2017) including the *CVP2* promoter reporter line as a treatment control. Overall, the 24-hour CLE45 treatment had different effects on each translational fusion line. Compared to MOCK conditions, *SMXL4*-YFP fusion protein signal was strongly reduced in protophloem strands of CLE45-treated plants with the notable exception that signal could always be detected in phloem initial cells even if SE differentiation was only affected higher up in roots (**Figure 14CC'**). The observation that, exclusively in phloem initial cells, *SMXL4*-YFP accumulation remains the same upon treatment is in line with *BAM3* expression starting in SE/procambium precursor cells (Hazak et al. 2017) whereas *SMXL4* is already expressed in phloem initial cells (Wallner et al. 2017).

Compared to *SMXL4* proteins, detecting the effect of the CLE45 treatment was more challenging for *SMXL3* and *SMXL5* proteins. Unlike *SMXL4* expression which is restricted to developing proto- and metaphloem strands, *SMXL3* and *SMXL5* are also expressed in neighbouring procambium cells, and *SMXL3* is further expressed in phloem pole pericycle (PPP) cells (Wallner et al. 2017). Under MOCK conditions, it was possible to identify *SMXL3/5*-YFP fusion protein signal in protophloem strands as opposed to neighbouring strands based on enhanced cell wall staining in differentiating SEs (**Figure 14BD**). Upon CLE45 treatment, signal for both *SMXL3*-YFP and *SMXL5*-YFP fusion proteins could still be detected, however, it was not possible to conclude whether these signals belonged to protophloem strands or neighbouring cells (**Figure 14B'D'**). Consequently, signal changes specific for developing protophloem strands were potentially masked by signal from neighbouring cells.

To test whether SMXL5 proteins were affected by CLE45 treatment specifically in protophloem strands, I generated and introduced a transgene expressing the SMXL5-VENUS fusion protein under the protophloem-specific *SMXL4* promoter into plants. As observed for SMXL4-YFP, SMXL5-VENUS fusion protein signal was clearly reduced in the protophloem strand after the treatment compared to the MOCK yet never lost in phloem initial cells (**Figure 14EE'**). These findings confirmed that SMXL5 proteins are affected by CLE45 specifically in *BAM3*-expressing cells of the developing protophloem.

Based on the observation that SMXL proteins driven by *pSMXL4* were not affected by exogenous CLE45 application in phloem initial cells where *BAM3* is not yet expressed, I assumed that loss of *BAM3* function would result in resistance of SMXL proteins to CLE45 signalling. Therefore, I generated a transgenic line expressing SMXL4-YFP under its endogenous promoter in the *bam3* background and repeated the treatment, finding that SMXL4-YFP fusion protein signal did not decrease, nor enhance noticeably, under CLE45 conditions compared to MOCK (**Figure 14FF'**).

Taken together, I show that CLE45/*BAM3*-mediated inhibition of SE differentiation affects SMXL4 and SMXL5 protein accumulation in developing protophloem strands. Importantly, CLE45 signalling influences SMXL protein accumulation exclusively in *BAM3*-expressing cells downstream of phloem initial cells. These findings further support the hypothesis that SMXLs play a crucial role in the establishment of the phloem lineage starting with phloem initial cells.

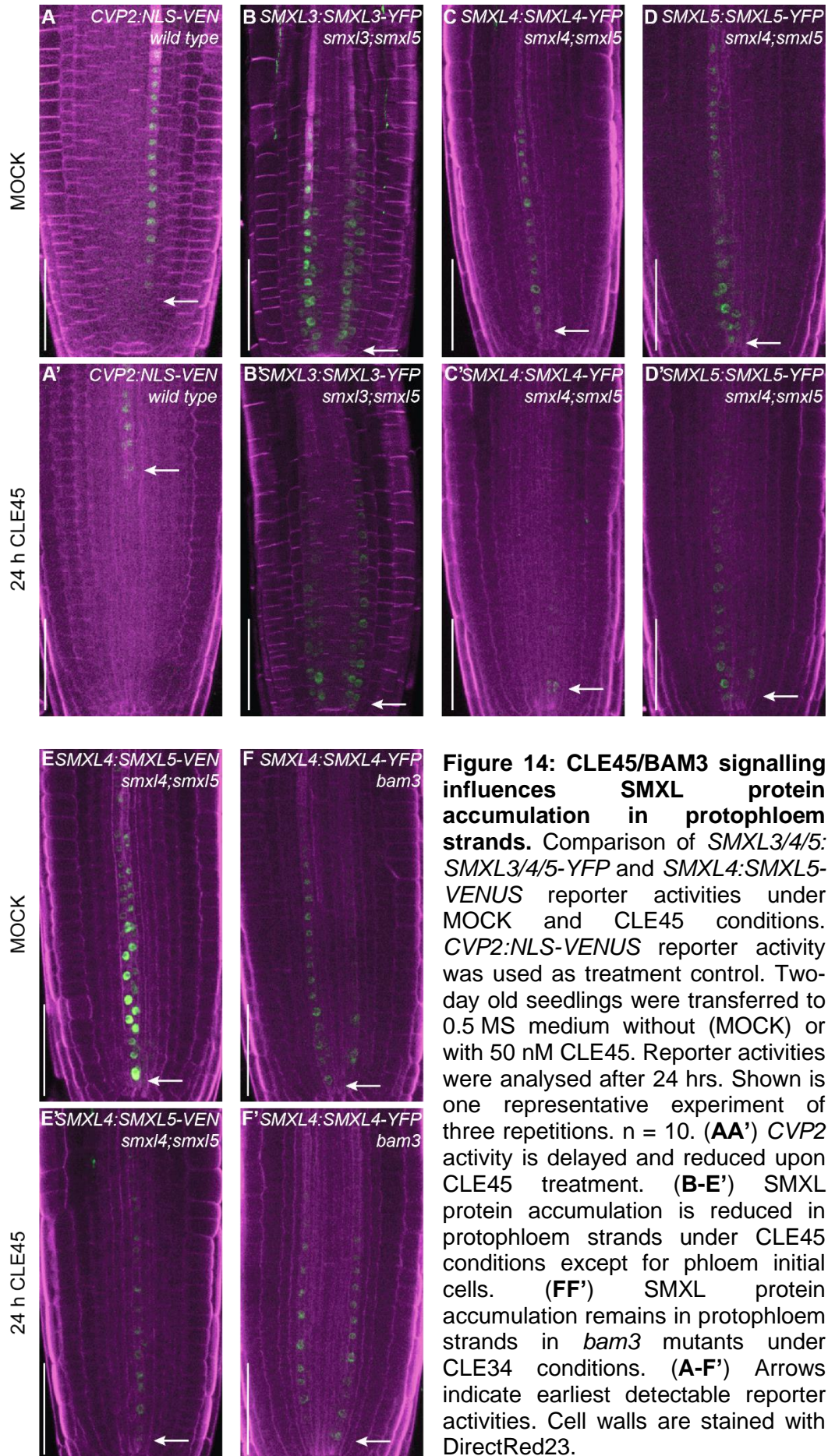


Figure 14: CLE45/BAM3 signalling influences SMXL protein accumulation in protophloem strands. Comparison of *SMXL3/4/5:SMXL3/4/5-YFP* and *SMXL4:SMXL5-VENUS* reporter activities under MOCK and CLE45 conditions. *CVP2:NLS-VENUS* reporter activity was used as treatment control. Two-day old seedlings were transferred to 0.5 MS medium without (MOCK) or with 50 nM CLE45. Reporter activities were analysed after 24 hrs. Shown is one representative experiment of three repetitions. $n = 10$. (**AA'**) *CVP2* activity is delayed and reduced upon CLE45 treatment. (**B-E'**) SMXL protein accumulation is reduced in protophloem strands under CLE45 conditions except for phloem initial cells. (**FF'**) SMXL protein accumulation remains in protophloem strands in *bam3* mutants under CLE45 conditions. (**A-F'**) Arrows indicate earliest detectable reporter activities. Cell walls are stained with DirectRed23.

3.8. **SMXL3/4/5 proteins are affected by BAM3-independent CLE26 signalling**

Previously, it was shown that not only CLE45, but also 14 other root-active CLE peptides cause a reduction in root length (Hazak et al. 2017). CLE26 is another root-active peptide involved in the suppression of protophloem differentiation and expressed towards the end of SE differentiation, but its effect is genetically separable from the effect of CLE45 (Hazak et al. 2017, Anne et al. 2018). While it is known that CLE45 binding is specific to BAM3 (Depuydt et al. 2013), a receptor that recognises the CLE26 peptide is still unknown.

To test whether my findings on *SMXL* promoter activities and *SMXL* protein accumulation are specific to CLE45/BAM3 signalling, I subjected the same *SMXL* promoter reporter, *SMXL* translational fusion, and *CVP2* promoter reporter lines as shown in **Figure 13** and **Figure 14** to exogenous CLE26 peptide for 24 hrs. Based on the fluorescent reporter proteins, *CVP2* promoter activity and thus SE differentiation were indeed impaired upon 24-hour CLE26 treatment while *SMXL3/4/5* promoter activities were unaffected (**Figure 15A-D'**). The effects on *SMXL*-YFP fusion protein signal after the CLE26 treatment also resembled those obtained after the CLE45 treatment. For *SMXL4*-YFP and *SMXL5*-VENUS fusion proteins, both driven by the protophloem-specific promoter of *SMXL4*, I detected fluorescence signal only in phloem initial cells as observed upon CLE45 treatment, deducing that the unknown CLE26-specific receptor is expressed in those cells (**Figure 15FF'HH'**). Resembling the results obtained after the CLE45 treatment, *SMXL3*-YFP and *SMXL5*-YFP fusion protein signals were still detectable upon CLE26 treatment. However, SE differentiation was impaired in those lines after the treatment based on reduced cell wall staining compared to MOCK conditions (**Figure 15E'G'**). Therefore, I inferred that *SMXL3*-YFP and *SMXL5*-YFP signals belonged to procambium (*SMXL3*, *SMXL5*) and PPP (*SMXL3*) cells. Furthermore, levels of *SMXL5*-YFP proteins expressed by *pSMXL4*

were clearly reduced upon CLE26 treatment, demonstrating that SMXL5-YFP proteins in protoxylem strands were indeed affected by CLE26 signalling.

Combining the results from CLE45 and CLE26 treatments of transgenic lines shown in **Figure 13**, **Figure 14** and **Figure 15**, CLE signalling pathways repressing protoxylem development induce changes in SMXL3/4/5 protein accumulation specifically in SE/procambium precursors and subsequent cell stages, while SMXL3/4/5 promoter activities remain unaffected.

Summary I

Together, I show that SMXL4/5 play crucial parts in the complex molecular network regulating xylem development in the RAM. SMXL4/5 function is required to initiate and promote the xylem developmental program including activities of *OPS*, *BRX*, *BAM3*, *CVP2* and *APL*. Furthermore, downstream of xylem initial cells, SMXL4/5 proteins are affected by CLE-mediated suppression of SE differentiation in developing xylem strands.

Figure 15 (next page): CLE26 signalling affects SMXL3/4/5 protein accumulation in protoxylem strands. SMXL3/4/5 promoter activities are not affected. Comparison of SMXL3/4/5:ER-YFP, SMXL3/4/5:SMXL3/4/5-YFP and SMXL4:SMXL5-VENUS reporter activities under MOCK and CLE26 conditions. CVP2:NLS-VENUS reporter activity was used as treatment control. Two-day old seedlings were transferred to 0.5 MS medium without (MOCK) or with 50 nM CLE45. Reporter activities were analysed after 24 hrs. Shown is one representative experiment of three repetitions. n = 10. **(AA')** CVP2 activity is delayed and reduced upon CLE45 treatment. **(B-D')** SMXL reporter activities display no apparent differences under MOCK and CLE26 conditions. **(E-H')** SMXL protein accumulation is reduced in protoxylem strands under CLE26 conditions except for xylem initial cells. **(A-H')** Arrows indicate earliest detectable reporter activities. Cell walls are stained with DirectRed23.

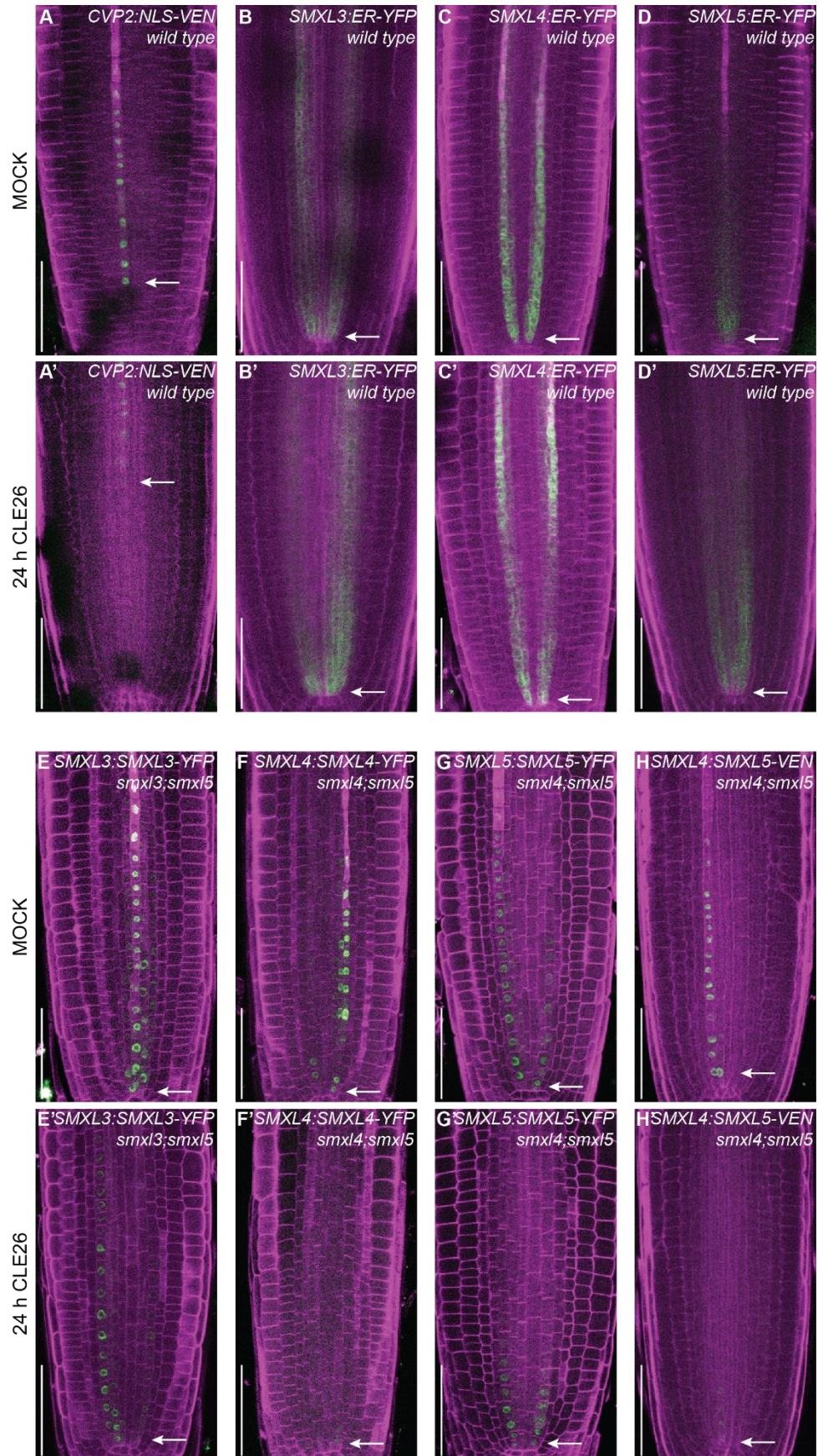


Figure 15: CLE26 signalling affects SMXL3/4/5 protein accumulation in protophloem strands. SMXL3/4/5 promoter activities are not affected.

3.9. SMXL5 protein function in protophloem cells is independent of the EAR motif

So far, it is unknown which domains are most crucial for the function of SMXL3/4/5 proteins in promoting protophloem development. One regulatory feature shared by all SMXL proteins is the conserved EAR motif, the most predominant transcription repression motif defined by the consensus sequence LxLxL (Jiang et al. 2013, Zhou et al 2013, Moturu et al. 2018, Walker et al. 2019, Ohta et al. 2001, Kagale and Rozwadowski 2011). To investigate whether the EAR motif of the SMXL5 protein is relevant to promote protophloem development, I started by testing whether protein accumulation was altered in EAR-mutated SMXL5 proteins *in planta*. Therefore, I generated a vector encoding a mutated, non-functional version of the SMXL5 EAR motif (LxLxL → AxAxA, 'mEAR') fused to the fluorescent VENUS protein and driven by the 35S promoter for transient coexpression in *Nicotiana benthamiana* leaves. Using a vector encoding a wild type SMXL5 protein (35S:SMXL5-VENUS) as reference, I found that both, SMXL5-VENUS and SMXL5^{mEAR}-VENUS accumulated in the nucleus (**Figure 16A**). Next, I generated a transgenic line expressing SMXL5^{mEAR}-VENUS driven by its endogenous promoter (SMXL5:SMXL5^{mEAR}-VENUS) in the *smxl4;smxl5* double mutant background to test whether the SMXL5^{mEAR}-VENUS fusion protein was also nuclear localised in Arabidopsis, and whether this mutated version of SMXL5 was functional to restore protophloem development and root length. As a control, I used a previously published translational fusion line expressing SMXL5-YFP under its endogenous promoter and restoring root length and phloem formation (SMXL5:SMXL5-YFP/*smxl4;smxl5*, Wallner et al. 2017). I found that, concomitant with my findings in *N. benthamiana*, SMXL5^{mEAR}-VENUS fusion proteins were also nuclear localised in developing protophloem strands (**Figure 16B**). Furthermore, analyses of SE differentiation in the RAM and root length measurements five days after germination showed that protophloem and root development were restored to wild type-like levels (**Figure 16CD**) indicating that SMXL5^{mEAR} proteins were functional.

Next, I tested whether root growth of plants expressing either SMXL5 or SMXL5^{mEAR} proteins under the endogenous *SMXL5* promoter was differentially affected by exogenous CLE45 application. Therefore, I grew respective translational fusion lines (*SMXL5:SMXL5-YFP/smxl4;smxl5*, *SMXL5:SMXL5^{mEAR}-VENUS/smxl4;smxl5*), wild type and *smxl4;smxl5* double mutants on MOCK and CLE45-containing medium and measured root length five days after germination. Notably, under MOCK conditions, primary roots of transgenic plants expressing SMXL5^{mEAR}-VENUS were slightly longer than roots of transgenic lines expressing SMXL5-YFP and wild type roots. When grown on CLE45-containing medium, however, primary roots of both transgenic lines and of wild type plants were reduced to the same length as *smxl4;smxl5* double mutants (**Figure 16D**). These findings suggested that SMXL5^{mEAR} protein function is as affected by CLE signalling as SMXL5 proteins.

Figure 16 (next page): EAR motif-mutated SMXL5 proteins are nuclear localised and restore protophloem development in *smxl4;smxl5* double mutants. (A) Transient expression of SMXL5-VENUS and SMXL5^{mEAR}-VENUS fusion proteins in nuclei of *Nicotiana benthamiana* leaves. Fusion proteins expressed under the 35S promoter. (B) Expression of SMXL5-YFP and SMXL5^{mEAR}-VENUS fusion proteins in *smxl4;smxl5* double mutants (Arabidopsis). SMXL5^{mEAR} proteins are nuclear localised and restore protophloem development. Asterisks depict protophloem strands. Cell walls are stained with DirectRed23. n = 5. Scale bars represent 50 µm. (C) Protophloem development five days after germination. Expression of SMXL5^{mEAR}-VENUS under the endogenous *SMXL5* promoter restores protophloem development in *smxl4;smxl5* double mutants. Transgenic lines expressing SMXL5-YFP under the endogenous *SMXL5* promoter were used as controls. Cell walls are stained by mPS-PI. Asterisks indicate protophloem strands. n = 10. Scale bars represent 50 µm. (D) Root length measurements five days after germination. Plants were grown on 0.5 MS medium without (MOCK) or with 50 nM CLE45. Under MOCK conditions, SMXL5^{mEAR}-VENUS fusion proteins expressed under the endogenous *SMXL5* promoter restore root length in the *smxl4;smxl5* background. Under CLE45 conditions, roots are reduced to the same length as *smxl4;smxl5* double mutants. Statistical groups (a, b, c, d) determined by one-way ANOVA and post-hoc Tukey's test (95 % CI). n = 17-46.

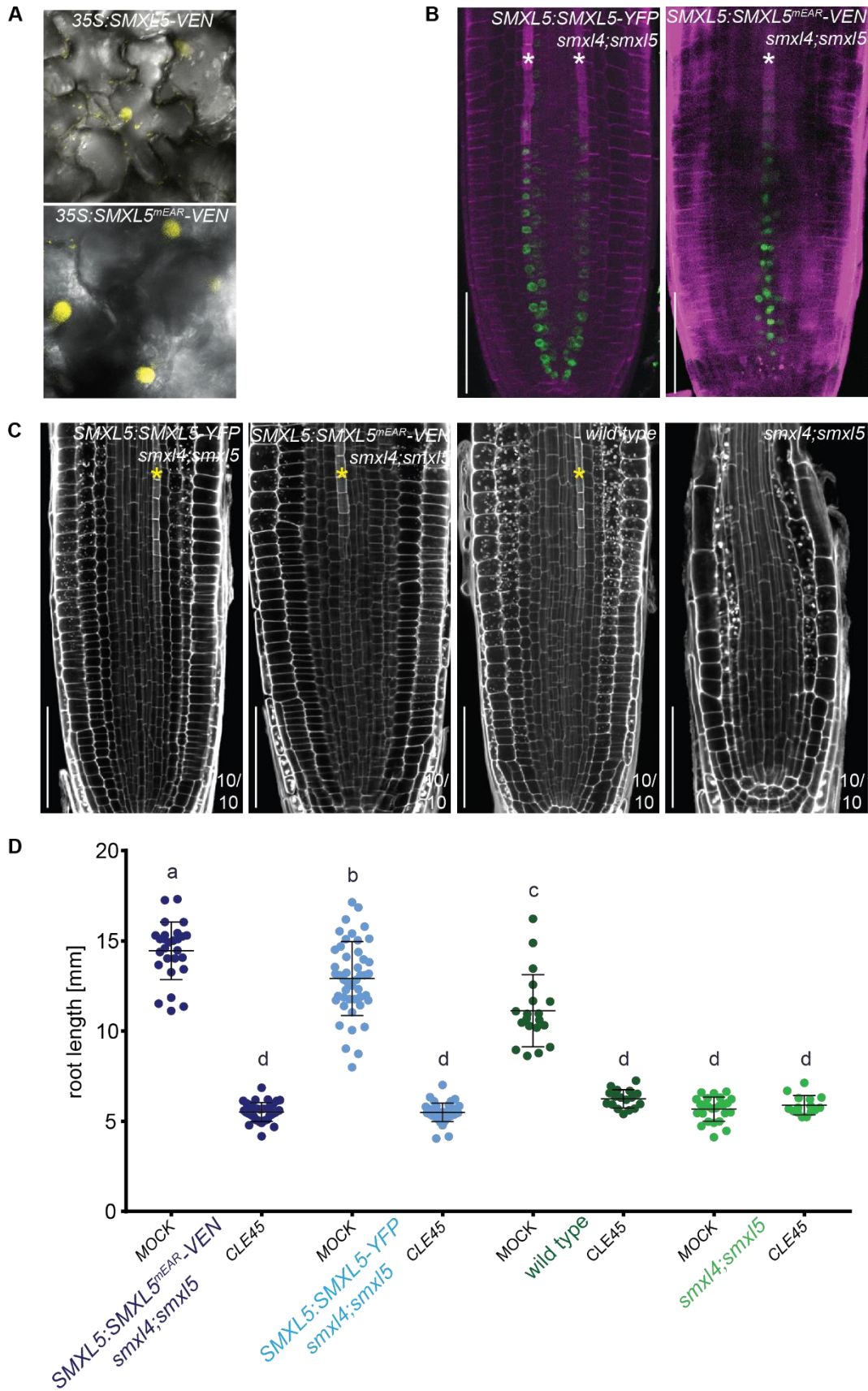


Figure 16: EAR motif-mutated SMXL5 proteins are nuclear localised and restore protophloem development in *smxl4;smxl5* double mutants.

3.10. SMXL5 proteins potentially interact with TPR2/4 corepressors

Having discovered that the SMXL5 EAR motif was not relevant for protein function in protophloem development, I raised the question whether it was yet relevant for interactions between SMXL5 and proteins that are known to be recruited by the EAR motif. The EAR motif has been viewed as 'hallmark' of transcription repressors interacting with TOPLESS (TPL) and TPL-RELATED (TPR) corepressors (Kagale and Rozwadowski 2011, Causer et al. 2012, Martin-Arevalillo et al. 2017). Moreover, EAR-mediated interactions between SMXLs and TPR2 have previously been discovered in rice, Arabidopsis, and barley (Smith and Li, 2014, Soundappan et al. 2015, Wang et al. 2015, Liu et al. 2017, Ma et al. 2017). Accordingly, EAR motif-mediated interaction of the SMXL5 protein with TPR corepressors would support a role of SMXL5 as 'EAR repressor' involved in transcription regulation. Furthermore, the TPR2-related protein TPR4 was previously identified as potential interaction partner of SMXL5 based in a Yeast-2-Hybrid screen previously performed in our group as described before (Legrain et al. 2001) using Hybrigenics (Evry, France). Therefore, I generated constructs to investigate localisation of TPR2-mGFP and TPR4-mGFP fusion proteins with SMXL5-mCherry fusion protein expressed under the 35S promoter after transient coexpression in *N. benthamiana* leaves. Co-localisation of SMXL5-mCherry and TPR2/4-mGFP fusion proteins in the nucleus was confirmed suggesting that SMXL5 and TPR2/4 proteins have the potential to interact physically (**Figure 17AB**). To see whether co-localisation was affected when the EAR motif was mutated in SMXL5 proteins, I also included the SMXL5^{mEAR}-mCherry fusion protein expressed under the 35S promoter in the analysis. However, after coexpression with SMXL5^{mEAR}-mCherry, no differences in protein accumulation or co-localisation of TPR2-mGFP fusion protein was detected compared to coexpression with SMXL5-mCherry (**Figure 17C**) again demonstrating that neither nuclear localisation of SMXL5, nor co-localisation with TPR2 was affected by mutations in the SMXL5 EAR motif.

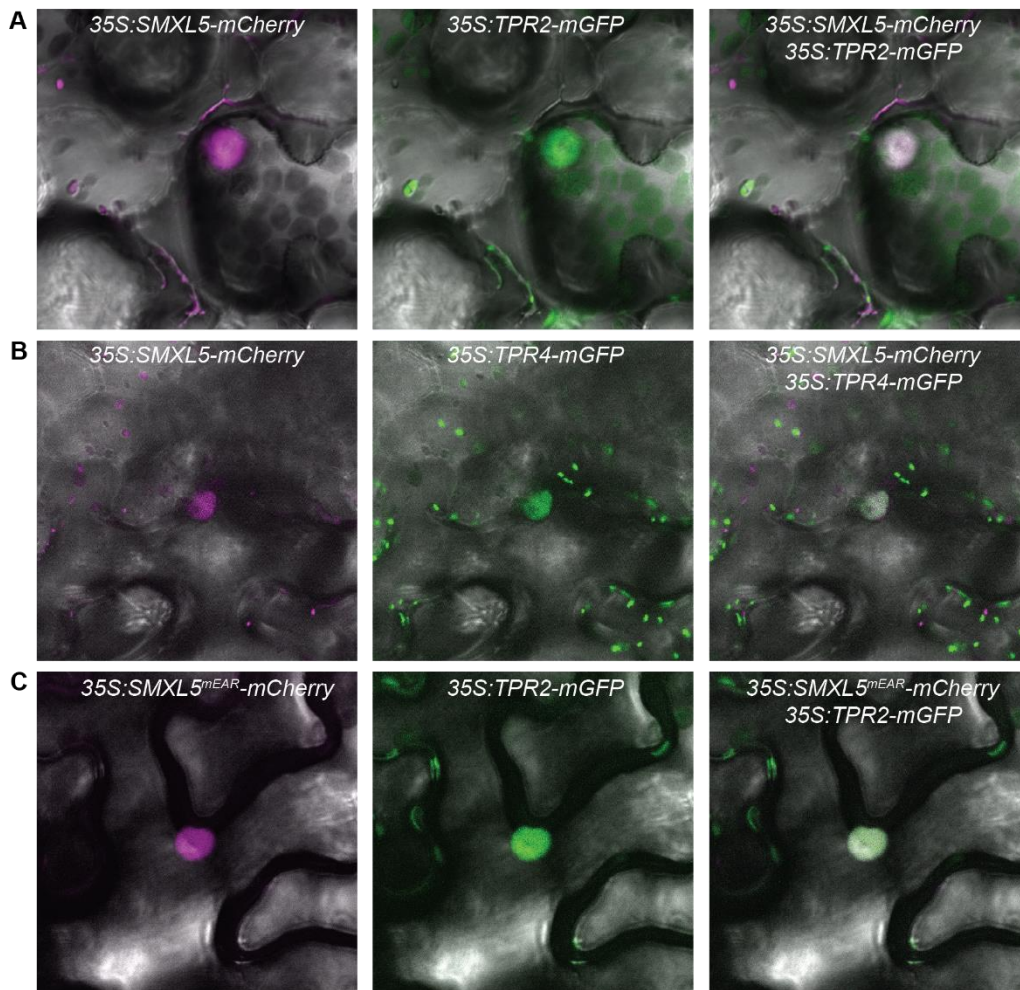


Figure 17: Transient expression of SMXL5-mCherry, SMXL5^{mEAR}-mCherry and TPR2/4-mGFP fusion proteins in nuclei of *Nicotiana benthamina*. (A) Co-expression of SMXL5-mCherry and TPR2-mGFP fusion proteins. (B) Co-expression of SMXL5-mCherry and TPR4-mGFP. (C) Co-expression of SMXL5^{mEAR}-mCherry and TPR2-mGFP. (A-C) Fusion proteins expressed under the 35S promoter.

Summary II

Taken together, I conclude that the SMXL5 EAR motif is neither required for SMXL5 protein accumulation in the nucleus nor essential for the function or dynamics of the SMXL5 protein in developing protophloem cells. Nevertheless, potential interaction of SMXL5 and TPR2/4 proteins remain to be tested.

3.11. EMS-based mutagenesis of *smxl4;smxl5* restored protophloem development

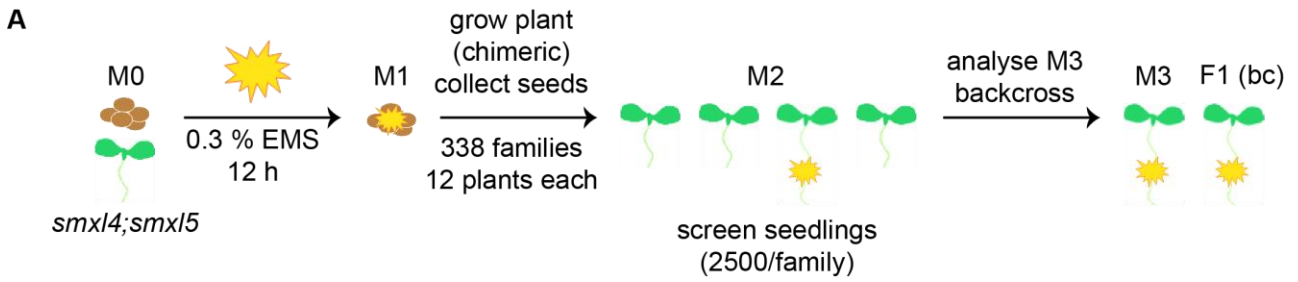
To identify genes that are functionally related to *SMXL4/5* during protophloem development, I performed a suppressor screen of *smxl4;smxl5* double mutants after mutagenesis using ethyl methanesulfonate (EMS) as mutagenic agent. EMS introduces random point mutations by nucleotide substitution (G:C → A:T) (Page and Grossniklaus 2002, Schröder et al. 2008) resulting in an increased percentage of unfertilised ovules, embryonic lethals, and embryonic chlorophyll mutants in mutagenised *Arabidopsis* seeds (van der Veen and Wirtz, 1968). Together with colleagues, we exposed approximately 8000 seeds of *smxl4;smxl5* double mutants (M0 generation) to a calculated sub-saturation level of EMS (0.3 %) for 12 hrs (Page and Grossniklaus, 2002). Immediately after, we transferred all M1 seeds to soil and let the plants grow to collect seeds in the M2 generation (**Figure 18A**). The presence of pale sectors in leaves or petioles resulting from embryonic chlorophyll mutants among M1 plants indicated that the mutagenesis was effective. It is also important to mention that in *Arabidopsis*, two embryonic cells contribute to the next generation. Therefore, M1 plants developing from mutagenised seeds are chimeric and consist of two sectors that (may) segregate differently for certain mutations (Page and Grossniklaus 2002).

To identify suppressors of the *smxl4;smxl5* phenotype in the M2 generation, seeds of twelve M1 parental plants were pooled and collected as one family. Next, approximately 2500 seedlings per M2 line (family) were sequentially screened for seedlings with suppressed *smxl4;smxl5* phenotype, i.e. with restored, wild type-like root length indicative of restored protophloem development. Of 338 families in total, three separate M2 lines (17-0159-1, 17-0159-2, 17-0159-3) were screened resulting in 56, 35, and 15 plants, respectively, with wild type-like, long roots. **Figure 18B** shows an example plate from the screening of M2 line 17-0159-2 highlighting seedlings with suppressed *smxl4;smxl5* phenotype. These numbers of long-rooted, wild type-like seedlings roughly reflected the expected number for a dominant suppressor mutation

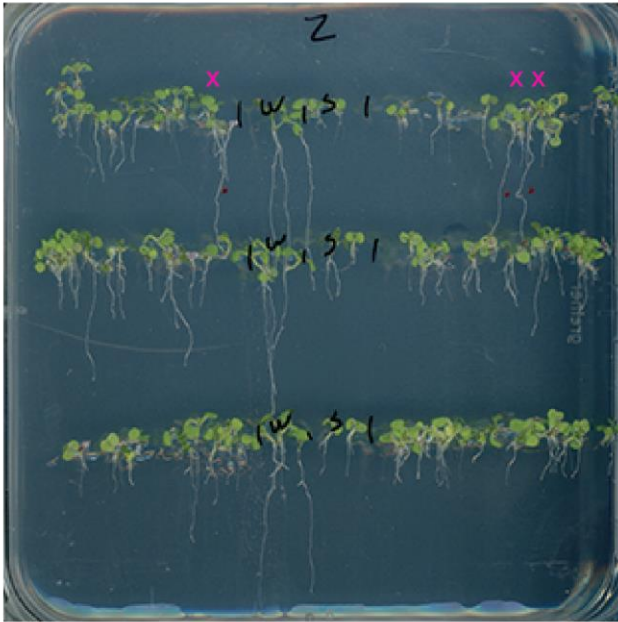
in the parent (M1) generation based on calculations with 12 plants/family, 2500 seeds, and a dominant (5:3) segregation rate (Page and Grossniklaus 2002). Continuing with M2 line 17-0159-2, all long-rooted seedlings were transferred to soil to analyse segregation rates in the M3 generation. Of those, five M3 lines were chosen randomly (17-1078-3, 17-1078-12, 17-1078-14, 17-1078-15, 17-1078-18) and of each, about 60 plants were grown on 0.5 MS medium to count the number of long and short roots seven days after germination. In these five M3 lines, analysing the percentage of long roots per line resulted in 5 % (17-1078-18), 57 % (17-1078-3), 72 % (17-1078-15), 85 % (17-1078-14) and 95 % (17-1078-12). These findings challenged the existence of one dominant second-site mutation suppressing the *smx4;smx15* mutant phenotype. Instead, the data suggested that a combination of mutations in the *smx14;smx15* background resulted in the restoration of long roots. Continuing with M3 line 17-1078-15 (roughly 75 % long roots) (**Figure 18C**), five seedlings with long and five with short roots were transferred to soil for further analysis in the next generation.

To eliminate background mutations, I backcrossed long-rooted plants of the M3 17-1078-15 line with *smx14;smx15* double mutants to analyse root growth in the F1 (bc) generation. Root analyses five days after germination revealed that in the F1 (bc) generation (X17-106) over 50 % of the plants developed long roots, indicating that the M3 parent (17-1078-15) was heterozygous for a putative dominant mutation (**Figure 18DD'**). Long-rooted seedlings were transferred to soil to collect seeds in the F2 (bc) generation.

Figure 18 (next page): EMS-based mutagenesis of *smx14;smx15* mutants yielding long-rooted, wild type-like plants. (A) Scheme of ethyl methanesulfonate (EMS)-based mutagenesis and suppressor screen of *smx14;smx15* double mutants. (B) Example of 0.5 MS plate showing seedlings in the M2 generation being screened for suppressors of the *smx14;smx15* short-root phenotype. wt – wild type, s4;s5 – *smx14;smx15* double mutant, X – suppressors of the *smx14;smx15* phenotype (collected). (C) Example of 0.5 MS plate showing seedlings in the M3 generation (72 % long-rooted). (DD') Example of 0.5 MS plate with seedlings in the F1 generation after backcrossing (F1 bc) (61 % long-rooted) and corresponding root length measurement five days after germination. n = 97.

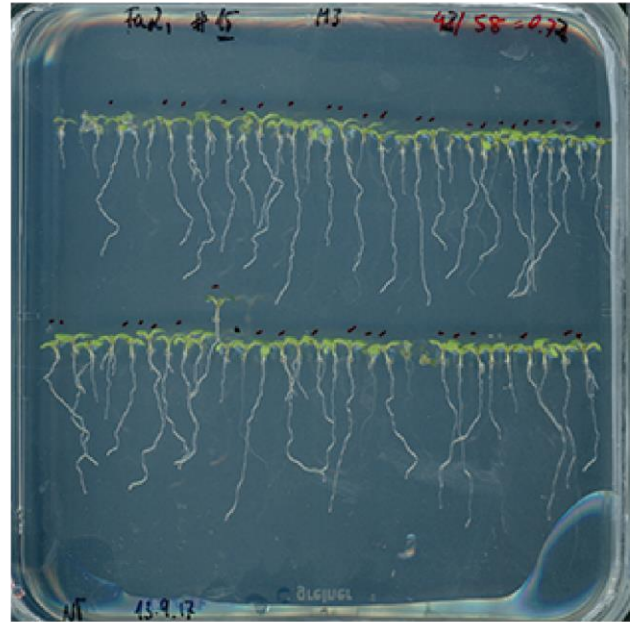


B M2 17-0159-2 | wt | s4;s5 | M2 17-0159-2

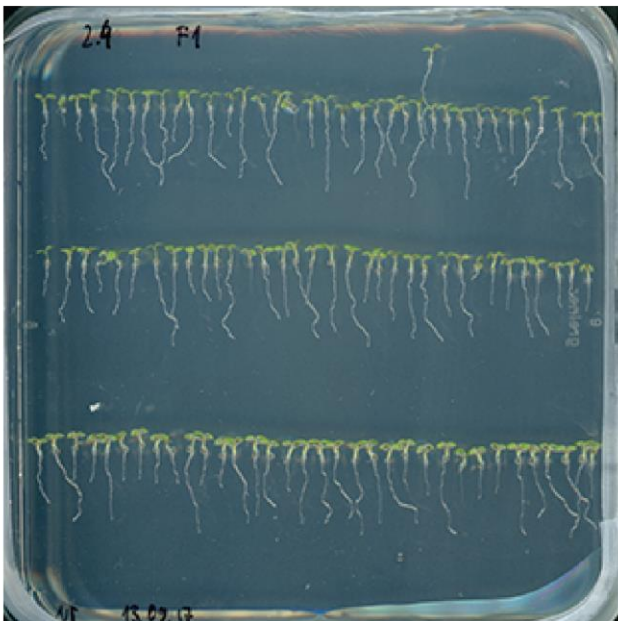


x suppressor the of *smx14;smx15* phenotype

C M3 17-1078-15 (72 % long roots)



D F1 (bc) X17-106 (61 % long roots)



D'

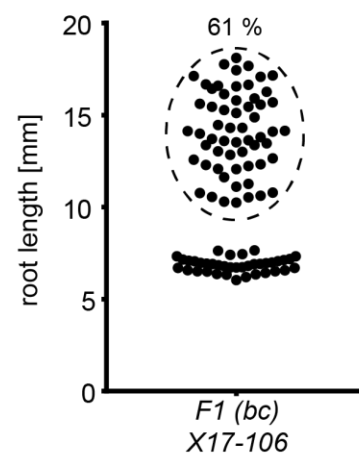


Figure 18: EMS-based mutagenesis of *smx14;smx15* mutants yielding long-rooted, wild type-like plants.

In parallel to backcrossing, I analysed root length of ten lines in the M4 generation derived from either long-rooted or short-rooted M3 17-1078-15 parents. In one of the five M4 lines (number 17-1506-24) derived from a long-rooted M3 parental plant, primary root growth resembled the wild type five days after germination (**Figure 19A**). In addition to root length measurements, I analysed the protophloem phenotype of the same line five days after germination, confirming that restored root length was concomitant with the development of continuous protophloem strands (**Figure 19A'**). Subsequently, I collected seeds and compared roots length of one M5 line (18-0031-24) derived from a long-rooted M4 parental plant (17-1506-24) and their predecessor in the M3 generation (17-1078-15) five days after germination. As controls, I included the respective parental lines in M4 and M3 as well as wild type and *smxl4;smxl5* double mutants. On average, primary roots growth in the M3, M4 and M5 generations resembled wild type. A closer look at the distribution of root lengths revealed that in the M3 generation, 54 % resembled *smxl4;smxl5* double mutants while 17 % exceeded the length of wild type roots. In M4 and M5 generations, the number of short-rooted seedlings decreased gradually compared to the M3 generation. In the M5 generation, average primary root length was distinctly higher than in wild type (**Figure 19B**). Additionally, I found that in the M4 generation, plants deriving from different short-rooted M3 (17-1078-15) parental plants developed short roots resembling the *smxl4;smxl5* phenotype (41-61 %) as well as long roots that frequently exceeded the length of wild type roots (**Figure 19C**). These findings again suggested that long roots did not result from one particular dominant mutation in the *smxl4;smxl5* background but from a combination of recessive mutations suppressing the *smxl4;smxl5* phenotype.

To exclude the possibility that long roots were based on genomic contamination by wild type plants, I genotyped for T-DNA insertions to confirm homozygous mutations of *SMXL4* and *SMXL5* genes. Genotyping was performed for long-rooted plants in the M3 generation (17-1506-22, 17-1506-24) and short- and long-rooted plants in the F2 (bc)

generation (17-1510-31-S/L, 17-1510-34-S/L). Wild type and *smxl4;smxl5* mutants were used as controls. Genotyped plants developed from mutagenised predecessors were homozygous for *SMXL4* and *SMXL5* gene mutations (**Figure 19DD'**), again confirming that restoration of root length and protophloem development resulted from second-site mutations suppressing the *smxl4;smxl5* phenotype. Next steps require the investigation of background mutations including genome mapping in the F2 (bc) generation and *smxl4;smxl5* double mutants as reference genome.

Summary III

EMS-based mutagenesis of *smxl4;smxl5* double mutants yielded plants with wild type-like root growth and protophloem development. These findings were an important first step toward identifying genes that are functionally related to *SMXL4/5* in protophloem development. Further analysis including genome mapping is required to identify candidate genes that result in the suppression of the *smxl4;smxl5* mutant phenotype.

Figure 19 (next page): Restored root length and protophloem development probably result from a combination of recessive, second-site mutations in the *smxl4;smxl5* background. (**AA'**) Root length and protophloem development of seedlings in the M4 generation resemble wild type plants. (A) Root length analysis five days after germination. Statistical groups (a, b, c) determined by one-way ANOVA and post-hoc Tukey's test (95 % CI). n = 32-85. (A') Protophloem development five days after germination. Cell walls are stained by mPS-PI. Asterisks indicate protophloem strands. n = 10. (**B**) Root length analysis of seedlings in the M3, M4 and M5 generation descending from long-rooted parents compared to wild type and *smxl4;smxl5* mutants five days after germination. n = 38-59. (**C**) Root length analysis of seedlings in the M4 generation descending from long-rooted (17-1506-24) and short-rooted (17-1506-26/27/29/30) parents compared to wild type and *smxl4;smxl5* mutants five days after germination. n = 13-34. (BC) Statistical groups (a, b, c) determined by one-way ANOVA and post-hoc Tukey's test (95 % CI). (**DD'**) Genotyping of *SMXL4* and *SMXL5* genes in long-rooted plants in the M3 generation (1, 2) and short- and long-rooted plants in the F2 (bc) generation (5-8). Except for wild type (3), plants were homozygous for *SMXL4* and *SMXL5* T-DNA insertions compared with the *smxl4;smxl5* control (4). 1,2 – M3 generation, 3 – wild type (ctrl), 4 – *smxl4;smxl5* (ctrl), 5/7 – F2 (bc) short-rooted, 6/8 – F2 (bc) long-rooted, 9 – water control.

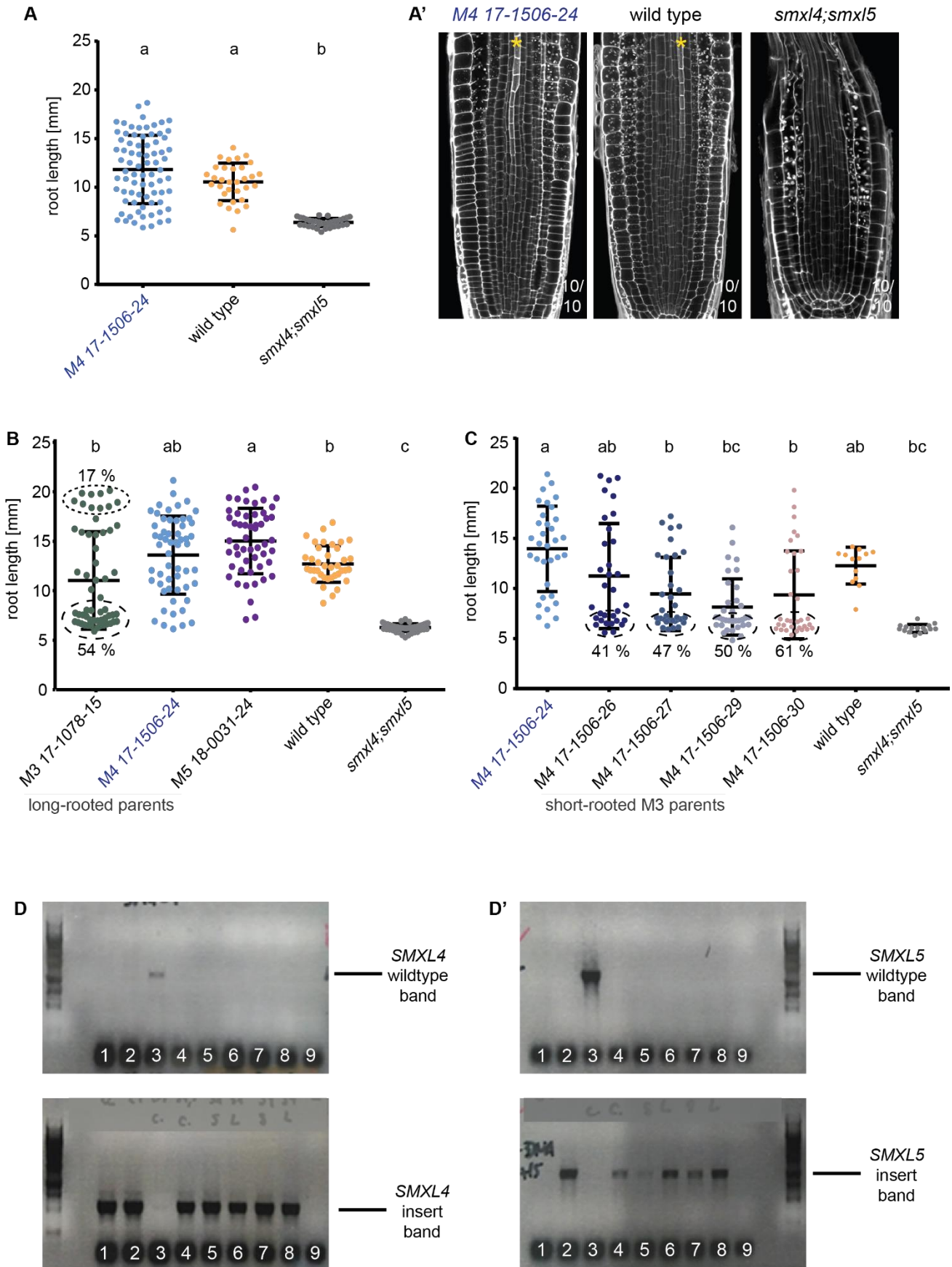


Figure 19: Restored root length and protophloem development probably result from a combination of recessive, second-site mutations in the *smx4;smx5* background.

4. Discussion

The integrity of phloem, the vascular tissue distributing sugars from source to sink organs, is essential to mediate root growth and overall plant body architecture (Wallner et al. 2017, Blob et al. 2018, Cho et al. 2018, John and Nimchuk 2019). Plant vascular development is a highly regulated process including four main developmental steps: specification of vascular cells from precursor cells, establishment of vascular tissue combining growth and patterning, maintenance, and differentiation of conductive cells including tracheary (xylem) and sieve (phloem) elements (De Rybel et al. 2015). In root tips, post-embryonic phloem development results in the formation of sieve element-companion cell (SE-CC) complexes, the functional transport units of the phloem infrastructure (Otero and Helariutta 2017, Cho et al. 2018). The root tip can be subdivided into four differential zones including the meristematic zone (RAM) followed by the transition zone, elongation zone, and differentiation zone (**Figure 2**) (Ivanov and Dubrovsky 2013). Of all known promoters of phloem development in Arabidopsis, *SUPPRESSOR OF MAX2 1-LIKE3 (SMXL3)*, *SMXL4*, and *SMXL5* are among those genes that are expressed earliest in phloem stem cells (initial cells) in the RAM (Wallner et al. 2017). Like other members of the *SMXL* family, these genes encode redundantly acting, cell-autonomous, nuclear localised proteins supposedly involved in transcriptional repression (Machin et al. 2019, Villaecija-Aguilar et al. 2019, Moturu et al. 2018, Walker et al. 2019). However, how *SMXL3/4/5* genes promote early steps of phloem development in interaction with other regulators has been obscure so far.

4.1. *SMXL3/4/5* genes promote phloem initiation and SE differentiation in roots

The formation of functional protophloem strands relies on sequential expression of antagonistically acting regulators, thereby mediating spatiotemporal phloem organisation in the RAM (Blob et al. 2018). Prominent events include two formative, periclinal cell divisions, the first giving rise to sieve element (SE) precursor cell and procambium strands, the second to proto- and metaphloem strands. SEs of proto- and

metaphloem strands are produced after a second periclinal cell division which mark the transition of SE precursor cells into developing SEs (Lucas et al. 2013) (**Figure 20**). Previous work showed that double mutants of *SMXL3/4/5* genes develop short primary roots with decreased RAM size as they grow. This phenotype correlates with defects during protophloem development where developing cells do not differentiate into functional SEs. Furthermore, this defect is preceded by a delay in the second periclinal cell division in developing protophloem strands (Wallner et al. 2017). Different from the total inability of double mutants of *SMXL3/4/5* genes to produce differentiated SEs in primary roots, loss of function of other early regulators of phloem development including *OCTOPUS (OPS)*, *BREVIS RADIX (BRX)*, *COTYLEDON VASCULAR PATTERN (CVP2)* and *CVP2-LIKE1 (CVL1)* results in discontinuous protophloem strands where differentiated SEs are intermitted by undifferentiated cells (*ops*, *brx*, *brx;ops*, *cvp2;cvl1*) (Truernit et al. 2012, Rodriguez-Villalon et al. 2014, Rodriguez-Villalon et al. 2015, Breda et al. 2017). So-called 'gap cells' exhibit features of developing SEs as well as CCs (Gujas et al. 2020). Based on early activities of *SMXL3/4/5* genes in phloem initial cells and total loss of functional protophloem strands in *smxl4;smxl5* double mutants (Wallner et al. 2017), I hypothesised that *SMXL4/5* gene activities are required to initiate protophloem development by activating the aforementioned phloem regulators.

Indeed, I discovered that gene expressions of *OPS*, *BRX*, and *CVP2* are reduced in *smxl4;smxl5* double mutants compared to wild type (**Figure 6**). Furthermore, the expression of *BARELY ANY MERISTEM3 (BAM3)* is reduced in double mutants as well, demonstrating that *SMXL4/5* not only activate genes that promote phloem development (*OPS*, *BRX*, *CVP2*) (Truernit et al. 2012, Rodriguez-Villalon et al. 2014, Rodriguez-Villalon et al. 2015, Breda et al. 2017), but also genes that inhibit phloem development (*BAM3*) (Depuydt et al. 2013). In conclusion, I found that *SMXL4/5* are required to initiate phloem formation by establishing the phloem-specific developmental program in phloem initial cells.

Interestingly, I discovered that *OPS* and *BRX* genes are expressed as early as *SMXL4/5* in phloem initial cells (**Figure 6**) which contradicts previous findings assigning *OPS* and *BRX* expression to start in SE/procambium precursor cells (Truernit et al. 2012) and SE precursor cells (Scacchi et al. 2009), respectively. Genetic interaction studies of *SMXL5* with *OPS* and *BRX* further indicate that the three genes conduct different roles in promoting phloem development. I demonstrated this by genetically combining *BRX/SMXL5* or *OPS/SMXL5* loss of functions which resulted in a combination of increased gap cells and loss of protophloem strands in *brx;smxl5* and *ops;smxl5* double mutants compared to *brx* and *ops* single mutants (**Figure 7**). Loss of protophloem strands was previously described for mutants with combined *BRX/OPS* loss of functions (Breda et al. 2017). As *smxl5* single mutants develop wild type-like protophloem strands without any gaps, the drastic enhancement of phloem defects when combining either *OPS* or *BRX* loss of function with *SMXL5* loss of function implies a crucial role of *SMXL5* not only to promote phloem initiation in the meristematic zone, but also to ensure the continuous formation of interconnected SEs in the transition zone. Furthermore, loss of *OPS* gene function does not affect *SMXL4/5* gene activity (**Figure 8**) but combinational loss of *SMXL4* and *SMXL5* functions strongly reduces *OPS* gene activity (**Figure 6**). This indicates that *SMXL4/5* genes act upstream of *OPS* during phloem development. Additionally, *BRX* driven by the protophloem-specific *SMXL4* promoter rescues phloem development in the *smxl4;smxl5* background (**Figure 9**) inferring that *SMXL4/5* act also upstream of *BRX*.

In conclusion, I propose that protophloem development is not only promoted by additive and dosage-dependent effects of *OPS*, *BRX* and *CVP2* genes (Rodriguez-Villalon et al. 2014) but depends initially on *SMXL4/5* gene activities upstream of those phloem regulators.

Other than reduced *OPS* and *BRX* expression, *CVP2* expression is both reduced and delayed in *smxl4;smxl5* double mutants (**Figure 6**). *CVP2* is involved in cell wall remodelling (thickening) of SEs and its expression marks the transition from SE precursor cells to developing SEs in the meristematic zone (Rodriguez-Villalon et al. 2015) (**Figure 20**). Discovering delayed expression of *CVP2* in *smxl4;smxl5* double mutants compared to wild type (**Figure 6**) complements previous findings showing delayed occurrence of the second formative, periclinal cell division in *smxl4;smxl5* double mutants compared to wild type (Wallner et al. 2017). Together, these observations suggest that in *smxl4;smxl5* double mutants, the occurrence of *CVP2*-expressing, developing SEs after the second periclinal cell division is delayed due to impeded transition of SE precursor cells. I presume that primary roots of *smxl4;smxl5* double mutants exhibit increased numbers of SE precursor cells compared to wild type, thus preventing sugar transport into the RAM and resulting in the ultimate death of primary roots. To test whether impaired protophloem development in *smxl4;smxl5* double mutants correlates with continued cell divisions of SE precursor cells, genetic markers specific to SE precursor cells would be required to perform comparative analyses between wild type and *smxl4;smxl5* double mutants.

Importantly, *SMXL5* expression under the promoters of *OPS* (phloem initial cells), *BAM3* (SE/procambium precursor cells) as well as *CVP2* (early developing SEs) is sufficient to restore phloem development and subsequent root growth in *smxl4;smxl5* double mutants (**Figure 9**). Combined with **Figure 6**, these findings show that *SMXL5* activity is required to promote activities of other phloem regulators that trigger SE differentiation. Conversely, *SMXL5* expression under the promoter of *ALTERED PLHOEM DEVELOPMENT (APL)* does not restore phloem development or root length in the *smxl4;smxl5* background (**Figure 9**). In wild type, *APL* is expressed in late developing SEs in the transition zone of the root and encodes a transcription factor that regulates enucleation of SEs after cell wall thickening (Bonke et al. 2003). Full

degradation of nuclei in differentiating SEs is promoted by joint protein functions of APL, its downstream targets NO APICAL MERISTEM45 (NAC45) and NAC86, and NAC45/86-DEPENDENT EXONUCLEASE-DOMAIN (NEN) proteins NEN1, NEN2 and NEN4 (**Figure 4, Figure 20**) (Bonke et al. 2003, Furuta et al. 2014, Blob et al. 2018). Finding that expression of *SMXL5* under the *APL* promoter does not restore phloem development in *smxl4;smxl5* double mutants can be explained by the observation that the *APL* promoter is not active in *smxl4;smxl5* mutants compared to wild type (**Figure 10**). This implies that *APL*-expressing cells which represent late developing SEs are not produced in primary roots of *smxl4;smxl5* double mutants and thus, SE differentiation cannot be finalised.

Taken together, my findings demonstrate that phloem development in primary roots of *smxl4;smxl5* double mutants progresses as far as producing early developing SEs, however, loss of *SMXL4* and *SMXL5* gene functions prevents final steps of SE differentiation including cell wall remodelling and enucleation to be performed. My data therefore indicate that *SMXL5* gene activity is not only required to establish the phloem-specific developmental program in phloem initial cells but also to promote timely differentiation SEs in developing phloem strands.

4.2. Delayed production of developing SEs *smxl4;smxl5* double mutants

Plants exhibiting defects in post-embryonic phloem development in roots suffer from deficient phloem sap transport to the RAM. This results in decreased RAM size and short primary roots (Bonke et al. 2003; Furuta et al. 2014, Wallner et al. 2017). Root length can thus serve as indicator for the degree of phloem defects in mutant backgrounds. Increasing degrees of protophloem impairment are also reflected by the gradual reduction in primary root length in *brx*, *ops*, *brx;smxl5*, *ops;smxl5*, and *smxl4;smxl5* mutants (**Figure 7**). Notably, increased accumulation of gap cells in the transition zone, continued proliferation of SE precursor cells in the meristematic zone,

or a combination of both result in the same short root phenotype resembling *smx14;smx15* mutants (**Figure 7**). This observation raised the question whether the molecular mechanisms suppressing phloem differentiation act in all these scenarios. Previously, the occurrence of gap cells was linked to locally increased activities of the membrane-associated receptor-like kinase (RLK) *BAM3* interacting with the root-active peptide hormone *CLAVATA3/EMBRYO SURROUNDING REGION45* (*CLE45*) in developing SEs (Depuydt et al. 2013, Rodriguez-Villalon et al. 2014, Breda et al. 2017; Kang and Hardtke 2016). Accordingly, I presumed that the effect of *CLE45/BAM3* signalling suppressing SE differentiation is more pronounced in the RAM of *smx14;smx15* double mutants compared to wild type as well. Interestingly, root length and RAM architecture of wild type and *smx1* single mutants treated with *CLE45* resemble *smx14;smx15* double mutants (**Figure 11**). However, enhanced *CLE45* signalling does not caused obvious alterations in RAM architecture or additional reduction in root length in the *smx14;smx15* background (**Figure 11**). *smx14;smx15* double mutants exhibit residual *BAM3* expression in developing protophloem strands (**Figure 6**) which shows the plants can still perceive and transmit *CLE45* signalling. This was confirmed based on reduced *CVP2* reporter activity in *smx14;smx15* double mutants after *CLE45* treatment (**Figure 12**).

Combining the findings on primary root length and *CVP2* reporter activity in *smx14;smx15* double mutants compared to wild type, I conclude that the effect of *CLE45/BAM3* signalling is already more pronounced in SE precursor cells in *smx14;smx15* double mutants than in wild type, consequently resulting in impeded transition from SE precursor cells into developing SEs. To confirm this hypothesis, relative gene expression levels of *BAM3* and positive regulators of phloem development (*BRX*, *OPS*) remain to be compared in developing phloem strands of wild type and *smx14;smx15* double mutants.

4.3. SMXL3/4/5 protein accumulation is affected by CLE signalling

Previous analyses showed that the establishment of the phloem cell lineage is alike in young roots of *smxl4;smxl5* and wild type plants based on the same timely occurrence of the first periclinal cell division preceding the production of SE precursor cells in both genetic backgrounds (Wallner et al. 2017). Considering that primary roots of *smxl4;smxl5* double mutants resemble CLE45-treated wild type plants, these findings point toward CLE45/BAM3-independent developmental steps preceding the first periclinal cell division in the RAM of wild type and *smxl4;smxl5* mutants. Consistent with essential roles of *SMXL3/4/5* genes to establish the phloem-specific developmental program, *SMXL3/4/5* promoter activities are not affected by enhanced CLE45 signalling (**Figure 13**). However, SMXL(3)/4/5 protein accumulation is attenuated in developing protophloem cells upon CLE45 treatment except when being expressed in the *bam3* background (**Figure 14**). Importantly, SMXL(3)/4/5 protein accumulation is not yet repressed phloem initial cells (**Figure 14**). These findings are in line with *BAM3* being first expressed in SE/procambium precursor cells (Hazak et al. 2017) but not yet in phloem initial cells (**Figure 20**). Together, these findings highlight the key role of SMXL4/5 to establish the phloem cell lineage from initial cells.

Interestingly, treatments with CLE26, another root-active peptide involved in the suppression of phloem differentiation but expressed towards the end of SE differentiation, resulted in similar effects as CLE45 treatments. As for CLE45, I found that *SMXL3/4/5* promoter activities are not affected upon CLE26 treatment (**Figure 15**). Furthermore, upon CLE26 treatment, SMXL(3)/4/5 protein accumulation is not affected in phloem initial cells yet attenuated in subsequent cells of the developing protophloem strand (**Figure 15**). Unlike for CLE45, the putative receptor recognising CLE26 is still unknown. Nevertheless, it was proposed that full perception of all root-active CLE peptides is mediated by a central heterodimer complex formed by the pseudokinase CORYNE (CRN) and the receptor kinase CLAVATA2 (CLV2) (Hazak et al. 2017). Both

membrane-associated proteins are expressed in most tissues in the root tip and accumulate in BAM3-expressing phloem cells (Somssich et al. 2016) (**Figure 20**). Therefore, I propose that SMXL3/4/5 proteins are regulated strands after phloem initiation in response to root-active CLE peptides via the CRN|CLV2 heterodimer in developing phloem. This could be tested by analysing the effect of various root-active, CRN-dependent CLE peptides on SMXL3/4/5 protein accumulation in *crn* mutants.

Taken together, as SMXL3/4/5 proteins are not affected by CLE26/45 treatments in phloem initial cells but subsequently in developing phloem cells, I suggest an additional function of SMXL3/4/5 proteins in fine-tuning SE differentiation during phloem development, for example, by indirect attenuation of CLE-mediated inhibitory pathways.

4.4. Additional role of SMXL3/4/5 proteins in fine-tuning SE differentiation?

Above, I show that SMXL(3/4)5 protein accumulation is affected by CLE signalling components (**Figure 14, Figure 15**) and suggest that SMXL4/5 proteins potentially play an additional role in fine-tune the timing of SE differentiation in the meristematic zone. As SMXL3/4/5 proteins are nuclear localised, it is possible that they attenuate CLE45/BAM3 signalling indirectly by differential upregulation of *OPS*, *BRX* and *CVP2* gene activities compared to *BAM3* activity in developing phloem strands. Eventually, SEs undergo differentiation events including wall remodelling (thickening) and connect via sieve plates to form continuous phloem strands in the transition zone (Dettmer et al. 2014). Previously, it was shown that the phosphoinositide-5-phosphatase CVP2 regulates phosphatidylinositol-4,5-bisphosphate (PI(4,5)P₂) levels in developing SEs by conversion of PI(4,5)P₂ into phosphatidylinositol-4-phosphate (PI4P), thus balancing the timing of cell wall thickening and SE differentiation (Carland and Nelson 2009, Rodriguez-Villalon et al. 2015). My findings show that *CVP2* expression in turn depends on the activity of *SMXL4/5* genes (**Figure 6**). Furthermore, in developing protophloem

strands, PI(4,5)P₂ is mainly produced from PI4P by the PI4P5-KINASE1 (PIP5K1) which is recruited by and co-localises with membrane-associated proteins BRX and PROTEIN KINASE ASSOCIATED WITH BRX (PAX). As for *CVP2*, *BRX* expression also depends on *SMXL4/5* gene activity (**Figure 6**). Antagonistic activities of *CVP2* and PIP5K1 enzymes regulate the PI(4,5)P₂ level which promotes the membrane localisation of PAX as well as endocytosis of the plasma membrane integral PIN-FORMED (PIN) protein PIN1 (Marhava et al. 2020). PIN proteins are polarly localised efflux carriers for the phytohormone auxin (Benjamins and Scheres 2008). Tightly controlled auxin minima act as signals to trigger the developmental switch from dividing into differentiating cells (Di Mambro et al. 2017, Soyars et al. 2016). In the RAM, PIN1 mediates rootward auxin flow within the root meristem towards the quiescent centre and is expressed highest in stele initial cells. Protophloem and related cells lose *PIN1* expression in the transition zone of the meristem (Omelyanchuk et al. 2016). During phloem development in roots, PI(4,5)P₂-mediated PIN1 endocytosis from the plasma membrane results in intracellular auxin build up eventually leading to SE differentiation. At the same time, PI(4,5)P₂-mediated PAX localisation stabilises PIN1 and BRX localisation which mutually inhibit and promote the efflux of auxin, respectively (Marhava et al. 2020).

Together, timing of SE differentiation is at least regulated by synergistic effects of enzymes balancing PI(4,5)P₂ levels (*CVP2*, PIPK51), membrane-associated BRX|PAX complexes regulating PIN1 localisation, and local accumulation of auxin. Furthermore, *BAM3* expression is regulated by *BRX* to counteract the inhibitory effect of BAM3/CLE45-signalling on SE differentiation (Depuydt et al. 2013, Breda et al. 2019). Additionally, OPS proteins physically interact with BAM3 proteins at the membrane, thereby alleviating CRN|CLV2-mediated CLE signalling (Breda et al. 2019). I complement this picture by proposing that *SMXL3/4/5* are required in fine-tuning SE differentiation, putatively via upregulation of *OPS*, *BRX* and *CVP2* expression.

However, *SMXL3/4/5*-mediated upregulation of *BAM3* might then result in the suppression of *SMXL3/4/5* protein functions by CLE signalling components (**Figure 20**). It would be interesting to test whether a hyperactive version of the *SMXL5* protein rescues phloem defects in related mutants exhibiting deficient SE differentiation such as *ops*, *brx*, and *cvp2;cvl1* (Truernit et al. 2012, Rodriguez-Villalon et al. 2015, Breda et al. 2017).

4.5. The *smxl4;smxl5* phenotype can be suppressed by second-site mutagenesis

In Arabidopsis, the phloem suppressor gene *BAM3* was identified after second-site mutagenesis of *brx* mutants as null mutations in *BAM3* suppressed the gap cell phenotype and restored root length to wild type level (Depuydt et al. 2013). Second-site mutation in the *BAM3* gene also suppresses the *ops* mutant phenotype (Breda et al. 2017). Together, these findings led to the discovery of *BRX* and *OPS* as antagonists of *CLE45/BAM3*-mediated signalling which inhibits SE differentiation (Breda et al. 2017; Kang and Hardtke 2016). To identify genes that are functionally related to *SMXL4/5* genes during protophloem development, I performed a suppressor screen of *smxl4;smxl5* double mutants after mutagenesis using ethyl methanesulfonate (EMS) as mutagenic agent (Page and Grossniklaus 2002, Schröder et al. 2008). Indeed, EMS-based mutagenesis of *smxl4;smxl5* double mutants yielded plants with wild type-like roots and restored protophloem development (**Figure 18**). These findings are an important first step toward identifying novel genes that are functionally related to *SMXL4/5* genes in (proto)phloem development.

So far, my analysis indicates that a combination of recessive genes results in the suppression of the *smxl4;smxl5* phenotype (**Figure 19**). However, these candidate genes remain to be identified and their functions to be characterised in the context of phloem development. For now, different scenarios are conceivable: It is possible be that in mutagenised *smxl4;smxl5* double mutants, expression levels of other *SMXL*

genes are enhanced or altered and thus substitute the functions of *SMXL3/4/5* genes. It was shown that compared to other *SMXL* genes, the expression level of *SMAX1* is highest in seedlings whereas in roots, *SMXL7* transcripts are second most abundant after *SMXL3* (Stanga et al. 2013). Additionally, it was proposed that *SMAX1* and *SMXL7* genes play overlapping roles in root skewing (Swarbreck et al. 2019) and lateral root development (Villaecija-Aguilar et al. 2019). Furthermore, it was shown that *SMAX1* expressed under the promoter of *SMXL5* can replace *SMXL5* function and thus rescue phloem development in *smxl4;smxl5* double mutants (Wallner et al. 2017). Therefore, it is possible that altered genes functions or expression patterns of *SMAX1*, *SMXL7*, or other *SMXLs* result in the restoration of phloem development in EMS-treated *smxl4;smxl5* double mutants. Alternatively, combined expression levels or gene activities of other positive regulators of phloem development (*OPS*, *BRX*, *CVP2*) might be enhanced in *smxl4;smxl5* primary roots after mutagenesis, thus restoring phloem formation in an additive way.

Reversely, the CLE signalling pathway inhibiting phloem development might be affected in *smxl4;smxl5* primary roots after mutagenesis. Altered genes could include CLE signalling components such as *CLE45*, *BAM3*, *CRN*, or *CLERK* (Depuydt et al. 2013, Hazak et al. 2017, Anne et al. 2018). Other than *BAM3* which is a CRN-dependent receptor of the *CLE45* peptide in developing SEs (Depuydt et al. 2013, Hazak et al. 2017), *CLERK* recognises the *CLE25* peptide (Ren et al. 2019) and its signalling is independent of CRN (Anne et al. 2018). Loss of function of the *CLERK* gene causes premature production of SE precursor cells as visualised by earlier expression of *CVP2* in *clerk* mutants compared to wild type (Anne et al. 2018). Thus, during early steps of phloem initiation, *CLE25/CLERK* might function antagonistically to the *SMXL3/4/5*, and loss of function in either *CLERK* or *CLE25* genes could rescue the *smxl4;smxl5* phenotype.

Further analyses including genome mapping are now required to identify those candidate genes that result in the suppression of the *smx14;smx15* mutant phenotype.

4.6. Synchronised development of SEs and CCs via translational control of *SMXL5*?

The phloem functions as plant-wide communication network integrating post-embryonic development and cellular energy status in a plastic manner (Cho et al. 2018, De Rybel et al. 2015). Formation of functional SEs is accompanied by selective elimination of subcellular organelles including the nucleus, remodelling of the cell wall to form connective sieve plates along phloem strand and plasmodesmata between SEs and neighbouring CCs (Mähönen et al. 2000, Oparka and Turgeon 1999; Otero and Helariutta 2017, Evert and Eichhorn 2006, Cho et al. 2018). Compared to other tissues, protophloem strands are the earliest to differentiate in the root tip before the end of the transition zone while other cell types are still elongating (Bonke et al. 2003, Blob et al. 2018). Higher up in roots, in the elongation zone, protophloem strands are functionally replaced by metaphloem strands (Lalonde et al. 2003, Mähönen et al. 2014) which again connect with CCs through plasmodesmata (**Figure 2**).

So far, little is known about how *SMXL3/4/5* functions are regulated in the context of phloem development or how their regulation might be linked to CC development. However, it was proposed that sucrose functions as signalling molecule to integrate source-sink relationships into phloem development by local control of *SMXL5* translation via RNA binding proteins (RBPs) (Cho et al. 2018-2). RBPs play a central role in translational regulation of phloem differentiation, potentially due to long-distance transport of mRNAs from SE-CC complexes into undifferentiated phloem cells (Cho et al. 2018, Cho et al. 2018-2). Of those, the RBP JULG1 (*JUL1*) is expressed specifically in phloem and cambium regions in the stem, and in vascular bundles of roots in the elongation and maturation zones (Cho et al. 2018). *JUL1* binds to *SMXL5* transcripts in differentiated SEs, subsequently suppressing *SMXL5* translation when sucrose

levels are high (Cho et al. 2018, Gonzali et al. 2006). Conversely, SMXL5 translation is undisturbed by JUL1 in SE precursor cells due to low sucrose levels.

Other than protophloem SE differentiation, maturation of CC occurs early in the transition zone and can be marked by the CC-specific gene *SODIUM POTASSIUM ROOT DEFECTIVE1 (NaKR1)* (Gujas et al. 2020). It was shown that CC differentiation is affected in mutants exhibiting gap cells, and that CLE45-mediated inhibition of phloem development suppresses the expression of the CC-specific *SUCROSE TRANSPORTER2 (SUC2)* gene (Rodriguez-Villalon et al. 2014). These findings imply that CLE45 signalling is not restricted to BAM3-expressing phloem cells but extends radially to CCs. This also suggests that SE and CC development are highly interconnected. In fact, recent findings confirmed that protophloem SE surrounding cells, visualised by the activity of the *SISTER OF APL (SAPL)* gene, perceive CLE signalling when triggered by several peptides including CLE25, CLE26 and CLE45 (Gujas et al. 2020). Additionally, CLE45 signalling is perceived by the RECEPTOR PROTEIN LIKE KINASE2 (RPK2) in protophloem SE-surrounding cells and procambial cells toward the end of the meristematic zone (Gujas et al. 2020). Together, it was proposed that CLE peptides are secreted from SEs and distributed radially into CCs where they are perceived by RPK2. Subsequently, RPK2 restricts SE identity to developing phloem strands (Gujas et al. 2020).

Interestingly, the authors found that CLE45 treatments do not alter gene expression of *SMXL3* in phloem initial cells which is in line with my data on CLE treatments (**Figure 13, Figure 14, Figure 15**) and supports the hypothesis that CLE45 signalling has no effect on *SMXL3/4/5* during the initiation of phloem development. Furthermore, it was shown that gap cells exhibit features of both SEs and CCs based on simultaneous gene activities of *CVP2* (SEs), *NaKR1* (CCs), *SAPL* and *RPK2* ('surrounding cells'). It was therefore proposed that SEs and CCs can be 'swapped' during early phloem

development in the meristematic/transition zone, thus ensuring continuous and plastic growth of phloem strands (Gujas et al. 2020). In the context of *smxl4;smxl5* double mutants, phloem development is inhibited due to impaired differentiation of SEs in the primary root (Wallner et al. 2017) including reduced expression of genes regulating phloem development in developing protophloem strands (**Figure 6**). Highlighting the delayed appearance of *CVP2*-expressing, developing SEs (**Figure 12**) subsequent to the second periclinal cell division (Wallner et al. 2017) in *smxl4;smxl5* mutants compared to wild type, I then proposed that impaired phloem formation in *smxl4;smxl5* double mutants correlates with continued cell divisions of SE precursor cell in the RAM. As root tips eventually fail to develop distinct transition, elongation and differentiation zones in the *smxl4;smxl5* background, I presume that CC maturation is also impaired in these mutants. Analyses of double marker lines visualising promoter activities of genes representative for developing SEs (*CVP2*) (Rodriguez-Villalon et al. 2014) and CCs (*NaKR1*, *SUC2*) (Gujas et al. 2020, Rodriguez-Villalon et al. 2014) in *smxl4;smxl5* double mutants compared to wild type could be a start to test hypothesis.

4.7. Non-identical roles of *SMXL3/4/5* in primary and secondary phloem development

SMXL3/4/5 genes promote phloem development not only in the root, but also in aerial parts of Arabidopsis including the stem (Wallner et al. 2020). Unlike in the RAM where primary phloem strands derive from precursor cells that also give rise to procambium strands (Mähönen et al. 2000, Lucas et al. 2013), secondary phloem tissues in the stem base derive from cambial cells. Cambial cells maintain a radial, secondary meristem and produce secondary vasculature (Lucas et al. 2013, Jouannet et al. 2015, Shi et al. 2019). Due to different cellular origins, it is intriguing to investigate whether the molecular mechanisms involving *SMXL3/4/5* genes and promoting primary and secondary phloem development share similar features.

Indeed, in *smx14;smx15* double mutants, activities of phloem regulators including *BRX*, *BAM3* and *APL* are not only reduced in developing protophloem strands (**Figure 6**) but also during phloem formation in the stem base. The latter was discovered by comparing transcript levels in the stem base of *smx14;smx15* mutants and wild type (Wallner et al. 2020). Furthermore, similar to delayed phloem development in *smx14;smx15* primary roots possibly due to increased number of undifferentiated SE precursor cells, impaired phloem formation in the stem base results from increases number of undifferentiated cambium-derived cells compared to wild type (Wallner et al. 2020, Cho et al. 2018, Wallner et al. 2017). Unlike in the RAM, however, *SMXL5* loss of function has a stronger impact on phloem differentiation in the cambium. In the RAM of *smx15* single mutants, the second periclinal cell division forming protophloem strands is delayed compared to wild type, yet not as delayed as in *smx14;smx15* double mutants (Wallner et al. 2019). Furthermore, primary roots of *smx15* single mutants eventually form functional phloem strands and resemble wild type roots (Wallner et al. 2017). Conversely, loss of *SMXL5* function already results in the absence of secondary phloem in the stem base (Wallner et al. 2020). Different from the RAM, *SMXL3* is not expressed during secondary phloem formation in the cambium which implies a dominant role of *SMXL5* in secondary compared to primary phloem formation (Wallner et al. 2020).

Taken together, molecular mechanism featuring *SMXL3/4/5* genes to promote phloem development in below- and above-ground tissues are probably shared, but not identical (Wallner et al. 2020), and need further studies.

4.8. Role of *SMXL5* in non-phloem related cell fate regulation in the SAM?

Formation of post-embryonic vasculature in root tips of *Arabidopsis* derives from embryonic, provascular cells and gives rise to vascular stem cells in the RAM. Conversely, vascular tissues in aerial parts of the plant do not originate in the shoot

apical meristem (SAM) but derive from non-vascular, procambium cells which start to differentiate in the cotyledons and subsequently in the axis (Bauby et al. 2007, Lucas et al. 2013). Interestingly, several components related to the molecular network regulating post-embryonic phloem development in the RAM play roles in balancing cell division and differentiation in the SAM. These components include CLE peptides, BAM receptors, CLV2, CRN and RPK2 (Lee et al. 2019, Yamaguchi et al. 2016, Soyars et al. 2016). Considering this combination of molecular players opens room for speculation that SMXL5 may be involved in other, non-phloem related mechanisms such as SC maintenance. To maintain the SC population in the SAM, the homeodomain transcription factor WUSCHEL (*WUS*), expressed in the organising centre (OC), moves to the above-located central zone (CZ) via plasmodesmata where it represses differentiation and activates the expression of the CLE peptide CLAVATA3 (*CLV3*). In turn, *CLV3* is secreted from the CZ and diffuses into the OC where it is perceived by the homomeric receptor kinase CLAVATA1(*CLV1*)|*CLV1*, subsequently dampening the expression of *WUS* which causes a negative feedback loop between *CLV3*-*WUS* signalling and thus restricts the number of SCs in the CZ (Soyars et al. 2016, Yamaguchi et al. 2016). Additionally, *CLV3* bind to *CLV1*|*CLV1* in the rib meristem (RM) below the OC causing a repression of *BAM* genes (Nimchuk et al. 2015). Heteromeric receptor kinase complexes including *BAM1*|*BAM2* (DeYoung et al. 2006) and *CLV2*|*CRN* (Müller et al. 2008, Nimchuk et al. 2011) also bind *CLV3* in the RM and subsequently dampen *WUS* expression (Nimchuk et al. 2015, Soyars et al. 2016). Furthermore, the receptor kinase *RPK2* is involved in the perception of *CLV3* signalling (Shinohara and Matsubayashi 2015) yet it remains unclear which additional component binds the *CLV3* peptide.

Other than in the root tip, *BAMs* and *CLV2*|*CRN* do not interact physically to enhance CLE peptide signalling in the SAM (Nimchuk et al. 2015). Intriguingly, one of the genes promoting *WUS* activity in the SAM is *OBERON3* (*OBE3*) (Lin et al. 2016). *OBE3*

encodes protein that contains a plant homeodomain (PHD)-finger motif which is known to bind to specifically modified histone tails indicative for actively transcribed or silent chromatin regions (Sanchez and Zhou 2011). In the SAM, *OBE3* appears to act downstream of *WUS* and both gene activities reinforce each other's expression in a positive feedback loop (Lin et al. 2016). Recent findings show that *OBE3* is also involved in cell fate regulation in the RAM (Wallner et al. 2019). Here, *OBE3* proteins form a functional unit with *SMXL5* proteins during protophloem development, supposedly promoting chromatin remodelling and/or transcriptional regulation of downstream targets (Wallner et al. 2019). Furthermore, *obe3;smxl5* double mutant seedlings are short-rooted and develop the same protophloem defects as *smxl4;smxl5* double mutants, indicating that *OBE3*-*SMXL5* complex-dependent formation of a distinct chromatin profile that is essential to establish a general phloem-specific developmental program (Wallner et al. 2019).

Taken together, several molecular players mediating CLE signalling are shared in post-embryonic phloem development in the RAM as well as SC homeostasis in the SAM. Furthermore, genetic interactions between *SMXL5-OBE3* and *OBE3-WUS* in the RAM and SAM, respectively, and the potential involvement of *SMXL5-OBE3* protein complexes in chromatin remodelling and/or transcriptional regulation open room for speculation that *SMXL5* might be involved in cell fate regulation independent of the phloem lineage. To test this hypothesis, potential expression of *SMXL5* in the SAM remains to be analysed and compared to *OBE3* expression. If *SMXL5* is not expressed in the SAM but exclusively in developing vascular cells, *SMXL5* might instead regulate phloem development of early vascular cells upon leaving the SAM, putatively in interaction with *OBE3*.

4.9. SMXL5 protein function is independent of the EAR motif

Like other members of the *SMXL* family, these genes encode redundantly acting, cell-autonomous, nuclear localised proteins supposedly involved in transcriptional repression during various developmental processes (Machin et al. 2019, Villacéija-Aguilar et al. 2019, Moturu et al. 2018, Walker et al. 2019). However, whether specific protein domains are relevant for SMXL3/4/5 protein function during phloem development is largely unknown. Recently, it was proposed that OBE3-SMXL5 protein interactions promote the formation of a distinct chromatin profile is essential to establish the phloem-specific developmental program (Wallner et al. 2019). Interestingly, Arabidopsis SMXL proteins all share one conserved ETHYLENE-RESPONSIVE ELEMENT BINDING FACTOR-ASSOCIATED AMPHIPHILIC REPRESSION (EAR) motif (LxLxL/I) (Soundappan et al. 2015, Ma et al. 2017, Wallner et al. 2017) which represents the most predominant transcriptional repression motif identified in plants (Ohta et al. 2001). However, the significance of the EAR motif for SMXL protein function is still unclear. In fact, my data show that SMXL5 protein localisation is independent of the EAR motif (**Figure 16**). Furthermore, root growth and phloem development is restored in *smxl4;smxl5* double mutants expressing EAR motif-mutated SMXL5 proteins, thus demonstrating that it is not essential for the function or dynamics of the SMXL5 protein in developing protophloem cells (**Figure 16**). It was also shown that deletion of the EAR motif of the SMXL7 protein has no effect on its localisation or degradation in Arabidopsis. Furthermore, while leaf morphology and branch angle are independent of the SMXL7 EAR motif, branch number and plant height are altered upon loss of the EAR motif suggesting different sensitivities to the EAR motif and distinct downstream mechanisms of SMXL7 (Liang et al. 2016). These findings are further supported by previously performed bioinformatics analyses revealing that for a notable number of Arabidopsis proteins, their EAR motif might have no functional relevance after all (Kagale and Rozwadowski 2010).

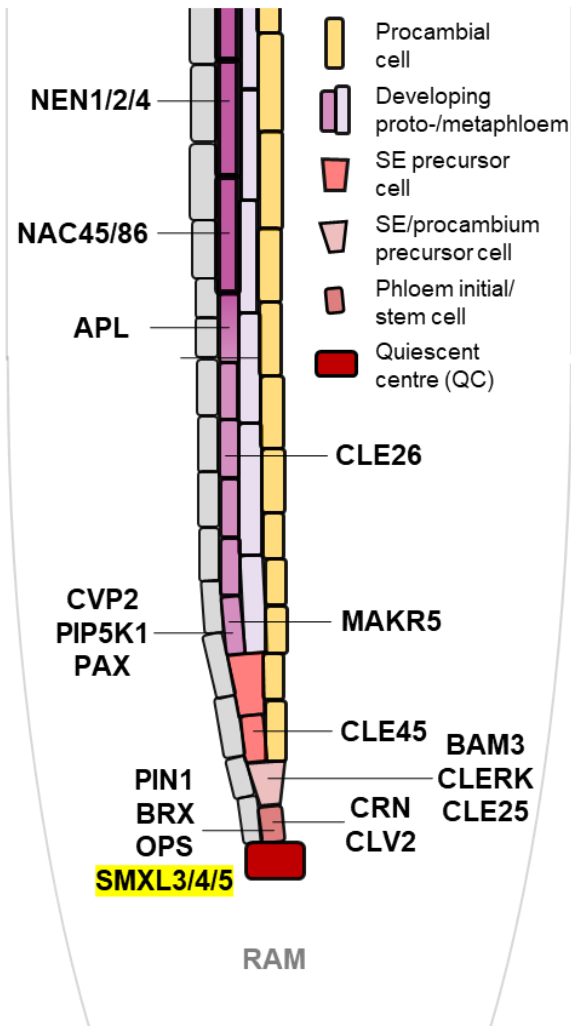
Nevertheless, the EAR motif has been viewed as a 'hallmark' of transcription repressors through interaction with TOPLESS (TPL) and TPL-RELATED (TPR) corepressors which play a key role in hormone signalling and development (Long et al. 2006, Krogan and Long 2009, Causier et al. 2012, Martin-Arevalillo et al. 2017, Kagale and Rozwadowski 2011). EAR-mediated interactions between SMXLs (SMXL6/7/8) and TPR2 have previously been discovered in rice, Arabidopsis, and barley (Smith and Li, 2014, Soundappan et al. 2015, Wang et al. 2015, Ma et al. 2017). My data show that SMXL5 protein indeed co-localises with TPR2 and TPR4 proteins in nuclei of *Nicotiana benthamiana* and mutating the SMXL5 EAR motif does not change its co-localisation with TPR2 (**Figure 17**). However, these findings do not provide information on protein-protein interaction between SMXL5 and TPR2/4. To investigate protein-protein interactions *in planta*, transient coexpression and subsequent co-immunoprecipitation assays of native and EAR motif-mutated SMXL5 proteins with TPR2/4 proteins remain to be performed. In this way, a conclusive answer could be found as to whether SMXL5 proteins interact with TPR corepressors in an EAR-dependent manner.

Conclusion

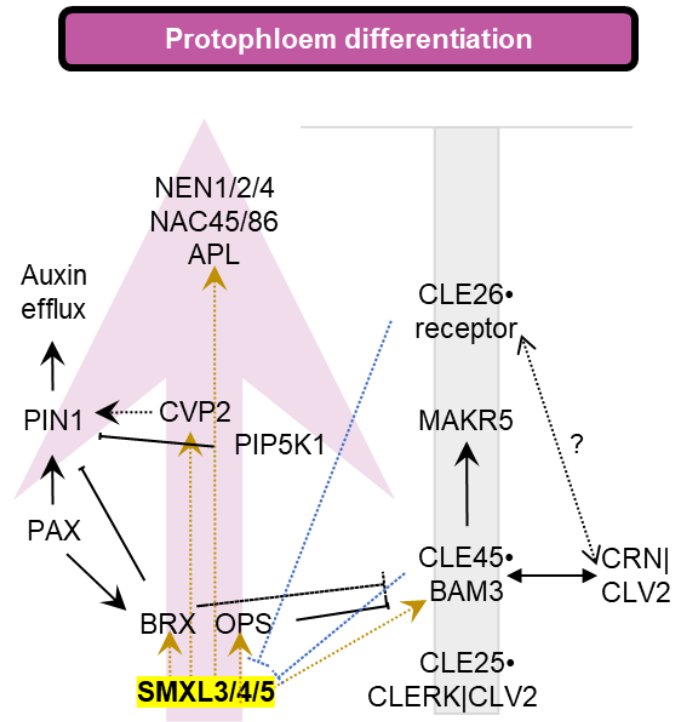
In conclusion, I postulate that *SMXL3*, *SMXL4* and *SMXL5* genes are essential to establish the post-embryonic phloem lineage in the RAM through sequential upregulation of genes that subsequently regulate phloem development. Genes activated by *SMXL4/5* include *OCTOPUS (OPS)*, *BREVIS RADIX (BRX)*, *BARELY ANY MERISTEM (BAM3)*, *COTYLEDON VASCULAR PATTERN (CVP2)* and *ALTERED PHLOEM FORMATION (APL)* which regulate the phloem-specific developmental program in a spatiotemporal manner. Additionally, *SMXL3/4/5* functions are putatively required to attenuate inhibitory pathways (CLE signalling) and balance final steps of SE differentiation (cell wall remodelling, enucleation) in the transition zone. Together, a complex, tightly balanced network of molecular players depending on *SMXL3/4/5* activities ensures the formation of phloem within the root system (**Figure 20**).

Figure 20 (next page): A complex, tightly balanced network of molecular players depending on *SMXL3/4/5* regulates the formation of functional phloem strands in the root. **(A)** *SMXL3*, *SMXL4* and *SMXL5* genes are required to establish the phloem lineage in the RAM and activate sequential expression of subsequent regulators. Different from previous publications (**Figure 4**), *OPS* and *BRX* are already expressed in phloem initial cells. **(B)** *SMXL3/4/5* promote expression of phloem regulators starting in phloem initial cells and are regulated by CLE signalling components in developing SEs. Solid lines indicate physical interaction, dotted lines indicate interaction via (unknown) downstream signalling, dot after CLE peptide indicates binding to receptor. Yellow lines indicate *SMXL3/4/5* activities, blue lines indicate pathways suppressing *SMXL3/4/5*. (A) Illustration based on own data, (AB) regulators and scheme based on this dissertation and data published in Rodriguez-Villalon et al. 2014, Rodriguez-Villalon et al. 2015, Hazak et al. 2017, Depuydt et al. 2013, Bonke et al. 2003, Wallner et al. 2017, Anne et al. 2018, Somssich et al. 2016, Gujas et al. 2020, Kang and Hardtke 2016, Blob et al. 2018, Furuta et al. 2014, Omelyanchuk et al. 2016, Marhava et al. 2018, Marhava et al. 2020.

A Sequential expression of regulators



B Proposed molecular mechanisms



Positive regulators:

- NEN** NAC45/86-DEPENDENT EXONUCLEASE-DOMAIN
- NAC** NO APICAL MERISTEM
- APL** ALTERED PHLOEM DEVELOPMENT
- CVP2** COTYLEDON VASCULAR PATTERN
- PIN1** PIN-FORMED1
- PIP5K1** PI4P5-KINASE1
- PAX** PROTEIN KINASE ASSOCIATED WITH BRX
- BRX** BREVIS RADIX
- OPS** OCTOPUS
- SMXL** SMAX1-LIKE

Negative regulators:

- CLE** CLAVATA3/EMBRYO SURROUNDING REGION
- MAKR5** MEMBRANE ASSOCIATED KINASE REGULATOR5
- BAM3** BARELY ANY MERISTEM3
- CLERK** CLE-RESISTANT RECEPTOR KINASE
- CRN** CORYNE
- CLV2** CLAVATA2

Figure 20: *SMXL3/4/5* initiate and modulate the phloem-specific developmental program in roots.

List of Figures

Figure 1:	
Vascular tissues in Arabidopsis organs.	2
Figure 2:	
Early phloem development in root tips.	5
Figure 3:	
Sugar transport from source to sink organs.	7
Figure 4:	
Early regulators of phloem development.	15
Figure 5:	
Developmental involvement and functional domains of SMXL proteins.	20
Figure 6 :	
Activities of early phloem genes are reduced in <i>smxl4;smxl5</i> double mutants.	40
Figure 7:	
Genetic interaction of <i>SMXL5</i> with <i>BRX</i> and <i>OPS</i> .	45
Figure 8:	
<i>OPS</i> is not required to stimulate <i>SMXL4</i> and <i>SMXL5</i> gene activities during early steps of protophloem development.	46
Figure 9:	
<i>SMXL5</i> expression restores protophloem development under the control of heterologous promoters.	48
Figure 10:	
<i>APL</i> is not active in <i>smxl4;smxl5</i> double mutants.	50
Figure 11:	
CLE45-treated plants resemble <i>smxl4;smxl5</i> double mutants.	52
Figure 12:	
<i>smxl4;smxl5</i> double mutants perceive enhanced CLE45/BAM3 signalling.	54

Figure 13:	
<i>SMXL3/4/5</i> promoter activities are not affected by CLE45/BAM3 signalling.	56
Figure 14:	
CLE45/BAM3 signalling influences SMXL protein accumulation in protophloem strands.	59
Figure 15:	
CLE26 signalling affects SMXL3/4/5 protein accumulation in protophloem strands.	61
Figure 16:	
EAR motif-mutated SMXL5 proteins are nuclear localised and restore protophloem development in <i>smx14;smx15</i> double mutants.	64
Figure 17:	
Transient expression of SMXL5-mCherry, SMXL5 ^{mEAR} -mCherry and TPR2/4-mGFP fusion proteins in nuclei of <i>Nicotiana benthamina</i> .	67
Figure 18:	
EMS-based mutagenesis of <i>smx14;smx15</i> mutants yielding long-rooted, wild type-like plants.	69
Figure 19:	
Restored root length and protophloem development probably result from a combination of recessive, second-site mutations in the <i>smx14;smx15</i> background.	72
Figure 20:	
<i>SMXL3/4/5</i> initiate and modulate the phloem-specific developmental program in roots.	95

List of Tables

Table 1:	
Arabidopsis lines used in this dissertation.	24
Table 2:	
Primers used for mutant genotyping in this dissertation.	28
Table 3:	
Primers used for gene cloning in this dissertation.	30
Table 4:	
Entry vectors cloned and used in this dissertation.	31
Table 5:	
Destination vectors cloned in this dissertation.	32

Bibliography

- Aguila Ruiz Sola, M., Coiro, M., Crivelli, S., Zeeman, S. C., Schmidt Kjølner Hansen, S. and Truernit, E. (2017) 'OCTOPUS-LIKE 2, a novel player in Arabidopsis root and vascular development, reveals a key role for OCTOPUS family genes in root metaphloem sieve tube differentiation', *New Phytologist*. doi: 10.1111/nph.14751.
- Aichinger, E., Kornet, N., Friedrich, T. and Laux, T. (2012) 'Plant Stem Cell Niches', *Annual Review of Plant Biology*. doi: 10.1146/annurev-arplant-042811-105555.
- Anne, P., Amiguet-Vercher, A., Brandt, B., Kalmbach, L., Geldner, N., Hothorn, M. and Hardtke, C. S. (2018) 'CLERK is a novel receptor kinase required for sensing of root-active CLE peptides in arabidopsis', *Development (Cambridge)*, 145(10). doi: 10.1242/dev.162354.
- Anne, P. and Hardtke, C. S. (2018) 'Phloem function and development — biophysics meets genetics', *Current Opinion in Plant Biology*. doi: 10.1016/j.pbi.2017.12.005.
- Bauby, H., Divol, F., Truernit, E., Grandjean, O. and Palauqui, J. C. (2007) 'Protophloem differentiation in early Arabidopsis thaliana development', *Plant and Cell Physiology*. doi: 10.1093/pcp/pcl045.
- Benjamins, R. and Scheres, B. (2008) 'Auxin: The Looping Star in Plant Development', *Annual Review of Plant Biology*. doi: 10.1146/annurev.arplant.58.032806.103805.
- Blob, B., Heo, J. and Helariutta, Y. (2018) 'Phloem differentiation: an integrative model for cell specification', *Journal of Plant Research*, 131(1). doi: 10.1007/s10265-017-0999-0.
- Bonke, M., Thitamadee, S., Mähönen, A. P., Hauser, M. T. and Helariutta, Y. (2003) 'APL regulates vascular tissue identity in Arabidopsis', *Nature*. doi: 10.1038/nature02100.
- Breda, A. S., Hazak, O. and Hardtke, C. S. (2017) 'Phosphosite charge rather than shootward localization determines OCTOPUS activity in root protophloem', *Proceedings of the National Academy of Sciences*, 114(28). doi: 10.1073/pnas.1703258114.
- Breda, A. S., Hazak, O., Schultz, P., Anne, P., Graeff, M., Simon, R. and Hardtke, C. S. (2019) 'A Cellular Insulator against CLE45 Peptide Signaling', *Current Biology*. doi: 10.1016/j.cub.2019.06.037.
- Bythell-Douglas, R., Rothfels, C. J., Stevenson, D. W. D., Graham, S. W., Wong, G. K. S., Nelson, D. C. and Bennett, T. (2017) 'Evolution of strigolactone receptors by gradual neofunctionalization of KAI2 paralogues', *BMC Biology*. doi: 10.1186/s12915-017-0397-z.
- Carland, F. M., Berg, B. L., Fitzgerald, J. N., Jinamornphongs, S., Nelson, T. and Keith, B. (1999) 'Genetic regulation of vascular tissue patterning in Arabidopsis', *Plant Cell*. doi: 10.1105/tpc.11.11.2123.
- Carland, F. and Nelson, T. (2009) 'CVP2- and CVL1-mediated phosphoinositide signaling as a regulator of the ARF GAP SFC/VAN3 in establishment of foliar vein patterns', *Plant Journal*. doi: 10.1111/j.1365-313X.2009.03920.x.
- Causier, B., Ashworth, M., Guo, W. and Davies, B. (2012) 'The TOPLESS interactome: A framework for gene repression in Arabidopsis', *Plant Physiology*. doi: 10.1104/pp.111.186999.
- Chen, L. Q., Qu, X. Q., Hou, B. H., Sosso, D., Osorio, S., Fernie, A. R. and Frommer, W. B. (2012) 'Sucrose efflux mediated by SWEET proteins as a key step for phloem transport', *Science*. doi: 10.1126/science.1213351.

- Cho, H., Cho, H. S., Nam, H., Jo, H., Yoon, J., Park, C., Dang, T. V. T., Kim, E., Jeong, J., Park, S., Wallner, E. S., Youn, H., Park, J., Jeon, J., Ryu, H., Greb, T., Choi, K., Lee, Y., Jang, S. K. *et al.* (2018) 'Translational control of phloem development by RNA G-quadruplex-JULGI determines plant sink strength', *Nature Plants*. doi: 10.1038/s41477-018-0157-2.
- Cho, H., Cho, H. S., and Hwang, I. (2018). 'In vivo action of RNA G-quadruplex in phloem development', *BMB reports*. doi: 10.5483/BMBRep.2018.51.11.253
- Clough, S. J. and Bent, A. F. (1998) 'Floral dip: A simplified method for Agrobacterium-mediated transformation of *Arabidopsis thaliana*', *Plant Journal*. doi: 10.1046/j.1365-313X.1998.00343.x.
- Cock, J. M. and McCormick, S. (2001) 'A large family of genes that share homology with *Clavata3*', *Plant Physiology*. doi: 10.1104/pp.126.3.939.
- Conn, C. E., Bythell-Douglas, R., Neumann, D., Yoshida, S., Whittington, B., Westwood, J. H., Shirasu, K., Bond, C. S., Dyer, K. A. and Nelson, D. C. (2015) 'Convergent evolution of strigolactone perception enabled host detection in parasitic plants', *Science*. doi: 10.1126/science.aab1140.
- Depuydt, S., Rodriguez-Villalon, A., Santuari, L., Wyser-Rmili, C., Ragni, L. and Hardtke, C. S. (2013) 'Suppression of *Arabidopsis* protophloem differentiation and root meristem growth by CLE45 requires the receptor-like kinase BAM3', *Proceedings of the National Academy of Sciences*. doi: 10.1073/pnas.1222314110.
- Dettmer, J., Ursache, R., Campilho, A., Miyashima, S., Belevich, I., O'Regan, S., Mullendore, D. L., Yadav, S. R., Lanz, C., Beverina, L., Papagni, A., Schneeberger, K., Weigel, D., Stierhof, Y. D., Moritz, T., Knoblauch, M., Jokitalo, E. and Helariutta, Y. (2014) 'CHOLINE TRANSPORTER-LIKE1 is required for sieve plate development to mediate long-distance cell-to-cell communication', *Nature Communications*. doi: 10.1038/ncomms5276.
- DeYoung, B. J., Bickle, K. L., Schrage, K. J., Muskett, P., Patel, K. and Clark, S. E. (2006) 'The CLAVATA1-related BAM1, BAM2 and BAM3 receptor kinase-like proteins are required for meristem function in *Arabidopsis*', *Plant Journal*. doi: 10.1111/j.1365-313X.2005.02592.x.
- Dolan, L., Janmaat, K., Willemsen, V., Linstead, P., Poethig, S., Roberts, K. and Scheres, B. (1993) 'Cellular organisation of the *Arabidopsis thaliana* root', *Development*.
- Durand, M., Mainson, D., Porcheron, B., Maurousset, L., Lemoine, R. and Pourtau, N. (2018) 'Carbon source–sink relationship in *Arabidopsis thaliana*: the role of sucrose transporters', *Planta*. doi: 10.1007/s00425-017-2807-4.
- Evert, R. F., and Eichhorn, S. E. (2006) 'Meristems, Cells, and Tissues of the Plant Body: Their Structure, Function, and Development. Esau's Plant Anatomy, 3rd edn', *Wiley InterScience, MA, USA*.
- Fukuda, H. and Hardtke, C. S. (2019) 'Peptide signaling pathways in vascular differentiation', *Plant Physiology*. doi: 10.1104/pp.19.01259.
- Furuta, K. M., Yadav, S. R., Lehesranta, S., Belevich, I., Miyashima, S., Heo, J. ok, Vatén, A., Lindgren, O., De Rybel, B., Van Isterdael, G., Somervuo, P., Lichtenberger, R., Rocha, R., Thitamadee, S., Tähtiharju, S., Auvinen, P., Beeckman, T., Jokitalo, E. and Helariutta, Y. (2014) 'Plant development. *Arabidopsis* NAC45/86 direct sieve element morphogenesis culminating in enucleation.', *Science (New York, N.Y.)*. doi: 10.1126/science.1253736.
- Gonzali, S., Loreti, E., Solfanelli, C., Novi, G., Alpi, A. and Perata, P. (2006) 'Identification of sugar-modulated genes and evidence for in vivo sugar sensing in *Arabidopsis*', *Journal of Plant Research*. doi: 10.1007/s10265-005-0251-1.

- Gujas, B., Alonso-Blanco, C. and Hardtke, C. S. (2012) 'Natural arabidopsis brx loss-of-function alleles confer root adaptation to acidic soil', *Current Biology*. doi: 10.1016/j.cub.2012.08.026.
- Gujas, B., Kastanaki, E., Sturchler, A., Cruz, T. M. D., Ruiz-Sola, M. A., Dreos, R., Eicke, S., Truernit, E. and Rodriguez-Villalon, A. (2020) 'A Reservoir of Pluripotent Phloem Cells Safeguards the Linear Developmental Trajectory of Protophloem Sieve Elements', *Current Biology*. doi: 10.1016/j.cub.2019.12.043.
- Hazak, O., Brandt, B., Cattaneo, P., Santiago, J., Rodriguez-Villalon, A., Hothorn, M. and Hardtke, C. S. (2017) 'Perception of root-active CLE peptides requires CORYNE function in the phloem vasculature', *EMBO reports*, 18(8). doi: 10.15252/embr.201643535.
- Ivanov, V. B. and Dubrovsky, J. G. (2013) 'Longitudinal zonation pattern in plant roots: Conflicts and solutions', *Trends in Plant Science*. doi: 10.1016/j.tplants.2012.10.002.
- Jiang, L., Liu, X., Xiong, G., Liu, H., Chen, F., Wang, L., Meng, X., Liu, G., Yu, H., Yuan, Y., Yi, W., Zhao, L., Ma, H., He, Y., Wu, Z., Melcher, K., Qian, Q., Xu, H. E., Wang, Y. *et al.* (2013) 'DWARF 53 acts as a repressor of strigolactone signalling in rice', *Nature*. doi: 10.1038/nature12870.
- John, A. and Nimchuk, Z. L. (2019) 'A little goes a long way: CLE peptides mediate phloem initiation', *Journal of Integrative Plant Biology*. doi: 10.1111/jipb.12868.
- Jouannet, V., Brackmann, K. and Greb, T. (2015) '(Pro)cambium formation and proliferation: Two sides of the same coin?', *Current Opinion in Plant Biology*. doi: 10.1016/j.pbi.2014.10.010.
- Kagale, S., Links, M. G. and Rozwadowski, K. (2010) 'Genome-Wide Analysis of Ethylene-Responsive Element Binding Factor-Associated Amphiphilic Repression Motif-Containing Transcriptional Regulators in Arabidopsis', *PLANT PHYSIOLOGY*. doi: 10.3390/s18103522.
- Kagale, S. and Rozwadowski, K. (2011) 'EAR motif-mediated transcriptional repression in plants: An underlying mechanism for epigenetic regulation of gene expression', *Epigenetics*. doi: 10.4161/epi.6.2.13627.
- Kang, Y. H. and Hardtke, C. S. (2016) 'Arabidopsis MAKR5 is a positive effector of BAM3-dependent CLE45 signaling', *EMBO reports*. doi: 10.15252/embr.201642450.
- Kieffer, M., Stern, Y., Cook, H., Clerici, E., Maulbetsch, C., Laux, T. and Davies, B. (2006) 'Analysis of the transcription factor WUSCHEL and its functional homologue in Antirrhinum reveals a potential mechanism for their roles in meristem maintenance', *Plant Cell*. doi: 10.1105/tpc.105.039107.
- Knoblauch, M., Knoblauch, J., Mullendore, D. L., Savage, J. A., Babst, B. A., Beecher, S. D., Dodgen, A. C., Jensen, K. H. and Holbrook, N. M. (2016) 'Testing the Münch hypothesis of long distance phloem transport in plants', *eLife*. doi: 10.7554/eLife.15341.
- Krogan, N. T. and Long, J. A. (2009) 'Why so repressed? Turning off transcription during plant growth and development', *Current Opinion in Plant Biology*. doi: 10.1016/j.pbi.2009.07.011.
- Lalonde, S., Tegeder, M., Throne-Holst, M., Frommer, W. B. and Patrick, J. W. (2003) 'Phloem loading and unloading of sugars and amino acids', *Plant, Cell and Environment*. doi: 10.1046/j.1365-3040.2003.00847.x.
- Lampropoulos, A., Sutikovic, Z., Wenzl, C., Maegele, I., Lohmann, J. U. and Forner, J. (2013) 'GreenGate - A novel, versatile, and efficient cloning system for plant transgenesis', *PLoS ONE*. doi: 10.1371/journal.pone.0083043.

- Lee, H., Jun, Y. S., Cha, O. K. and Sheen, J. (2019) 'Mitogen-activated protein kinases MPK3 and MPK6 are required for stem cell maintenance in the Arabidopsis shoot apical meristem', *Plant Cell Reports*. doi: 10.1007/s00299-018-2367-5.
- Li, S., Chen, L., Li, Y., Yao, R., Wang, F., Yang, M., Gu, M., Nan, F., Xie, D. and Yan, J. (2016) 'Effect of GR24 Stereoisomers on Plant Development in Arabidopsis', *Molecular Plant*. doi: 10.1016/j.molp.2016.06.012.
- Liang, Y., Ward, S., Li, P., Bennett, T. and Leyser, O. (2016) 'SMAX1-LIKE7 signals from the nucleus to regulate shoot development in Arabidopsis via partially EAR motif-independent mechanisms', *Plant Cell*. doi: 10.1105/tpc.16.00286.
- Lin, T. F., Saiga, S., Abe, M. and Laux, T. (2016) 'OBE3 and WUS interaction in shoot meristem stem cell regulation', *PLoS ONE*. doi: 10.1371/journal.pone.0155657.
- Long, J. A., Ohno, C., Smith, Z. R. and Meyerowitz, E. M. (2006) 'TOPLESS regulates apical embryonic fate in Arabidopsis', *Science*. doi: 10.1126/science.1123841.
- López-Salmerón, V., Cho, H., Tonn, N. and Greb, T. (2019) 'The Phloem as a Mediator of Plant Growth Plasticity', *Current Biology*, 29(5). doi: 10.1016/j.cub.2019.01.015.
- Lucas, W. J., Groover, A., Lichtenberger, R., Furuta, K., Yadav, S. R., Helariutta, Y., He, X. Q., Fukuda, H., Kang, J., Brady, S. M., Patrick, J. W., Sperry, J., Yoshida, A., López-Millán, A. F., Grusak, M. A. and Kachroo, P. (2013) 'The Plant Vascular System: Evolution, Development and Functions', *Journal of Integrative Plant Biology*. doi: 10.1111/jipb.12041.
- Ma, H., Duan, J., Ke, J., He, Y., Gu, X., Xu, T. H., Yu, H., Wang, Y., Brunzelle, J. S., Jiang, Y., Rothbart, S. B., Xu, H. E., Li, J. and Melcher, K. (2017) 'A D53 repression motif induces oligomerization of TOPLESS corepressors and promotes assembly of a corepressor-nucleosome complex', *Science Advances*. doi: 10.1126/sciadv.1601217.
- Machin, D. C., Hamon-Josse, M. and Bennett, T. (2019) 'Fellowship of the rings: a saga of strigolactones and other small signals', *New Phytologist*. doi: 10.1111/nph.16135.
- Mähönen, A. P., Bonke, M., Kauppinen, L., Riikonen, M., Benfey, P. N. and Helariutta, Y. (2000) 'A novel two-component hybrid molecule regulates vascular morphogenesis of the Arabidopsis root', *Genes and Development*. doi: 10.1101/gad.189200.
- Mähönen, A. P., Tusscher, K. Ten, Siligato, R., Smetana, O., Díaz-Triviño, S., Salojärvi, J., Wachsman, G., Prasad, K., Heidstra, R. and Scheres, B. (2014) 'PLETHORA gradient formation mechanism separates auxin responses', *Nature*. doi: 10.1038/nature13663.
- Di Mambro, R., De Ruvo, M., Pacifici, E., Salvi, E., Sozzani, R., Benfey, P. N., Busch, W., Novak, O., Ljung, K., Di Paola, L., Marée, A. F. M., Costantino, P., Grieneisen, V. A. and Sabatini, S. (2017) 'Auxin minimum triggers the developmental switch from cell division to cell differentiation in the Arabidopsis root', *Proceedings of the National Academy of Sciences of the United States of America*. doi: 10.1073/pnas.1705833114.
- Marhava, P., Aliaga Fandino, A. C., Koh, S. W. H., Jelínková, A., Kolb, M., Janacek, D. P., Breda, A. S., Cattaneo, P., Hammes, U. Z., Petrášek, J. and Hardtke, C. S. (2020) 'Plasma Membrane Domain Patterning and Self-Reinforcing Polarity in Arabidopsis', *Developmental Cell*. doi: 10.1016/j.devcel.2019.11.015.
- Marhava, P., Bassukas, A. E. L., Zourelidou, M., Kolb, M., Moret, B., Fastner, A., Schulze, W. X., Cattaneo, P., Hammes, U. Z., Schwechheimer, C. and Hardtke, C. S. (2018) 'A molecular rheostat adjusts auxin flux to promote root protophloem differentiation', *Nature*, 558(7709), pp. 297–300. doi: 10.1038/s41586-018-0186-z.

- Martin-Arevalillo, R., Nanao, M. H., Larrieu, A., Vinos-Poyo, T., Mast, D., Galvan-Ampudia, C., Brunoud, G., Vernoux, T., Dumas, R. and Parcy, F. (2017) 'Structure of the Arabidopsis TOPLESS corepressor provides insight into the evolution of transcriptional repression', *Proceedings of the National Academy of Sciences of the United States of America*. doi: 10.1073/pnas.1703054114.
- Miyashima, S., Sebastian, J., Lee, J. Y. and Helariutta, Y. (2013) 'Stem cell function during plant vascular development', *EMBO Journal*. doi: 10.1038/emboj.2012.301.
- Moturu, T. R., Thula, S., Singh, R. K., Nodzyński, T., Vařeková, R. S., Friml, J. and Simon, S. (2018) 'Molecular evolution and diversification of the SMXL gene family', *Journal of Experimental Botany*. doi: 10.1093/jxb/ery097.
- Mouchel, C. F., Briggs, G. C. and Hardtke, C. S. (2004) 'Natural genetic variation in Arabidopsis identifies BREVIS RADIX, a novel regulator of cell proliferation and elongation in the root', *Genes and Development*. doi: 10.1101/gad.1187704.
- Münch, E. (1930) 'Die Stoffbewegungen in der Pflanze', *Jena: Gustav Fischer*.
- Nimchuk, Z. L., Zhou, Y., Tarr, P. T., Peterson, B. A. and Meyerowitz, E. M. (2015) 'Plant stem cell maintenance by transcriptional cross-regulation of related receptor kinases', *Development (Cambridge)*. doi: 10.1242/dev.119677.
- Ohta, M., Matsui, K., Hiratsu, K., Shinshi, H. and Ohme-Takagi, M. (2001) 'Repression Domains of Class II ERF Transcriptional Repressors Share an Essential Motif for Active Repression', *The Plant Cell*. doi: 10.1105/tpc.010127.
- Omelyanchuk, N. A., Kovrizhnykh, V. V., Oshchepkova, E. A., Pasternak, T., Palme, K. and Mironova, V. V. (2016) 'A detailed expression map of the PIN1 auxin transporter in Arabidopsis thaliana root', *BMC Plant Biology*. doi: 10.1186/s12870-015-0685-0.
- Oparka, K. J. and Turgeon, R. (1999) 'Sieve elements and companion cells - Traffic control centers of the phloem', *Plant Cell*. doi: 10.1105/tpc.11.4.739.
- Page, D. R. and Grossniklaus, U. (2002) 'The art and design of genetic screens: Arabidopsis thaliana', *Nature Reviews Genetics*. doi: 10.1038/nrg730.
- Pauwels, L., Barbero, G. F., Geerinck, J., Tilleman, S., Grunewald, W., Pérez, A. C., Chico, J. M., Bossche, R., Vanden, Sewell, J., Gil, E., García-Casado, G., Witters, E., Inzé, D., Long, J. A., De Jaeger, G., Solano, R. and Goossens, A. (2010) 'NINJA connects the co-repressor TOPLESS to jasmonate signalling', *Nature*. doi: 10.1038/nature08854.
- Ren, S. C., Song, X. F., Chen, W. Q., Lu, R., Lucas, W. J. and Liu, C. M. (2019) 'CLE25 peptide regulates phloem initiation in Arabidopsis through a CLERK-CLV2 receptor complex', *Journal of Integrative Plant Biology*. doi: 10.1111/jipb.12846.
- Rodrigues, A., Santiago, J., Rubio, S., Saez, A., Osmont, K. S., Gadea, J., Hardtke, C. S. and Rodriguez, P. L. (2009) 'The short-rooted phenotype of the brevis radix mutant partly reflects root abscisic acid hypersensitivity1[C][W][OA]', *Plant Physiology*. doi: 10.1104/pp.108.133819.
- Rodriguez-Villalon, A. (2016) 'Wiring a plant: Genetic networks for phloem formation in Arabidopsis thaliana roots', *New Phytologist*, 210(1). doi: 10.1111/nph.13527.
- Rodriguez-Villalon, A., Gujas, B., Kang, Y. H., Breda, A. S., Cattaneo, P., Depuydt, S. and Hardtke, C. S. (2014) 'Molecular genetic framework for protophloem formation', *Proceedings of the National Academy of Sciences of the United States of America*. doi: 10.1073/pnas.1407337111.
- Rodriguez-Villalon, A., Gujas, B., van Wijk, R., Munnik, T. and Hardtke, C. S. (2015) 'Primary root protophloem differentiation requires balanced phosphatidylinositol-4,5-bisphosphate levels and systemically affects root branching', *Development (Cambridge)*. doi: 10.1242/dev.118364.

- Ross-Elliott, T. J., Jensen, K. H., Haaning, K. S., Wager, B. M., Knoblauch, J., Howell, A. H., Mullendore, D. L., Monteith, A. G., Paultre, D., Yan, D., Otero, S., Bourdon, M., Sager, R., Lee, J. Y., Helariutta, Y., Knoblauch, M. and Oparka, K. J. (2017) 'Phloem unloading in arabidopsis roots is convective and regulated by the phloempole pericycle', *eLife*, 6. doi: 10.7554/eLife.24125.
- Ruonala, R., Ko, D. and Helariutta, Y. (2017) 'Genetic Networks in Plant Vascular Development', *Annual Review of Genetics*, 51(1). doi: 10.1146/annurev-genet-120116-024525.
- De Rybel, B., Mähönen, A. P., Helariutta, Y. and Weijers, D. (2016) 'Plant vascular development: From early specification to differentiation', *Nature Reviews Molecular Cell Biology*. doi: 10.1038/nrm.2015.6.
- Sabatini, S., Beis, D., Wolkenfelt, H., Murfett, J., Guilfoyle, T., Malamy, J., Benfey, P., Leyser, O., Bechtold, N., Weisbeek, P. and Scheres, B. (1999) 'An auxin-dependent distal organizer of pattern and polarity in the Arabidopsis root', *Cell*. doi: 10.1016/S0092-8674(00)81535-4.
- Sanchez, R. and Zhou, M. M. (2011) 'The PHD finger: A versatile epigenome reader', *Trends in Biochemical Sciences*. doi: 10.1016/j.tibs.2011.03.005.
- Scacchi, E., Osmont, K. S., Beuchat, J., Salinas, P., Navarrete-Gómez, M., Trigueros, M., Ferrándiz, C. and Hardtke, C. S. (2009) 'Dynamic, auxin-responsive plasma membrane-to-nucleus movement of Arabidopsis BRX', *Development*. doi: 10.1242/dev.035444.
- Scacchi, E., Salinas, P., Gujas, B., Santuari, L., Krogan, N., Ragni, L., Berleth, T. and Hardtke, C. S. (2010) 'Spatio-temporal sequence of cross-regulatory events in root meristem growth', *Proceedings of the National Academy of Sciences of the United States of America*. doi: 10.1073/pnas.1014716108.
- Schröder, P., Herzig, R., Bojinov, B., Ruttens, A., Nehnevajova, E., Stamatiadis, S., Memon, A., Vassilev, A., Caviezel, M. and Vangronsveld, J. (2008) 'Bioenergy to save the world: Producing novel energy plants for growth on abandoned land', *Environmental Science and Pollution Research*. doi: 10.1065/espr2008.03.481.
- Schürholz, A. K., López-Salmerón, V., Li, Z., Forner, J., Wenzl, C., Gaillochet, C., Augustin, S., Barro, A. V., Fuchs, M., Gebert, M., Lohmann, J. U., Greb, T. and Wolf, S. (2018) 'A comprehensive toolkit for inducible, cell type-specific gene expression in Arabidopsis', *Plant Physiology*. doi: 10.1104/pp.18.00463.
- Shi, D., Lebovka, I., López-Salmerón, V., Sanchez, P. and Greb, T. (2019) 'Bifacial cambium stem cells generate xylem and phloem during radial plant growth', *Development (Cambridge)*. doi: 10.1242/dev.171355.
- Shinohara, H. and Matsubayashi, Y. (2015) 'Reevaluation of the CLV3-receptor interaction in the shoot apical meristem: Dissection of the CLV3 signaling pathway from a direct ligand-binding point of view', *Plant Journal*. doi: 10.1111/tbj.12817.
- Slewinski, T. L., Zhang, C. and Turgeon, R. (2013) 'Structural and functional heterogeneity in phloem loading and transport', *Frontiers in Plant Science*. doi: 10.3389/fpls.2013.00244.
- Smith, S. M. and Li, J. (2014) 'Signalling and responses to strigolactones and karrikins', *Current Opinion in Plant Biology*. doi: 10.1016/j.pbi.2014.06.003.
- Somssich, M., Bleckmann, A. and Simon, R. (2016) 'Shared and distinct functions of the pseudokinase CORYNE (CRN) in shoot and root stem cell maintenance of Arabidopsis', *Journal of Experimental Botany*. doi: 10.1093/jxb/erw207.

- Soundappan, I., Bennett, T., Morffy, N., Liang, Y., Stanga, J. P., Abbas, A., Leyser, O., Nelsona, D. C. and Nelson, D. C. (2015) 'SMAX1-LIKE/D53 family members enable distinct MAX2-dependent responses to strigolactones and karrikins in arabidopsis', *Plant Cell*. doi: 10.1105/tpc.15.00562.
- Soyars, C. L., James, S. R. and Nimchuk, Z. L. (2016) 'Ready, aim, shoot: Stem cell regulation of the shoot apical meristem', *Current Opinion in Plant Biology*. doi: 10.1016/j.pbi.2015.12.002.
- Stadler, R., Wright, K. M., Lauterbach, C., Amon, G., Gahrtz, M., Feuerstein, A., Oparka, K. J. and Sauer, N. (2005) 'Expression of GFP-fusions in Arabidopsis companion cells reveals non-specific protein trafficking into sieve elements and identifies a novel post-phloem domain in roots', *Plant Journal*. doi: 10.1111/j.1365-313X.2004.02298.x.
- Stanga, J. P., Smith, S. M., Briggs, W. R. and Nelson, D. C. (2013) 'SUPPRESSOR OF MORE AXILLARY GROWTH2 1 controls seed germination and seedling development in Arabidopsis', *Plant Physiology*. doi: 10.1104/pp.113.221259.
- Swarbreck, S. M., Guerringue, Y., Matthus, E., Jamieson, F. J. C. and Davies, J. M. (2019) 'Impairment in karrikin but not strigolactone sensing enhances root skewing in Arabidopsis thaliana', *Plant Journal*. doi: 10.1111/tbj.14233.
- Szemenyei, H., Hannon, M. and Long, J. A. (2008) 'TOPLESS mediates auxin-dependent transcriptional repression during Arabidopsis embryogenesis', *Science*. doi: 10.1126/science.1151461.
- Tonn, N. and Greb, T. (2017) *Radial plant growth*, *Current Biology*. doi: 10.1016/j.cub.2017.03.056.
- Truernit, E., Bauby, H., Belcram, K., Barthélémy, J., Palauqui, J. C. J.-C., Barthelemy, J. and Palauqui, J. C. J.-C. (2012) 'OCTOPUS, a polarly localised membrane-associated protein, regulates phloem differentiation entry in Arabidopsis thaliana', *Development*. doi: 10.1242/dev.072629.
- Truernit, E., Bauby, H., Dubreucq, B., Grandjean, O., Runions, J., Barthélémy, J. and Palauqui, J. C. (2008) 'High-resolution whole-mount imaging of three-dimensional tissue organization and gene expression enables the study of phloem development and structure in Arabidopsis', *Plant Cell*. doi: 10.1105/tpc.107.056069.
- Villaécija-Aguilar, J. A., Hamon-Josse, M., Carbonnel, S., Kretschmar, A., Schmidt, C., Dawid, C., Bennett, T. and Gutjahr, C. (2019) 'SMAX1/SMXL2 regulate root and root hair development downstream of KAI2-mediated signalling in Arabidopsis', *PLoS Genetics*. doi: 10.1371/journal.pgen.1008327.
- Walker, C. H., Siu-Ting, K., Taylor, A., O'Connell, M. J. and Bennett, T. (2019) 'Strigolactone synthesis is ancestral in land plants, but canonical strigolactone signalling is a flowering plant innovation', *BMC biology*. doi: 10.1186/s12915-019-0689-6.
- Wallner, E. S. (2018) 'Early events in phloem formation: Exploring the molecular network of SMXL3/4/5 (Doctoral dissertation)', *Heidelberg*. doi: 10.11588/heidok.00025313.
- Wallner, E.-S., Tonn, N., Wanke, F., Lopéz-Salmerón, V., Gebert, M., Wenzl, C., Lohmann, J. U., Harter, K. and Greb, T. (2019) 'OBERON3 and SUPPRESSOR OF MAX2 1-LIKE proteins form a regulatory module specifying phloem identity', *bioRxiv*. doi: 10.1101/2019.12.21.885863.
- Wallner, E. S., López-Salmerón, V., Belevich, I., Poschet, G., Jung, I., Grünwald, K., Sevilem, I., Jokitalo, E., Hell, R., Helariutta, Y., Agustí, J., Lebovka, I. and Greb, T. (2017) 'Strigolactone- and Karrikin-Independent SMXL Proteins Are Central Regulators of Phloem Formation', *Current Biology*. doi: 10.1016/j.cub.2017.03.014.

- Wallner, E. S., Tonn, N., Shi, D., Jouannet, V. and Greb, T. (2020) 'SUPPRESSOR OF MAX2 1-LIKE 5 promotes secondary phloem formation during radial stem growth', *Plant Journal*. doi: 10.1111/tpj.14670.
- Wang, L., Wang, B., Jiang, L., Liu, X., Li, X., Lu, Z., Meng, X., Wang, Y., Smith, S. M., Li, J. and Lia, J. (2015) 'Strigolactone Signaling in Arabidopsis Regulates Shoot Development by Targeting D53-Like SMXL Repressor Proteins for Ubiquitination and Degradation', *Plant Cell*. doi: 10.1105/tpc.15.00605.
- Glazebrook, J., and Weigel, D. (2002) 'Arabidopsis: A laboratory manual', *Cold Spring Harbor Laboratory Press, New York*.
- Wippel, K. and Sauer, N. (2012) 'Arabidopsis SUC1 loads the phloem in suc2 mutants when expressed from the SUC2 promoter', *Journal of Experimental Botany*. doi: 10.1093/jxb/err255.
- Wu, Y. Y., Hou, B. H., Lee, W. C., Lu, S. H., Yang, C. J., Vaucheret, H. and Chen, H. M. (2017) 'DCL2- and RDR6-dependent transitive silencing of SMXL4 and SMXL5 in Arabidopsis dcl4 mutants causes defective phloem transport and carbohydrate over-accumulation', *Plant Journal*. doi: 10.1111/tpj.13528.
- Yamaguchi, M., Ohtani, M., Mitsuda, N., Kubo, M., Ohme-Takagi, M., Fukuda, H. and Demura, T. (2010) 'VND-INTERACTING2, a NAC Domain Transcription Factor, Negatively Regulates Xylem Vessel Formation in Arabidopsis', *The Plant Cell*. doi: 10.1105/tpc.108.064048.
- Zhou, F., Lin, Q., Zhu, L., Ren, Y., Zhou, K., Shabek, N., Wu, F., Mao, H., Dong, W., Gan, L., Ma, W., Gao, H., Chen, J., Yang, C., Wang, D., Tan, J., Zhang, X., Guo, X., Wang, Jiulin *et al.* (2013) 'D14-SCF D3 -dependent degradation of D53 regulates strigolactone signalling', *Nature*. doi: 10.1038/nature12878.
- Zhu, Z., Xu, F., Zhang, Yaxi, Cheng, Y. T., Wiermer, M., Li, X. and Zhang, Yuelin (2010) 'Arabidopsis resistance protein SNC1 activates immune responses through association with a transcriptional corepressor', *Proceedings of the National Academy of Sciences of the United States of America*. doi: 10.1073/pnas.1002828107.

Acknowledgements / Danksagungen

I am truly grateful for everyone who accompanied, supervised and chaperoned me in the past three years and nine months!

First of all, thank you, Thomas, for offering me this PhD project, for giving me the freedom to figure out my way of doing research, and, if in doubt, for nudging me to pursue a more promising direction. Thank you, Rüdiger Hell and Sebastian Wolf, for completing my Thesis Advisory Committee and improving my project with your suggestions. Thank you, too, Karin Schumacher and Steffen Lemke, for agreeing to evaluate my dissertation.

Many thanks go to all current and former members of the Greb lab. Sophie und Theresa, tausend Dank euch, Vadir, muchas gracias, and Laura, grazie mille. You guys helped me get through any struggle that came along the way. I am very lucky to call you my co-workers and friends. And to Dongbo a special ありがとう for your scientific advice and critical input on my thesis.

More thanks belong to all first-floor people for providing a respectful and friendly work environment. Thanks also to those familiar faces in the seminar room, not to mention Denis, Yossi, and Michael. I do not know how our scientific discussions ended up at the most peculiar topics, but it has been a pleasure working and pausing with you.

A comprehensive thank you goes to the whole COS community and everyone who worked hard on keeping the spirit and mutual support alive. Danke, Mädels, für eure positive Energie und all die unterstützenden Worte, die mich immer wieder aufgebaut haben. Anka, Eli, Jana, Naima, Viola, fühlt euch umarmt. Dankeschön, liebe Anna, für die produktiven Minipausen mit dir. Unsere shotgun conversations zwischen perfekt ausgemachten Laboreinheiten haben mich immer ein Stückchen aufgemuntert und weitergebracht. Bleib' dran, bald ist es geschafft!

And thank you, Rik, for your scientific input and moral support especially during the final phase. Recharging with you kept me going.

Ganz besonderer Dank gilt auch euch da draußen außerhalb des COS, Andrea, Leander, Roman, Laura, Katha, Lisa, Nadia und Helen. Danke für mittägige Beratungsgespräche, abendliche Sporteinheiten, nächtliche Laborbesuche, unzählige Telefonate und alles, was mich ab und zu aus dem PhD-Trott herausgerissen hat. Andrea, Roman, Lisa, Nadia, Helen – toitoitoi für die letzten Meter!

Und natürlich: liebe Viola, Linda, Sonja, Mama, lieber Adi und Papa, vielen Dank, dass ihr mir immer wieder das Gefühl vermittelt habt, dass das, was ich mache, etwas Besonderes ist. Ihr habt mich aufgefangen und aufgebaut und ich könnte mir keine tollere Familie vorstellen.

Abschließend richte ich vielen Dank an das Cusanuswerk für die finanzielle und ideelle Unterstützung. Ich bleibe euch gerne als Alumna verbunden.

Finite Incantatem

